SEISMIC ANALYSIS OF STEEL FRAME / WOOD PANEL SHEAR WALLS

By

Félix-Antoine Boudreault

Department of Civil Engineering and Applied Mechanics
McGill University, Montreal, Québec, Canada

June 2005

A thesis submitted to the Faculty of Graduate and Postdoctoral Studies
in partial fulfillment of the requirements of the
Degree of Master of Engineering

© Félix-Antoine Boudreault, 2005

Library and
Archives Canada

Published Heritage
Branch

395 Wellington Street
Ottawa ON K1A 0N4
Canada

Bibliothèque et
Archives Canada

Direction du
Patrimoine de l'édition

395, rue Wellington
Ottawa ON K1A 0N4
Canada

Your file Votre référence
ISBN: 978-0-494-22631-5
Our file Notre référence
ISBN: 978-0-494-22631-5

NOTICE:
The author has granted a non-exclusive license allowing Library and Archives Canada to reproduce, publish, archive, preserve, conserve, communicate to the public by telecommunication or on the Internet, loan, distribute and sell theses worldwide, for commercial or non-commercial purposes, in microform, paper, electronic and/or any other formats.

The author retains copyright ownership and moral rights in this thesis. Neither the thesis nor substantial extracts from it may be printed or otherwise reproduced without the author's permission.

AVIS:
L'auteur a accordé une licence non exclusive permettant à la Bibliothèque et Archives Canada de reproduire, publier, archiver, sauvegarder, conserver, transmettre au public par télécommunication ou par l'Internet, prêter, distribuer et vendre des thèses partout dans le monde, à des fins commerciales ou autres, sur support microforme, papier, électronique et/ou autres formats.

L'auteur conserve la propriété du droit d'auteur et des droits moraux qui protège cette thèse. Ni la thèse ni des extraits substantiels de celle-ci ne doivent être imprimés ou autrement reproduits sans son autorisation.

In compliance with the Canadian Privacy Act some supporting forms may have been removed from this thesis.

While these forms may be included in the document page count, their removal does not represent any loss of content from the thesis.

Conformément à la loi canadienne sur la protection de la vie privée, quelques formulaires secondaires ont été enlevés de cette thèse.

Bien que ces formulaires aient inclus dans la pagination, il n'y aura aucun contenu manquant.

Canada

"EARTHQUAKES DON'T KILL PEOPLE,

BUILDINGS DO"

CHARLES RICHTER, INVENTOR OF THE RICHTER SCALE

SEISMIC ANALYSIS OF STEEL FRAME / WOOD PANEL SHEAR WALLS

Félix-Antoine Boudreault

ABSTRACT

The use of steel frame / wood panel shear walls as a seismic force resisting system (SFRS) in residential and/or commercial buildings is expected to increase in the future. At the moment, in Canada, however, no specific guidelines in line with the seismic provisions of the National Building Code of Canada (NBCC) exist with which the engineer can design a building consisting of these shear walls. An extensive research program has therefore been undertaken at McGill University to develop a design method through the testing of different configurations of steel frame / wood panel shear walls loaded with monotonic and reversed cyclic protocols. A total of 16 wall configurations (109 walls) were tested over the course of the study. The CUREE Ordinary Ground Motions loading protocol was selected to represent the reversed cyclic regime because it was found to best correspond to the demand that would be imposed on a steel frame / wood panel shear wall during a typical seismic event.

The analysis of test results in order to extract the principal design information was carried out using an Equivalent Energy Elastic-Plastic (EEEP) model. A ductility related (R_d) and an overstrength related (R_o) force modification factor are required for the calculation of equivalent static seismic loads following the 2005 NBCC design provisions. Values of $R_o = 1.8$ and $R_d = 2.5$ have been determined and are recommended on a preliminary basis.

The Stewart hysteretic model was found to best represent the strength and stiffness characteristics of a steel frame / wood panel shear wall component. The subsequent evaluation of building models that incorporate the Stewart model using non-linear time history dynamic analyses could then be carried out to validate the assumptions made by the EEEP method on the system ductility and the corresponding force modification factors.

ANALYSE SISMIQUE DES MURS DE REFEND À OSSATURE EN ACIER RECOUVERTS DE PANNEAUX DE BOIS

Félix-Antoine Boudreault

RÉSUMÉ

Les murs de refend à ossature en acier laminé à froid recouverts de panneaux de bois sont de plus en plus utilisés dans l'industrie de la construction résidentielle et commerciale comme système de résistance aux charges latérales. Par contre, aucune directive spécifique à ce type de construction n'est disponible à ce jour aux ingénieurs canadiens qui désirent l'utiliser tout en respectant les normes établies dans le Code national du bâtiment du Canada (CNB). Afin de pallier à cette carence, un important programme expérimental a été entrepris à l'université McGill afin d'enrichir la base de données empiriques nécessaire à l'élaboration de directives concernant le design de murs de refend à ossature d'acier recouverts de panneaux de bois. Un protocole de chargement monotone et le protocole de chargement cyclique développé par CUREE ont été appliqué à 16 différentes configurations de murs (pour un total de 109 tests). Ce dernier protocole cyclique a été choisi parmi plusieurs autres car il a été jugé celui qui représentait le mieux la demande en énergie que pourra impliquer un véritable séisme à ce type de construction.

Une méthode dite d'énergie équivalente (Equivalent Energy Elastic-Plastic (EEEP)) a été utilisée afin d'extraire, des résultats obtenus, certaines données nécessaires au design. Le CNB 2005 propose l'utilisation de deux facteurs de réduction de force; un premier lié à la ductilité du système (R_d) et un second lié à la sur-résistance (R_o). Des valeurs préliminaires ont été déterminées lors de cette recherche ($R_o = 1.8$ et $R_d = 2.5$), lesquelles devront être vérifiées par des essais sur table vibrante et analyses non linéaires.

Afin d'effectuer ces analyses non linéaires, il est nécessaire de modéliser les murs de refend par un modèle hystérétique sachant reproduire les caractéristiques intrinsèques de l'assemblage. Le modèle hystérétique Stewart remplit ces conditions et il est donc recommandé pour la modélisation lors d'analyses non linéaires.

ACKNOWLEDGEMENTS

First and foremost, I would like to express my deepest gratitude to my supervisor, Professor Colin A. Rogers. Your infinite availability, your profound openness and incommensurable patience will be forever remembered. Thank you.

À mes parents adorés qui ont su m'enseigner que « l'instruction se donne à l'école, l'éducation à la maison ». Merci aussi pour votre appui moral tout au long de mes études et autres escapades africaines. Merci enfin à ma grande sœur pour ses encouragements répétés et parce qu'elle a été, sans vraiment le savoir, un modèle tout au long de ces années d'études. Merci Catherine.

À ce cercle d'amis que j'ai depuis si longtemps malgré mes absences quelques fois prolongées, je vous remercie de votre fidélité. En voulant chacun réussir au mieux ce qu'il entreprend, vous m'avez poussé à me dépasser. Une pensée toute spéciale pour Martin, Hubert, Olivier, David, Émilie, Stéphanie, Philippe-Olivier, Patrice.

A thank you is also especially reserved for my master's companion since the beginning of this McGill adventure, Aaron Branston. Acknowledgements are also extended to all the other graduate and undergraduate students I had the chance to work with; Changyi Chen, Katherine Hikita, Regis Lambert, Damien Soulier and Caroline Blais.

Finally, I would like to thank the Natural Sciences and Engineering Research Council of Canada, the Department of Civil Engineering and Applied Mechanics, the Canada Foundation for Innovation, the Canadian Sheet Steel Building Institute, Bailey Metal Products Ltd., Simpson Strong-Tie Co. Inc., Grabber Construction Products, the Canadian Plywood Association, and the Canam Group Inc. for their support in terms of finances, testing equipment and test specimens.

TABLE OF CONTENTS

LIST OF FIGURES

LIST OF TABLES

CHAPTER 1

INTRODUCTION

1.1 BACKGROUND

In most situations the lateral forces imposed on a structure are the result of wind or seismic actions. Shear walls are generally used as the main lateral force resisting system in residential and small industrial or commercial buildings in North America. However, for the structure to resist the lateral forces, the shear walls must act together with the horizontal diaphragms (roof and floors) and the foundations. The general load path, illustrated in Figure 1-1, is as follows: lateral loads are transferred from the horizontal diaphragm to the shear walls, and then the shear walls themselves transfer the same loads to the foundations. The efficiency of the system is typically limited by the effectiveness of the connections, whether it is the connectors that join a diaphragm to a shear wall to the foundations, or a sheathing panel to a frame member within a shear wall itself.

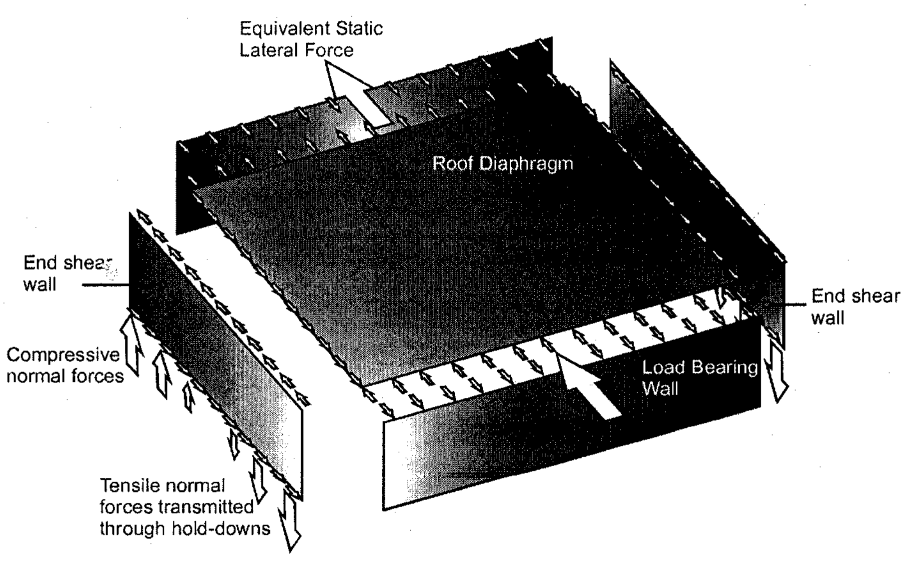

Figure 1-1 : Lateral forces load path (Branston 2004)

For centuries, home builders in North America and other parts of the world, such as Australia and Japan, have used wood as their construction material of choice due to its availability, renewability and low cost. However, in recent years light gauge steel sections have been specified more and more as primary framing components of residential homes and small industrial or commercial buildings (Figure 1-2). Light gauge steel sections are also often selected because of the consistent quality, resistance to fire, rot and termites and because they are available in a variety of shapes.

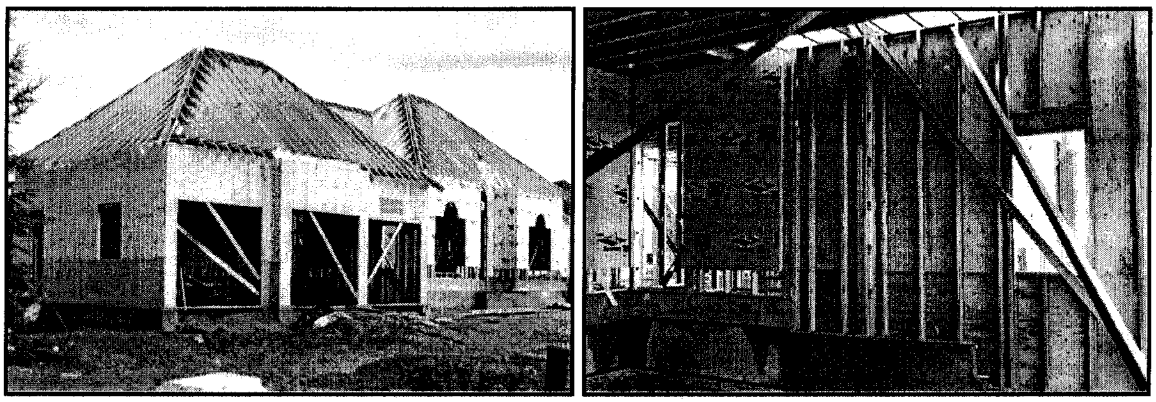

Figure 1-2 : Light gauge steel frame members in residential housing

Residential structures, although being the biggest contributor to wealth (Gad *et al.* 1999-B), tend to be the subject of research less often than larger commercial or industrial structures. As an example, in North America, design methodologies for light framed wood shear walls were based largely on results from monotonic loading tests, i.e. shear loads applied in the plane of the wall in one direction only. However, after the Northridge earthquake in 1994, which caused quite extensive damage to wood structures[1], the evaluation of shear wall performance by cyclic load tests was encouraged. It was believed that a reversed cyclic protocol can represent a better approximation of the imposed energy on a structure that has been submitted to a seismic event.

Since the use of light-gauge steel framing is becoming more common across North America, an increase in the probability that a light gauge steel frame / wood panel

[1] An estimated 48 000 wood frame residences were affected, resulting in an estimated 40 billion USD in property damage and 24 of the 25 recorded fatalities occurred in wood structures (Krawinkler *et al.* 2000)

structure will be subjected to the demands of a severe earthquake or wind event exists. Even though steel frame and wood frame shear walls are constructed in a similar fashion, and hence share some performance characteristics, their behaviour in the non-linear range and at the onset of failure is somewhat different. Firstly, the presence of thin cold-formed steel sections introduces the possibility of compression failure in the chord studs of a shear wall. Secondly, the wood-to-steel screw connections do not exhibit the same behaviour as wood-to-wood nail connections because of the thinness of the steel framing members and the rigidity of the screw fasteners themselves. At present, no Canadian document has been published with which engineers can design light gauge steel frame / wood panel shear walls subjected to lateral in-plane loading. Given this variation in behaviour from wood shear walls and the fact that a Canadian design document which covers the effects of lateral loading is not available, a research program on steel frame / wood panel shear walls was undertaken.

1.2 OBJECTIVES OF THE RESEARCH

In view of supplying Canadian engineers with guidelines on how to design light gauge steel frame / wood panel shear walls, the present research, which is part of a larger research programme (Branston, 2004; Chen, 2004), consists of the following objectives:

i) To review existing reversed cyclic loading protocols for light framed shear walls and to select the most appropriate for use in testing.
ii) To carry out a suite of shear wall tests and to determine the appropriate design information from the test results.
iii) To provide a preliminary recommendation of seismic force modification factors for ductility and overstrength for use with the 2005 National Building Code of Canada based on the analysis results derived from these tests.
iv) To determine an hysteretic model that corresponds to the shear resistance vs. deflection behaviour of a light gauge steel frame / wood panel shear wall submitted to a reversed cyclic loading protocol.

v) To determine the material properties of the wood sheathing in shear. And,

vi) To provide recommendations for future studies of light gauge steel frame / wood panel shear walls.

1.3 Scope of Study

An extensive shear wall testing programme (109 tests) was carried out during the summer of 2003 in order to establish a bank of data for various wall configurations constructed with Canadian steel frame (1.12 mm (0.044") thick 230 MPa (33 ksi) grade) and wood sheathing products (Douglas Fir Plywood (CSA O121, 1978), Canadian Softwood Plywood (CSA O151, 1978), Performance Rated OSB (CSA O325, 1992)). Three screw fastener spacing distances (152, 102 and 76 mm (6", 4" and 3")) were used for the perimeter sheathing to framing connections, and in all cases, industry standard hold-downs (Simpson, 2001) were installed at the base of the chord studs. Of the total 109 tests that were completed, the author was solely responsible for 20 wall specimens that measured 1220 x 2440 mm (4' x 8'). All test data, results and observation sheets were assembled in a stand-alone document (Branston *et al.*, 2004). Four existing reversed cyclic protocols were investigated in detail, with the most appropriate being selected for use in testing. The resulting test data from all of the shear walls tests was then incorporated into this study to establish the seismic force modification factors and to recommend an hysteretic model.

1.4 Limitations of Study

A number of factors can play a role in the behaviour of a shear wall subjected to an earthquake. For time and economic reasons only a limited number of these factors were considered to be variables. The single storey shear walls tested in the present study were of limited sizes (610, 1220, 2440 mm (2', 4', 8') in length), were subjected to in-plane displacements without vertical gravity loads, were supported laterally and contained no upper floor diaphragm. These aspects were considered beyond the scope of this thesis. Also, some of the articles and documents referred to in the literature review consist of research on wood framed shear walls only, and although it is generally accepted that the behaviour of the two types of shear walls share some, but not all, of their characteristics, a few differences exist such as the failure mechanisms.

1.5 Document Organization

This thesis contains four main parts. Chapter 2 consists of a general literature review of existing loading protocols and summarizes past research in which a comparison of the different loading protocols, especially reversed cyclic, is found.

Chapter 3 describes the testing program, starting with comparative tests on nominally identical walls of a particular configuration subjected to two preselected reversed cyclic protocols, namely a "ramped" cyclic protocol used by Serrette (2002) and the CUREE ordinary ground motion protocol (Krawinkler *et al.*, 2000). The results of ancillary materials tests are provided, as well as values for strength and stiffness design parameters.

Chapter 4 examines the measured ductility of each shear wall assembly and proposes possible values of seismic force modification factors (commonly called R-Factors) for light gauge steel frame / wood panel shear walls for use with the 2005 National Building Code of Canada (NRCC, 2004).

Chapter 5 first summarizes the hysteresis characteristics of typical light gauge steel frame shear walls and then proposes an hysteretic model that can be used for dynamic non-linear time history analysis.

Finally, Chapter 6 provides conclusions for this study and recommendations for further research on light gauge steel frame / wood panel shear walls.

CHAPTER 2

LITERATURE REVIEW

2.1 *SUMMARY OF PREVIOUS RESEARCH ON SHEAR WALLS*

Included in this thesis is a brief summary of previous research on shear walls reviewed by Zhao (2002), Branston (2004) and Chen (2004). For an extensive literature review of previous shear wall studies, an interested reader is invited to consult their theses.

Zhao (2002) provided a detailed review of previous shear wall test programs in North America. Most notably, Zhao covered the research programs carried out by Gad *et al.* (1997, 1998, 1999a,b, 2000), Salenikovich *et al.* (2000), Serrette *et al.* (1996, 1997) and COLA-UCI (2001). Results from some of the previous test programs were used by Zhao to evaluate various lateral force design methods and to determine a preliminary ductility based force modification factor for use in the seismic design of steel frame / wood panel shear walls following the equivalent static approach prescribed by the 1995 National Building Code of Canada (NRCC, 1995). Based on this investigation, Zhao recommended that a preliminary ductility related force modification factor (R_d) of 2.0 is suitable for use in the design of steel frame / wood panel shear walls.

Branston (2004) also included a complete literature review of previous shear wall testing programs as well as an extensive review of existing data interpretation methodologies. A total of 42 shear wall specimens measuring 1220 x 2440 mm (4' x 8') of various sheathing type (CSP, DFP, OSP) and screw pattern (76/305, 102/305 and 152/305 mm (3"/12", 4"/12" and 6"/12")) were tested and analysed by Branston. The equivalent energy elastic-plastic (EEEP) analysis technique was employed to evaluate the test data to deduce key design parameters such as the yield wall resistance, elastic stiffness, and system ductility for the wall systems under study (steel frame / wood panel shear walls). Branston provided specified strength and unit elastic stiffness values for use in design according to given perimeter fastener schedules and sheathing type. It was found that a resistance factor (Φ) of 0.7 provided sufficient reliability and a reasonable factor of safety under the 2005 NBCC (NRCC, 2004) wind loading case. Branston also recommended that this resistance factor be used for seismic design of steel frame / wood panel shear walls.

Chen (2004) investigated the performance characteristics of various configurations of steel frame / wood panel shear walls under monotonic and reversed cyclic loading. Chen tested and analyzed a total of 46 steel frame / wood panel shear wall specimens using the EEEP method as recommended by Branston (2004). The configuration of the specimens varied in terms of wall length (610, 1220 and 2440 mm (2', 4' and 8')), sheathing type (CSP, OSB) and fastener schedule (76/305, 102/305, 152/305 mm (3"/12", 4"/12" and 6"/12")). A comparative study of relative shear wall performance based on the test results obtained by Branston, Chen and the author was presented. Chen also provided information on existing analytical design approaches for shear. Finally, an analytical method of mechanics approach to estimate wall displacement and strength was recommended.

2.2 Background of Loading Protocols

Light gauge steel frame / wood panel shear wall response can be influenced by various factors including the size of the wall, wood panel type and thickness, screw spacing pattern as well as the type of test protocol implemented, i.e. monotonic or reversed cyclic. Amongst these factors, the protocol selection is critical, especially when it comes to reversed cyclic testing, in order to replicate the possible wind conditions and seismic events that could occur and cause damage to the structure in its lifetime.

Standard racking tests, or monotonic tests as they are often called, have been used since the 1940s in order to measure the shear strength of wood shear walls. Very rapidly, researchers became aware of the lack of information provided by these unidirectional tests. Medearis and Young (1964) first developed and used a reversed cyclic testing protocol that allowed for the determination of more variables than the standard racking test; the most noticeable being the level of energy dissipation, deformation capacity, pinched hysteretic loops and the stiffness and strength degradations (refer to Chapter 5 for a more detailed description of these hysteresis characteristics). In fact, it has been found that the same factors which affect the behaviour of a monotonic test also affect the cyclic behaviour. In contrast, the reverse relationship is not true, i.e. the cyclic test response reveals new factors that are undetectable when a specimen is monotically tested (Heine, 2001), which explains the necessity of performing cyclic tests. Nevertheless, the results from monotonic tests (see Section 2.2.1) are yet necessary as they are used to simulate wind load conditions as well as to determine the reference displacement needed in the development of most cyclic protocols.

Over the years, many cyclic loading protocols have been established; from quasi-static to pseudodynamic as well as full-scale shaketable testing. It is therefore surprising to note that forty years after Medearis' and Young's first cyclic test, there are still no internationally accepted reversed cyclic protocols nor general guidelines, and that the choice of a cyclic protocol is still very subjective (Foliente and Zacher, 1994; Krawinkler, 1996). In some cases, the design values for light framed structures found in current building codes have been derived from results obtained from monotonic testing because, among other reasons, of the lack of a standardized protocol. Although seismic design values that originate from monotonic test results exist and are frequently used for a variety of structural systems, it is commonly believed by the scientific community that these design values are not representative of a structure's behaviour during a real earthquake (Gatto and Uang, 2002).

This Chapter presents an overview of the monotonic protocol typically utilized and four of the most commonly employed reversed cyclic protocols in use by the scientific community: SPD (Sequential Phased Displacement), ATC-24 (Applied Technology Council), ISO 16670 (International Organization of Standardization) and CUREE

(Consortium of Universities for Research in Earthquake Engineering). A discussion which focuses on a comparison of the reversed cyclic protocols follows their description.

2.3 OVERVIEW OF LOADING PROTOCOLS

2.3.1 MONOTONIC PROTOCOLS

Contrary to reversed cyclic protocols, monotonic racking protocols are usually very similar due to the fact that very few parameters need to be programmed by the experimentalist. The American Society for Testing and Materials Standard E 564 (ASTM, 1995) is generally used as a base for static tests, but some researchers have adapted and modified this standard in order to obtain results not provided by the basic standard alone. For instance, Serrette *et al.* (1996) introduced a modification to the ASTM E 564 protocol by unloading the wall to zero force at displacements of 12.7 mm (0.5") and 38.1 mm (1.5") in order to evaluate permanent set (Figure 2-1). In the experimental testing program carried out by the author and described in Chapter 3, the monotonic protocol implemented was similar to that followed by Serrette *et al.* (1996, 1997, 2002).

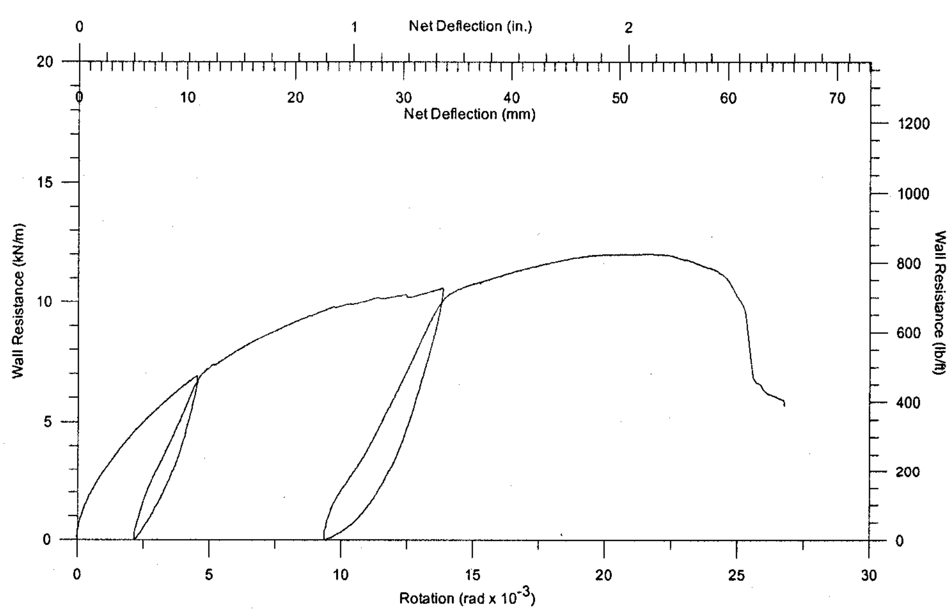

Figure 2-1 : Wall Resistance vs. Displacement Curve for a Typical Monotonic Test

Although monotonic tests are generally relied on to evaluate the "static" type of loading used to simulate wind load conditions on a building, other reasons exist for the implementation of static racking tests. First of all, it is generally easier to evaluate the progressive failure mechanism compared with a rapid cyclic test. Also, not all laboratories are equipped with test frames that can perform reversed-cyclic experiments. Finally, a static racking test is often needed to evaluate the reference displacement needed in the calibration of most cyclic protocols.

2.3.2 SPD (Sequential Phased Displacement) (1987)

Initially developed by Porter (1987) for the Joint Technical Coordinating Committee on Masonry Research (TCCMAR), the Sequential Phased Displacement (SPD) protocol has been modified and adapted specifically for woodframe shear wall testing by the Structural Engineers Association of Southern California (SEAOSC, 1997). The procedure consists of a series of reversed-cyclic excursions that increase in magnitude based on a reference displacement known as the First Major Event (FME). The FME is generally described as the minimum displacement at which an event that demarks two behaviour states occurs or, in other words, the displacement at which the structural system yields (ASTM E 2126, 2005).

The displacement history is composed of two distinct zones: the "elastic" zone[1] where the amplitudes do not reach the anticipated yield point (FME), and the degradation zone where higher amplitude excursions are repeated in order to evaluate the extent of damage and its effect on the overall behavioural response. Table 2-1 presents the sequence of cycles that the SPD protocol follows and Figure 2-2 illustrates the displacement history.

---

[1] "Elastic zone" is used because it is the term employed by Porter (1987) but as shown in Chapter 5 of this thesis, such an "elastic zone" does not exist for the steel frame / wood panel shear wall response.

Table 2-1 : Sequence of amplitudes for SPD Cyclic Protocol

Cycles	Cycle Type	Amplitude (% of FME)
1-3	Initiation	25%
4-6	Initiation	50%
7-9	Initiation	75%
10	Primary	100%
11-13	Decay	75% / 50% / 25%
14-16	Stabilization	100%
17	Primary	125%
18-20	Decay	93.75% / 62.5% / 31.25%
21-23	Stabilization	125%
24	Primary	150%
25-27	Decay	112.5% / 75% / 37.5%
28-30	Stabilization	150%
31	Primary	175%
32-34	Decay	131.25% / 87.5% / 43.75%
35-37	Stabilization	175%
38	Primary	200%
39-41	Decay	150% / 100% / 50%
42-44	Stabilization	200%
45	Primary	250%
46-48	Decay	187.5% / 125% / 62.5%
49-51	Stabilization	250%
52-	Continue pattern, i.e. increase previous primary cycle amplitude by 50% and follow with three decay cycles and three stabilization cycles	

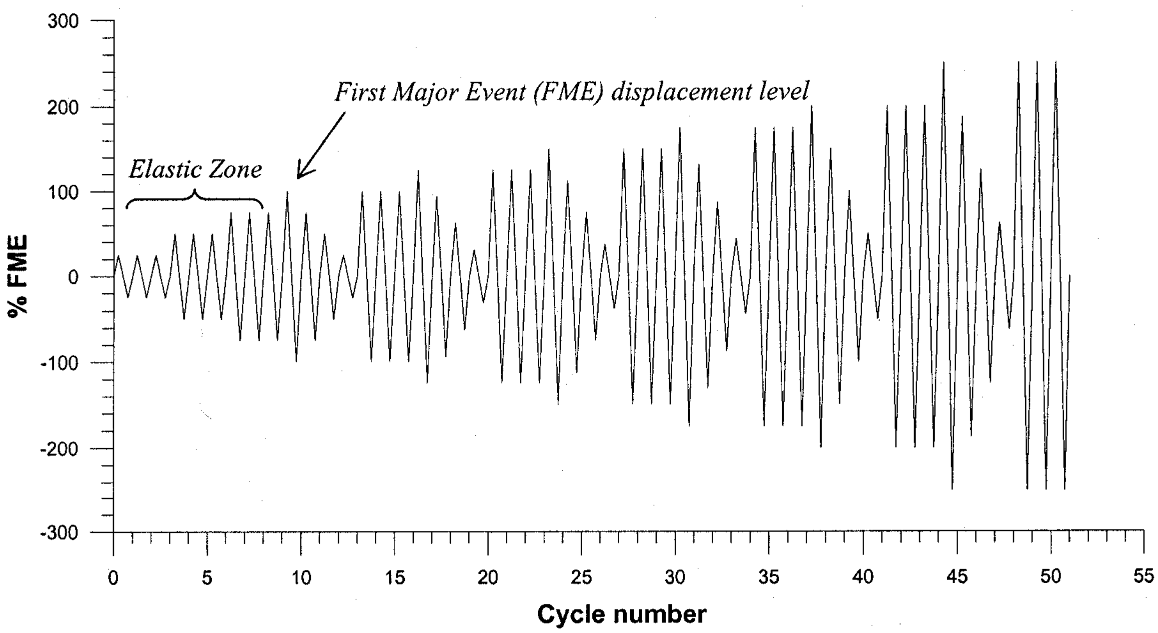

Figure 2-2 : SPD Protocol Displacement History

In the elastic part of the displacement history, three sets of three cycles are defined as 25%, 50% and 75% of the FME respectively. Then, a cycle with an amplitude equal to the theoretical yield point followed by trailing cycles of 75%, 50% and 25% of the primary cycle are included. To complete the pattern, cycles at the identical displacement level as the previous primary cycle (in this case, 100% FME) are repeated three times. This pattern (one primary cycle followed by three stabilization cycles of 75%, 50% and 25% of the primary cycle amplitude, which is in turn followed by three cycles at equal amplitude to the primary cycle) is repeated for primary cycle values of 100%, 125%, 150%, 175%, 200%, 250% and by further increments of 50% if deemed necessary (ICC-ES, 2003). The degradation cycles (sometimes called decay cycles by other researchers) were initially introduced to determine a lower bound on displacement for energy dissipation purposes (Heine, 2001) and the stabilization cycles (also called trailing cycles in the literature) allow for observation of the specimen response in degradation when subjected to similar amplitude cycles (Gatto and Uang, 2002).

The determination of the FME requires prior monotonic or cyclic testing for each of the wall configurations that are included in the testing program. In the cyclic test for the determination of the reference displacement, the specimen is subjected to a special protocol in which sets of three constant amplitude cycles are applied. The displacement level for each set is slowly increased until yielding of the specimen occurs, which, according to SEAOSC (1997), is when the difference between the load reached during the first and last cycle in a set drops by five percent.

The Acceptance criteria for shear wall assemblies consisting of wood structural panel sheathing attached to cold-formed steel framing (ICC-ES, 2003) recommended a modified version of the SPD protocol that does not have decay cycles to reduce the energy demand imposed on a tested shear wall. However, the Acceptance Criteria for Prefabricated wood Shear Panels (ICC-ES, 2004) has not included the SPD protocol in its most recent revision.

2.3.3 ATC-24 PROTOCOL (1992)

In 1992, the Applied Technology Council (ATC) published the "Guidelines for Cyclic Seismic Testing of Components of Steel Structures", also called the ATC-24 guidelines (1992). Although specifically developed for steel structures, the protocol proposed in the above-mentioned document has been used by many researchers who have studied the cyclic behaviour of light framed shear walls (Krawinkler, 1996; Landolfo *et al.*, 2004). Based on Nassar's and Krawinkler's (1991) work, the displacement history prescribed under the ATC-24 protocol (Table 2-2 and Figure 2-3) follows a multiple step test (MST) pattern, which consists of stepwise increasing series of deformation cycles of constant maximum displacement amplitude (Krawinkler, 1996). Decaying cycles were not considered in the development of the ATC-24 guidelines because the primary intent of this loading pattern was to evaluate the sequence effect, i.e. the strength degradation observed at adjacent similar amplitude cycles.

Table 2-2 : Sequence of amplitudes for ATC-24 loading protocol

Cycles	Cycle Type	Amplitude (% δ_y)
1-3	Initiation	33%
4-6	Initiation	66%
7-9	Degradation	100%
10-12	Degradation	200%
13-15	Degradation	300%
16-17	Degradation	400%
18-19	Degradation	500%
20-	Continue pattern, i.e. increase previous degradation cycle amplitude by 100%	

The controlling deformation parameter in the case of the ATC-24 protocol is δ_y, which is the yield deformation deduced from measurements (obtained from prior testing) or predicted analytically (from non-linear analysis). The ATC-24 protocol has been superseded by the SAC Protocol (1997) standardized for cyclic testing of steel moment connections. This loading protocol, in which δ_y was replaced by the interstorey drift angle, defined as the interstorey lateral drift divided by the storey height, no longer requires that prior testing be carried out because specific drift based displacements specified by construction codes replace relative displacements. The displacement history is very similar to the original ATC-24 shown in Figure 2-3, except that additional initiation cycles are included at the beginning of the protocol.

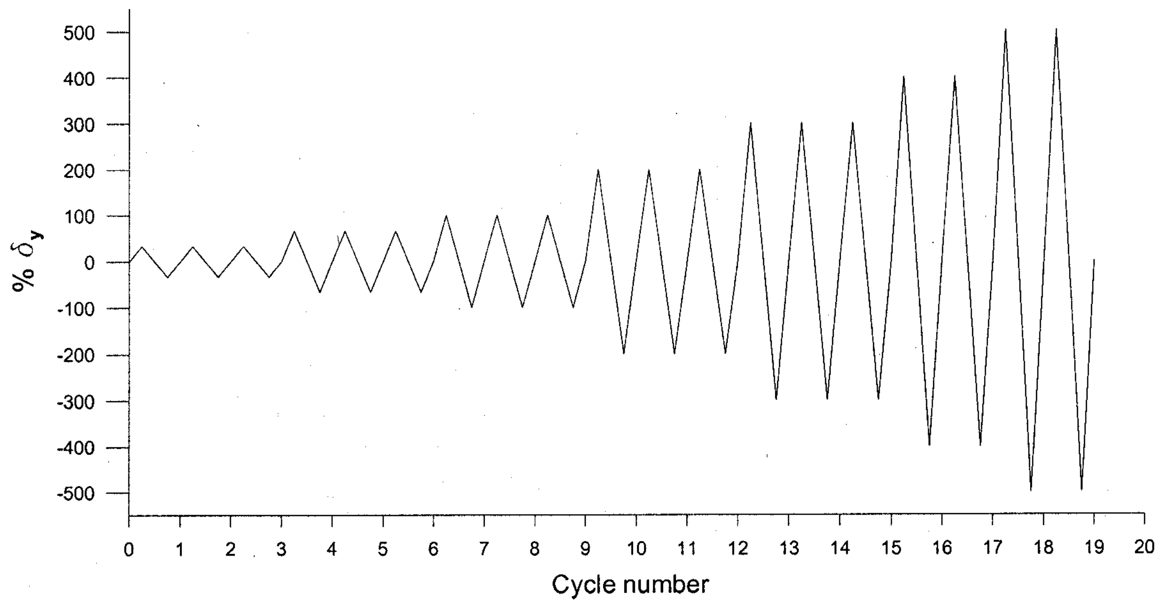

Figure 2-3 : ATC-24 Protocol Displacement History

2.3.4 ISO 16670 (INTERNATIONAL ORGANIZATION FOR STANDARDIZATION) (2002)

The International Organization for Standardization (ISO) developed a loading protocol under its Working Group 7 (Technical Committee on Timber Structures) following Foliente's (1994) observation that a universally used cyclic loading protocol will always be a compromise between a monotonic racking protocol and a fully reversed-cyclic protocol, such as the SPD protocol. The ISO Standard 16670 (ISO, 2002) is believed to be conservative for most practical cases (e.g. fastened timber joints and light framed shear walls as well).

The loading history (Table 2-3 and Figure 2-4) is a function of the ultimate displacement (v_u) obtained from prior monotonic tests on a matched group. The v_u value corresponds to the displacement at failure of the wall, which is defined by the displacement corresponding to 80% of the maximum load in the descending portion of the load-displacement curve.

Table 2-3 : Sequence of amplitudes for ISO 16670 Cyclic Protocol

Cycles	Cycle Type	Amplitude (% of v_u)
1	Initiation	1.25%
2	Initiation	2.5%
3	Initiation	5%
4	Initiation	7.5%
5	Initiation	10%
6-8	Degradation	20%
9-11	Degradation	40%
12-13	Degradation	60%
14-16	Degradation	80%
17-19	Degradation	100%
20-22	Degradation	120%
23-	Continue pattern, i.e. increase previous degradation cycle amplitude by 20% v_u	

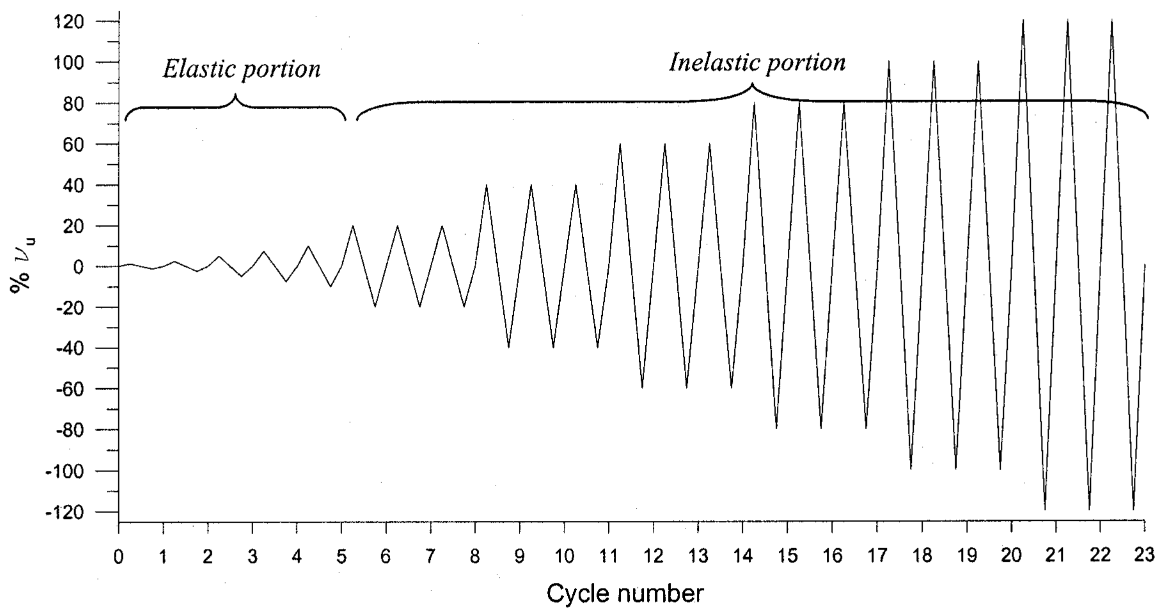

Figure 2-4 : ISO 16670 Protocol Displacement History

The loading history shown in Figure 2-4 consists of two distinct displacement patterns, so that sufficient data in the elastic and inelastic ranges are generated. The first displacement pattern constitutes five "elastic" reversed cycles of amplitudes of 1.25%, 2.5%, 5%, 7.5% and 10% of the ultimate displacement (v_u). In the second part of the protocol, inelastic groups of three symmetric cycles at displacements of 20%, 40%, 60%, 80%, 100% and 120% of the ultimate displacement (v_u) are imposed to the specimen in order to produce three envelope curves that may be used to evaluate strength degradation, ductility and yield displacement.

2.3.5 CUREE Ordinary Ground Motions Protocol (2000)

Among the four protocols developed as part of Task 1.3.2 of the CUREE (Consortium of Universities for Research in Earthquake Engineering) Woodframe Project, the Basic Loading History (Krawinkler *et al.*, 2000) is the displacement-controlled reversed cyclic protocol that is to be used to assess the performance of a structure subjected to an ordinary ground motions earthquake, i.e. not near-fault. The protocol was developed based on the statistical analysis of non-linear dynamic modeling of typical light framed wood buildings situated in California.

As in the case of the ISO Protocol, the reference deformation (Δ) necessary to calibrate the CUREE Basic Loading History protocol is derived from the ultimate resistance values evaluated with the help of prior monotonic tests. After performing a monotonic test and plotting the force-displacement curve, the monotonic deformation capacity (Δ_m) is found by determining the deformation at which the applied load reaches 80% of the peak lateral force on the descending segment of the force-displacement curve (Figure 2-5). Then, the equation:

$$\Delta = \gamma \Delta_m \qquad \textbf{(2-1)}$$

is applied to determine the reference deformation for the cyclic protocol. The factor γ accounts for the difference in deformation capacity between a monotonic test and a cyclic test and is suggested to be taken as 0.6 (Krawinkler *et al.*, 2000).

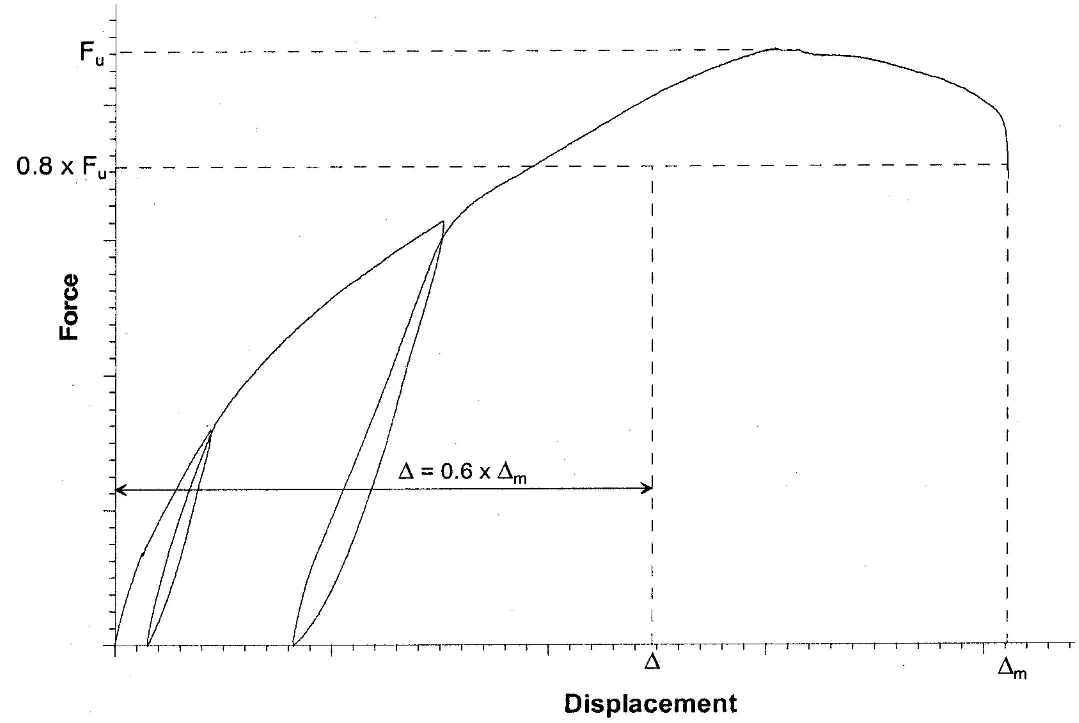

Figure 2-5 : Calculation of Δ and Δ_m for the CUREE Cyclic Protocol

The displacement history for a basic cyclic test should follow the pattern given in Table 2-4 and shown in Figure 2-6. The protocol involves displacement cycles increasing incrementally using the reference displacement (Δ), and consists of three types of cycles: initiation cycles, primary cycles and trailing cycles. The initiation cycles, executed at the beginning of the loading history, are of very low amplitude and are intended to simulate the effect of cumulative damage from possible past tremors. As well, this part of the protocol provides the experimentalist with an opportunity to check if the loading equipment and the measurement devices are working properly. Following the initiation cycles comes a single primary cycle, which reaches an amplitude higher than any previous cycles in the displacement history. Immediately afterwards, trailing cycles at 75% of the amplitude of the preceding primary cycle are imposed. This loading pattern is repeated until failure of the wall is observed.

Table 2-4 : Sequence of amplitudes for CUREE Cyclic Protocol

Cycles	Cycle Type	Amplitude (% of Δ)
1-6	Initiation	5%
7	Primary	7.5%
8-13	Trailing	5.625%
14	Primary	10%
15-20	Trailing	7.5%
21	Primary	20%
22-24	Trailing	15%
25	Primary	30%
26-28	Trailing	22.5%
29	Primary	40%
30-31	Trailing	30%
32	Primary	70%
33-34	Trailing	52.5%
35	Primary	100%
36-37	Trailing	75%
38-	Continue pattern, i.e. increase previous primary cycle amplitude by α ≤50%Δ and follow with two trailing cycles of 75% the amplitude of the primary cycle	

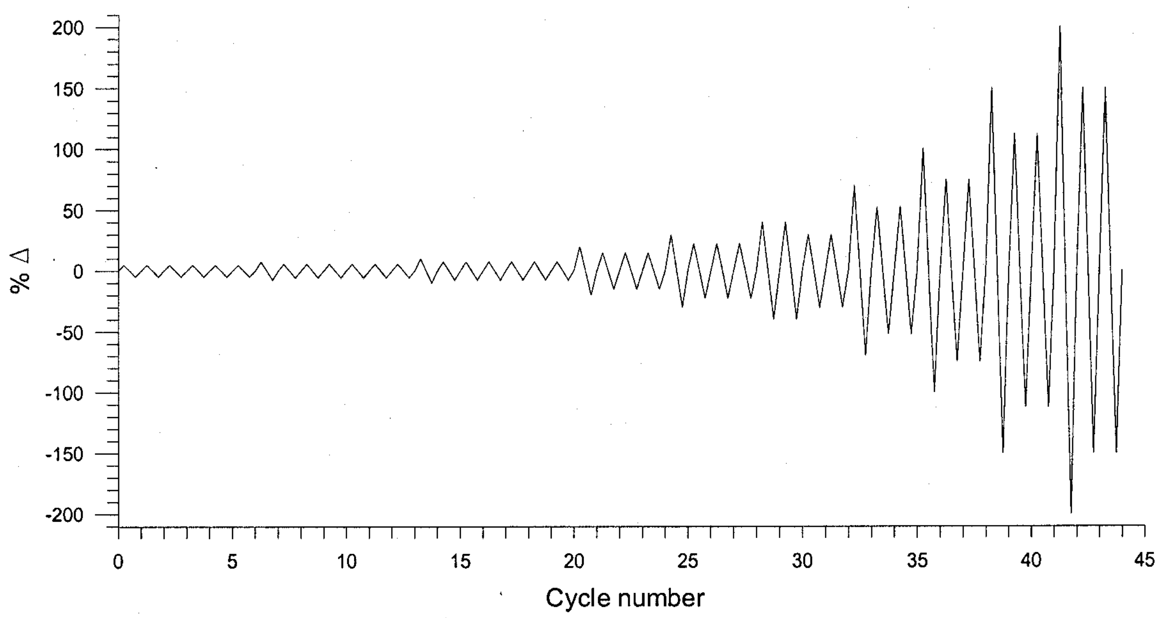

Figure 2-6 : Displacement history of CUREE Basic Loading Cyclic Protocol

2.4 *REVERSED CYCLIC PROTOCOL COMPARISON*

Karacabeyli and Ceccotti (1998)

Karacabeyli and Ceccotti explored the effects of different cyclic loading protocols on the response of shear walls composed of wood framing and plywood sheathing. Similarly built shear wall specimens of 4.88 m x 2.44 m (16' x 8') were tested using, among others, the SPD and the ISO protocols. Of interest was the ultimate load capacity, the displacement at ultimate load and the dissipated energy.

The shear fatigue failure of the nails was only observed under the SPD protocol. It was attributed to the high number of cycles and the corresponding high energy demand that ensues, as also experienced by Rose (1998). The ISO and the other protocols lead to a mix of nails pulling through the sheathing, nail withdrawal and nails tearing out the edges of the sheathing.

The ultimate load obtained from the specimen loaded with the ISO protocol was very similar to the ultimate load from the monotonic test (+3%), which allowed the authors to consider that monotonic testing could be used to determine the maximum design capacity. Tests performed under the SPD protocol produced a displacement at ultimate load that was significantly lower than all other tests (40% smaller than the monotonic displacement) and an energy demand that was radically higher than in the other cyclic tests. Karacabeyli and Ceccotti indicated that it would still be conservative to use the first envelope of the SPD hysteresis loops instead of the commonly used third envelope to obtain the design capacity. No explicit recommendations on which protocol to use were stated but many shortcomings of the SPD protocol were identified.

Dinehart and Shenton III (1998)

Dinehart and Shenton III investigated the relative performance of timber shear walls tested statically and dynamically[2]. Monotonic tests followed the ASTM E 564 protocol, whereas reversed cyclic tests were carried out using the SPD protocol with a FME of 6 mm (0.24"). More precisely, the purpose of this research was to evaluate and to compare the stiffness, ductility, ultimate load and failure mechanism of the walls for the two test methods. The testing program involved twelve identically constructed 2.4 m x 2.4 m (8' x 8') walls, four of which were tested monotonically and eight dynamically. Half of the specimens were sheathed with 11.9 mm (15/32") plywood and the other half with 12.7 mm (1/2") oriented strand board (OSB).

Previous research by He *et al.* (1998) concluded that the failure modes observed during static tests were significantly different than those of dynamic tests. Dinehart and Shenton III found the same results and noted that during the monotonic tests, the sheathing tended to pull away from the frame, pulling the nails along with it. Pull-through of the nails was only observed in a few instances along the edges of the sheathing. The bottom sill plate split parallel to the grain at the uplift corner, i.e. the corner in tension. Both the OSB and plywood sheathing failed in the same manner during the monotonic tests. As for the dynamic tests, most of the damage was concentrated in the sheathing-to-framing connectors. After being repetitively bent during the reversed cycles, nails either fatigued and/or sheared at the connection between the stud and the sheathing, or were pulled out from the stud. Nail fracture was more common than pull out. The OSB sheathed shear walls exhibited degradation near the corners in the later stages of the test, which was not observed in the tested plywood sheathed walls. Apart from that damage type, both OSB and plywood sheathed shear walls failed in a similar manner.

When comparing the load-deformation curves of the plywood and OSB sheathed specimens, Dinehart and Shenton III noted no major differences in either the monotonic

---

[2] Note: the dynamic tests that the authors refer to were actually quasi-static in nature

or cyclic regime. When looking at the static and dynamic responses of similarly sheathed shear walls, it was observed that both ultimate loads are comparable, but occurred at very different displacements, the dynamic tests having the lower displacements (66% less for plywood and 58% less for OSB). The dynamic ductility, defined as the ratio of the failure displacement to the yield displacement experienced under a dynamic test, was therefore less than the static ductility (34% reduction for plywood and 42% reduction for OSB). Dinehart and Shenton III were not able to conclude if these results were due to the rate of loading or the load history (cyclic protocol).

Because of the severe differences in the measured ductility between dynamic and static tests, Dinehart and Shenton III were in favour of the 25% reduction of the allowable shear loads listed in the UBC (*Uniform Building Code,* 1994) until more thorough research is carried out. This suggestion was made in the report *Findings and recommendation of the City of Los Angeles / SEASOC* (1994), where the task force investigating the Northridge earthquake recommended that a cyclic test program be carried out to determine reasonable load levels for light framed shear walls subjected to a seismic event.

Karacabeyli *et al.* (1999)

In a discussion of the paper by Dinehart and Shenton III (1998), Karacabeyli *et al.* revisited one of the conclusions, which stated that "the actual load factors[3] for a shear wall subjected to an earthquake will be significantly lower than the intended design". This statement is, according to Dinehart and Shenton III, verified if the fourth cycle envelope of the SPD protocol is used. However, Karacabeyli and Ceccotti (1998) stated that the load capacity under an earthquake of a light framed shear wall would be, in the worst case, comparable to the ultimate load obtained in the first cycle.

[3] Load factor = the ultimate load divided by the design allowable load

According to Karacabeyli *et al.*, the SPD loading protocol is not an earthquake simulation test, as it contains many more displacement cycles than would occur during a real seismic event. It was mentioned that it is desirable to utilize a testing protocol that would have similar velocity, energy demand and failure mode to that which would be expected in a real earthquake. The SPD protocol was found to have an energy demand three times greater than that associated with a typical earthquake. Karacabeyli *et al.* attributed the nail fatigue and nail shearing type of failures, which were not observed in shake table tests (Dolan, 1989) or in previous earthquakes, with this excessive energy demand. It was mentioned that an international effort would eventually lead to a widely recognized loading protocol, which would be more appropriate for the testing of light framed walls.

Heine (2001)

Before beginning his experimental testing program, Heine (2001) evaluated five cyclic loading protocols in order to select the most appropriate one. Only those that were considered to be relevant to the current study, the SPD and CUREE protocols, are presented in this Chapter.

In his review of the SPD protocol, Heine states that although the repetitive cycles at the same displacement level are useful to determine the stiffness degradation of the system and to assess a wall's structural performance after high wind events, they lead to an overestimate of the energy demand and thus to the fastener fatigue failure mode. Another drawback of the SPD protocol, according to Heine, is that the displacement history is based on the first major event (FME) displacement, or yield displacement, which, as opposed to idealized elastic plastic response of steel, is difficult to determine in the case of a sheathed stud shear wall.

Heine finally employed the CUREE protocol for his research program because of its scientific derivation, and the dependency of the displacement history on the ultimate displacement rather than the yield displacement. This made it less ambiguous and more adaptable in comparison with other standard protocols including the SPD and ISO.

Gatto and Uang (2002)

As part of Task 1.3.1 of the CUREE-Caltech Woodframe Project, a shear wall comparative testing program was carried out at the University of California in San Diego. The testing program involved 36 2.4 m x 2.4 m (8' x 8') wood framed wall specimens tested using different sheathing configurations, loading protocols and loading rates. This review will be focused on the findings of the CUREE study with respect to the different loading protocols.

Three different cyclic protocols, in addition to the monotonic protocol, were used to determine the loading protocol effect. The cyclic protocols were: CUREE Basic Loading Protocol, ISO cyclic protocol and finally the SPD protocol.

When comparing the backbone curves obtained from the reversed cyclic tests, the CUREE protocol produced results equivalent to that of the monotonic, especially for the positive excursions. The ISO protocol produced a lower capacity followed by a further reduced capacity for the SPD protocol (peak strength 20% lower than monotonic). As for the absorbed energy, it was stated by Gatto and Uang (2002) that it was directly dependent on the displacement history, the SPD protocol specimens being the ones that absorbed the greatest amount of energy due to the large number of cycles. The specimens tested using the CUREE and ISO protocols absorbed essentially the same amount of energy. As for the deformation capacities, the CUREE protocol lead to a deformation capacity similar to that produced by monotonic testing, followed by the ISO and SPD protocols respectively.

The researchers concluded that the loading protocols imposed on shear walls influence greatly their performance, and concluded that:

- The ISO protocol is simple and convenient to use, but the equal amplitude cycles exaggerate the demand imposed on the wall, leading to very conservative estimates of strength and ductility;
- The SPD protocol leads to fastener fatigue failures that are not representative of the demand imposed by a real seismic event. Gatto and Uang do not recommend the use of the SPD protocol for the cyclic evaluation of shear walls.
- The CUREE protocol produced strength and associated deformation similar to that of the monotonic tests. Because it has been developed especially for shear wall testing and the failure modes appear to be the most consistent with the ones observed during real earthquakes, the authors recommended that the CUREE protocol be established as the standard for future testing.

Salenikovich and Dolan (2003)

A comprehensive study that combined both experimental and numerical analyses of wood framed shear walls was undertaken by Salenikovich and Dolan to improve the understanding of shear wall performance. In a review of existing protocols, Salenikovich and Dolan mentioned that since the response of wood shear walls in the elastic range is strongly non-linear even at very low deflections, the magnitude of the first major event (FME) necessary for the SPD procedure is difficult to determine. It is reported that because researchers interpret the FME definition differently, values varying between 2.5 mm (0.1") (Jamieson, 1997) and 20.3 mm (0.8") (Serrette *et al.*, 1996 and 1997) have been used for similar wall assemblies.

A cyclic protocol, which is described as a hybrid of the SPD and ISO protocols, was used by Salenikovich and Dolan in order to obtain a response more similar to that observed during a monotonic test (Ceccotti, 1995; Daudeville *et al.*, 1998). This protocol was chosen because it was known that the use of the SPD protocol leads to cyclic responses with greatly reduced capacity and significantly decreased ductility due to the repetitive decay cycles, which lead to unrealistic energy demands (Dinehart and Shenton III, 1998;

Salenikovich *et al.*, 2000; Fulop and Dubina, 2004; Karacabeyli and Ceccotti, 1998). In brief, the decay cycles were eliminated from the standard SPD protocol, allowing for a significant reduction of the energy demand without affecting the wall response (Rose, 1998).

Although the energy demand imposed on a shear wall specimen by the modified SPD protocol was reduced compared with the original SPD protocol, some failure modes, such as nail fatigue were observed, that are typically present during monotonic tests and real earthquakes. It is recommended by Salenikovich and Dolan that for future research, importance is to be given to calibrate cyclic protocols with regards to reference displacements and the number of cycles that would represent more adequately deflections and energy demands imposed by an expected design level seismic event.

Landolfo *et al.* (2004)

The purpose of this experimental research on steel frame / wood panel shear walls was to generally evaluate the seismic response of a structural assembly, but more precisely to analyse the efficiency of the horizontal transfer from the floor to the vertical components and the effect of gravity load on the lateral response of shear walls. A database of 26 natural acceleration records was used to determine the possible deformation amplitudes of a cyclic loading protocol through a numerical analysis.

Two structural sub-assemblages, each of which was composed of two sheathed stud walls and a diaphragm acting as a roof, were tested. The first prototype was tested monotically and the second one was tested using a cyclic loading history inspired by the ATC-24. The amplitude reached during each cycle was defined such that the energy demand determined by the numerical analysis could be reproduced. The walls were designed according to capacity design principles, in order to develop the full shear resistance of the sheathing-to-framing fasteners, and not to fail other elements in the lateral load carrying path. The reversed cyclic loading protocol consisted of a series of multiple steps as described in the ATC-24 displacement history, with the exception that each displacement level was composed of three successive cycles. The reference displacement for the development of the cyclic test was taken as "the conventional yield limit state (YLS) displacement (d=6.0 mm (0.236"))". An explanation was not offered as to the selection of this displacement value.

A comparison between the response of the monotonic and cyclic tests revealed a reduced peak strength of 20% and 11% for the positive and negative excursions, respectively, when compared to the monotonic peak strength. These differences were probably due to the fact that the cyclic protocol used was very demanding in terms of energy when compared to a monotonic load regime, and therefore, a strength degradation was perceivable.

ASTM E 2126 (2005)

Standard reversed cyclic test methods were established by the Performance of Buildings Committee of ASTM to evaluate the shear stiffness, shear strength, and ductility of a shear wall assembly. It is specified that the standard is intended for shear wall specimens constructed from wood or metal framing with solid sheathing. The three recommended reversed cyclic loading protocols are the SPD, ISO 16670 and CUREE basic loading protocol. The recommended monotonic protocol is that documented by ASTM E 564.

The standard test method recommends the SPD protocol be used when a lower bound in displacement is required; that is, when increased hysteretic energy dissipation due to the presence of decay cycles occurs. An example where a lower bound displacement causing hysteretic energy dissipation may occur is a bolted connection through an over-drilled hole or any other slack system. Both the ISO and CUREE basic loading history protocols are said to adequately describe the elastic and inelastic cyclic properties of a shear wall, in addition to providing realistic failure modes expected during earthquake loading.

2.5 SUMMARY

In terms of the dynamic or seismic performance of shear walls, a synthesis of all previous research programs is difficult to accomplish and comparisons are usually not feasible because of the different test objectives, methodologies and load regimes that were employed by the different investigators. However, a main conclusion that can be drawn is that the majority of researchers are unanimous about the necessity to agree on a standard testing method in order to move forward in the area of shear wall research. Unfortunately, one aspect for which the researchers do not agree is in the selection of this cyclic standard. Dolan (1993) proposed to the American Society for Testing and Materials (ASTM) and the International Council for Building Research Studies and Documentation (CIB) the use of the SPD protocol. However, the SPD protocol is largely disputed as to its accuracy to represent the seismic demand on a light framed shear wall, as has been indicated in the preceding literature review. Although the repetitive cycles at the same displacement level are useful to determine the stiffness degradation of the system (Heine, 2001), many researchers have pointed out shortcomings of the SPD protocol:

1. The SPD protocol requires the evaluation of the yield displacement, or "first major event" (FME), which, because of the highly non-linear behaviour observed in the response, is very difficult to determine (Salenikovich and Dolan, 2003; Karacabeyli and Ceccotti, 1998; Heine, 2001). Researchers have used FME values ranging from 2.54 mm (0.1") to 20.3 mm (0.8") for similar wall assemblies, illustrating the difficulty in defining and determining an accurate FME value (Jamison, 1997; Serrette *et al.*, 1996 and 1997) ;
2. The energy demand imposed on a shear wall specimen tested using the SPD protocol was found to be three times higher than during a real major earthquake (Karacabeyli and Ceccotti, 1998; Rose, 1998), which leads to unrealistic modes of failure such as fastener fatigue. The modes of failure that have been observed following real earthquakes, such as Northridge, were fastener withdrawal or pull-through, but not fastener fatigue (Dinehart and Shenton III, 1998; He *et al.*, 1998);

3. The wall capacity observed during tests using the SPD protocol was reduced when compared to the monotonic response (Fulop and Dubina, 2004; Salenikovich *et al.*, 2000) which does not comply with the statement made by some researchers (Ceccotti, 1995; Daudeville *et al.*, 1998) that the backbone curve of a cyclic response should coincide with the monotonic load-deformation curve. Ductility was also found to be significantly decreased during the SPD test relative to the monotonic test (Dinehart and Shenton III, 1998).

Although fewer researchers mention the CUREE loading protocol, likely because of its recent development, it was found to be adequate for the testing of light framed shear walls because of its accurate scientific derivation from actual earthquake demands and its displacement history, which is based on a measure of the ultimate displacement rather than yield displacement (Heine, 2001). Also, cumulative damage concepts were used in the transformation of the time history responses into representative displacement history, which is more representative of the demand imposed on light frame structures during a seismic event (Krawinkler *et al.*, 2000). However, the noticeable drawbacks are that all the natural acceleration records used in the development of the loading regime were from the Los Angeles area and are therefore not representative of the possible seismic events that could occur elsewhere. Also, the protocol represents an ordinary ground motion whose probability of exceedance in 50 years is 10%, which does not comply with the recent recommendations, notably the seismic provisions of the 2005 Edition of the National Building Code of Canada (NRCC, 2004) which were developed for a design level earthquake having a 2% in 50 years probability of exceedance.

A comparative analysis of two cyclic protocols (a revised version of the ATC-24 by Serrette *et al.* (2002) and the CUREE Ordinary Ground Motions Cyclic protocol) is presented in Chapter 3 in order to determine which is most appropriate for the seismic evaluation of steel frame / wood panel shear walls. The choice of protocol was in part based on the information documented in the reports and papers reviewed in this Chapter.

CHAPTER 3

TEST SPECIMENS AND PROCEDURES

3.1 TEST FRAME SETUP AND BACKGROUND INFORMATION

In order to evaluate the performance of steel frame / wood panel shear wall test specimens, a self-equilibrating test frame was installed in the Jamieson Structures Laboratory of McGill University during the summer of 2002 (Figures 3-1 and 3-2). Designed by Zhao (2002), this test frame is currently equipped with a 250 mm (10") (± 125 mm (± 5")) stroke dynamic actuator and a 250 kN (55 kip) load cell. Its design allows for the installation of a 500 kN (110 kip) load cell and actuator, as well as an increased top of the wall displacement by lowering the actuator on the pinned column while maintaining the load cell height. Lateral movement of a test wall is restrained by the vertically positioned HSS braces. For more details about the design of the frame, refer to Zhao (2002).

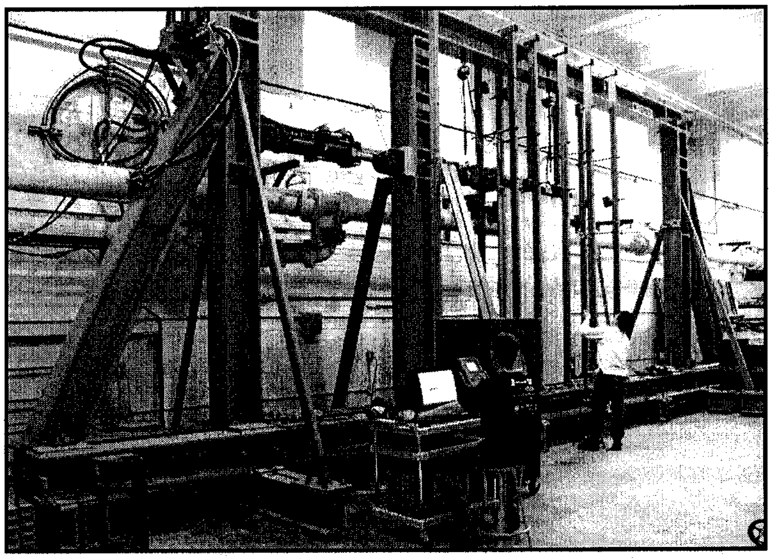

Figure 3-1: Shear Wall Test Frame

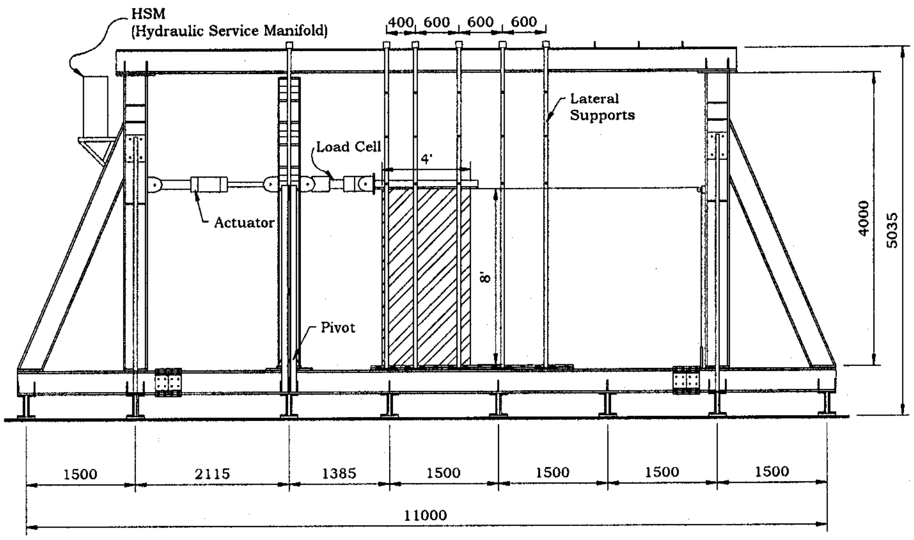

Figure 3-2: Schematic of Shear Wall Test Frame (Elevation)

A preliminary series of 12 test specimens was completed in the Fall of 2002. The scope of testing included specimens to match those carried out by Serrette *et al.* (1996) and COLA-UCI (2001), i.e. they were built with similar materials obtained from the US and loaded with the same monotonic and cyclic protocols as used in the original tests. It was possible to evaluate the functionality of the test frame by comparing the obtained wall responses with the existing data. Table 3-1 outlines the preliminary testing program carried out.

Table 3-1: Preliminary Testing Program to Match US Tests

Match Tests	Original Tests	Sheathing	Wall Size	Screw Pattern	Loading
OSB 4-8 US M-A,B,C	Serrette *et al.* (1996) OSB – 1D3,4	OSB [1]	1220mm x 2440mm	102mm / 305mm	Monotonic [3]
OSB 4-8 US C-A,B,C	Serrette *et al.* (1996) AISI OSB 3,4	OSB	1220mm x 2440mm	102mm / 305mm	Reversed [4] Cyclic
PLY 8-8 US M-A,B,C	Serrette *et al.* (1996) PLY-1A6,7	Plywood [2]	2440mm x 2440mm	152mm / 305mm	Monotonic
PLY 8-8 US C-A,B,C	COLA-UCI (2001) Group 14	Plywood	2440mm x 2440mm	152mm / 305mm	Reversed Cyclic

[1] OSB 11mm (7/16") APA Rated 24/16, Sheathing Exposure 1, Oriented Parallel to Framing;
[2] Plywood 12mm (15/32"), APA Rated 32/16, 4-ply Sheathing Exposure 1, Oriented Parallel to Framing;
[3] See Section 3.2.3 for a description of the monotonic protocol;
[4] Sequential Phased Displacement (SPD) (Porter 1987), 58 cycles version for OSB tests and 72 cycles version for PLY tests.

A comparison of the match test results with the control group revealed some differences, particularly concerning the stiffness of the walls. It was concluded that the discrepancy of the displacement at ultimate load between the match tests and the control group was due to the installation method utilized for the hold-downs. A variation in the results could also be attributed to inconsistent material properties between the match specimens and the control group. As a result of this preliminary testing experience, minor modifications were made to the lateral bracing system and installation procedure used for the hold-downs prior to the testing of the walls. A more detailed description and analysis of this preliminary testing program can be found in Branston *et al.* (2003).

3.2 STEEL FRAME / WOOD PANEL SHEAR WALLS TESTING PROGRAM

It was originally planned for the main testing program to include 100 shear wall specimens to be tested during the summer of 2003. Variations in the specimen configurations included wall dimensions, fastener schedule and sheathing type. For the majority of the shear wall configurations, three monotonic and three cyclic tests were carried out to ensure a minimum level of reliability / validity of the test data. In some cases, however, additional specimens had to be built and tested because differences in the measured response of the three nominally identical walls were greater than 10%. A total of 109 steel frame / wood panel shear walls were eventually included in the scope of this research, of which the author was responsible for the testing and data interpretation of 20 tests.

3.2.1 TEST MATRIX

The objective of the first 13 shear wall specimens tested by the author was primarily to determine which cyclic protocol to use for the remainder of the testing program. An additional wall configuration that consisted of Douglas Fir Plywood (DFP) (Groups 5 and 6) was also part of the author's research. Table 3-2 lists the details of wall specimens tested by the author, while Table 3-3 provides information on wall specimens included in the main test program but carried out by Branston (2004) and Chen (2004).

Table 3-2: Detailed Test Program Matrix

Specimen	Protocol	Wall Length (mm)	Wall Height (mm)	Sheathing Type	Sheathing Thickness (mm)	Fastener Schedule (mm)
1 – A,B,C	Monotonic [1]	1220	2440	CSP	12.5	102 / 305 [5]
1 – D,E,F	Monotonic	1220	2440	CSP [6]	12.5	102 / 305
2 – A	Cyclic [2]	1220	2440	CSP	12.5	102 / 305
3 – A,B,C	SPD [3]	1220	2440	CSP	12.5	102 / 305
4 – A,B,C	CUREE [4]	1220	2440	CSP	12.5	102 / 305
5 – A,B,C,D	Monotonic	1220	2440	DFP	12.5	102 / 305
6 – A,B,C	CUREE	1220	2440	DFP	12.5	102 / 305

[1] See Section 2.2.1 for a description of the monotonic protocol;
[2] Reversed cyclic test (small cycles) to determine the FME (First Major Event) for the SPD protocol;
[3] Serrette-SPD (2002) reversed cyclic protocol (see Section 3.3.1 for a detailed description);
[4] CUREE reversed cyclic protocol for ordinary ground motions (see Section 2.2.5 for a detailed description);
[5] Fastener Schedule (e.g. 102 / 305) refers to the spacing in millimetres between sheathing to framing screws around the edge of the panel and along intermediate studs (field spacing) respectively;
[6] CSP sheathing from Mill BC858 (Richply) was used, whereas panels from Mill AB244 (Alberta Plywood) were used for the remainder of CSP test specimens.

As noted in Table 3-2, wall configuration (1) required six monotonic tests instead of the usual three because the first three tests (A,B,C) resulted in unexpected stiffness values when compared to the cyclic series of the same configuration and to the walls in Groups 7, 8, 9 and 10 (Branston, 2004). These were the first tests that were carried out, and it is likely that inconsistency of the tightness of the anchor rods for the hold-downs could explain the difference in stiffness values. The second group (2), which consisted of a single reversed cyclic test, was necessary to determine the first major event (FME) for the Serrette *et al.* (2002) sequential phased displacement (SPD) tests (refer to Chapter 2 for more details). An additional test was also required for Group 5 because of the variation (>10%) in the measured ultimate capacity of the walls.

Table 3-3: Additional Wall Configurations Included in Main Test Program

Group ID[1]	Wall Dimensions (mm)	Sheathing Type	Fastener Schedule (mm)	Author
7, 8	1220 x 2440	CSP 12.5 mm	152 / 305	Branston (2004)
9, 10	1220 x 2440	CSP 12.5 mm	76 / 305	"
11, 12	1220 x 2440	DFP 12.5 mm	152 / 305	"
13, 14	1220 x 2440	DFP 12.5 mm	76 / 305	"
15, 16	610 x 2440	CSP 12.5 mm	152 / 305	Chen (2004)
17, 18	610 x 2440	CSP 12.5 mm	102 / 305	"
19, 20	610 x 2440	OSB 11 mm	152 / 305	"
21, 22	1220 x 2440	OSB 11 mm	152 / 305	Branston (2004)
23, 24	1220 x 2440	OSB 11 mm	102 / 305	"
25, 26	1220 x 2440	OSB 11 mm	76 / 305	"
27, 28	610 x 2440	OSB 11 mm	102 / 305	Chen (2004)
29, 30	2440 x 2440	CSP 12.5 mm	152 / 305	"
31, 32	2440 x 2440	CSP 12.5 mm	102 / 305	"
33, 34	2440 x 2440	CSP 12.5 mm	76 / 305	"

[1] Odd numbers represent monotonic testing, and even numbers represent CUREE cyclic protocol testing

3.2.2 Specimen Fabrication, Instrumentation and Test Setup

This section contains an overview of the specimen fabrication and the general testing setup used throughout the testing program. A more detailed step-by-step description of the shear wall fabrication and test setup can be found in Branston (2004).

The walls were fabricated from a combination of the following materials and components:

i. Wall sheathing on one side only, oriented vertically (strong axis or face grain parallel to framing), consisting of either 12.5 mm CSA O151 (1978) Canadian Softwood Plywood (CSP) sheathing or 12.5 mm CSA O121 (1978) Douglas Fir Plywood (DFP) sheathing (Figure 3-3) ;
ii. 92.1 x 41.3 x 12.7 mm (3-5/8" x 1-5/8" x 1/2") light gauge steel studs and 92.1 x 31.8 mm (3-5/8" x 1-1/4") light gauge steel tracks manufactured in Canada to ASTM A653 (2002) with nominal grade and thickness of 230 MPa (33 ksi) and 1.12 mm (0.044"), respectively. Studs were spaced at 610 mm (24") on centre;
iii. Back-to-back chord studs connected by two No. 10 x 19.1 mm (3/4") long Hex head self-drilling screws (Figure 3-4) at 305 mm (12") on centre to increase compression capacity;

iv. Simpson Strong-Tie® S/HD10 hold-down connectors (Simpson 2001) (Figure 3-5) connected to the back-to-back chord studs with 33 No. 10 x 19.1 mm (3/4") long Hex washer head self-drilling screws (Figure 3-4). An ASTM A307 (2000) 22.2 mm (7/8") diameter threaded anchor rod was used to transfer the uplift force from the tension chord / hold-down to the test frame (acting as the foundation);

v. 19.1 mm (3/4") diameter ASTM A325 (2002) bolts were used as shear anchors;

vi. No. 8 x 12.7 mm (½") long wafer head self-drilling framing screws (Figure 3-4) to connect the track and studs;

vii. No. 8 x 38.1 mm (1-½") long grabber SuperDrive® bugle head self-piercing sheathing screws (Figure 3-4) installed at an edge distance of 12.7 mm (½"). Screw spacing along the edges of the walls was 102 mm (4") and field screw spacing was 305 mm (12");

viii. No. 9 x 25.4 mm (1") long bugle head screws were needed at the lower corners of the shear walls where the hold-downs were installed to replace the No. 8 x 38.1 mm (1-½") screws that were too long.

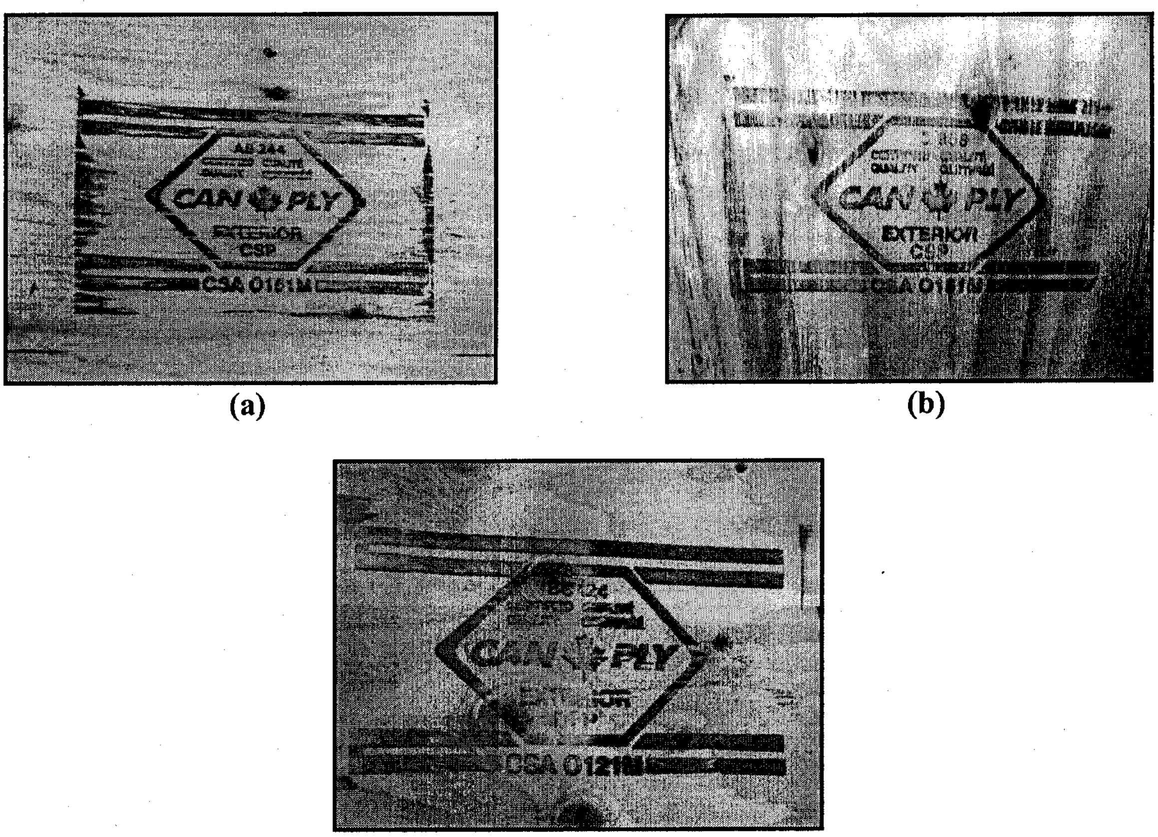

(a) (b)

(c)

Figure 3-3 : Panel Markings of (a) Alberta Plywood CSP (Mill: AB 244) ; (b) Richply CSP (Mill: BC 858) ; (c) Riverside DFP (Mill: BC 124)

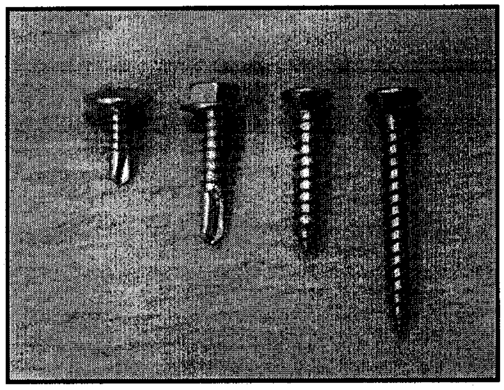

Figure 3-4: Screw Fasteners (left to right); No. 8 x 12.7 mm (1/2") wafer head framing screw, No. 10 x 19.1 mm (3/4") Hex washer head self-drilling screw, No. 9 x 25.4 mm (1") bugle head self-piercing sheathing screw and No. 8 x 38.1 mm (1-1/2") bugle head self-piercing sheathing screw

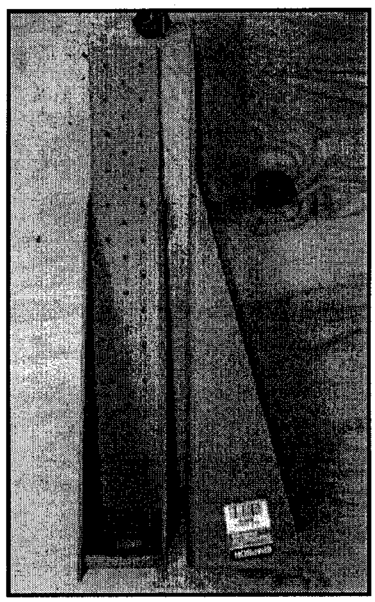

Figure 3-5: Simpson Strong-Tie S/HD10 hold-downs

Once each shear wall had been built, it was mounted into the test frame and attached to the loading beam and test frame base as shown in Figure 3-6. A 1" (25.4 mm) spacer plate was positioned both above and below the wall to allow the sheathing to rotate freely relative to the framing. The 7/8" ASTM A307 threaded anchor rods were placed through the Simpson Strong-Tie® hold-downs to transfer tension forces and to limit the global overturning under lateral loading (Figure 3-7). The hold-down anchor rods were first finger tightened until snug and then an additional half turn of the nut was completed using a wrench. Anchors were placed in the top and bottom tracks to transfer shear forces from the wall to the supporting test frame, acting as a floor and/or foundation. The top of the wall was bolted with six 3/4" diameter ASTM A325 bolts in order to uniformly apply the shear force from the loading beam over the entire length of the wall. Both the bottom and top shear anchors were tightened using an electric impact wrench. Steel plate washers 3/16" x 2.5"x 2.5" (4.8 x 63.5 x 63.5 mm) were placed at these shear anchor locations.

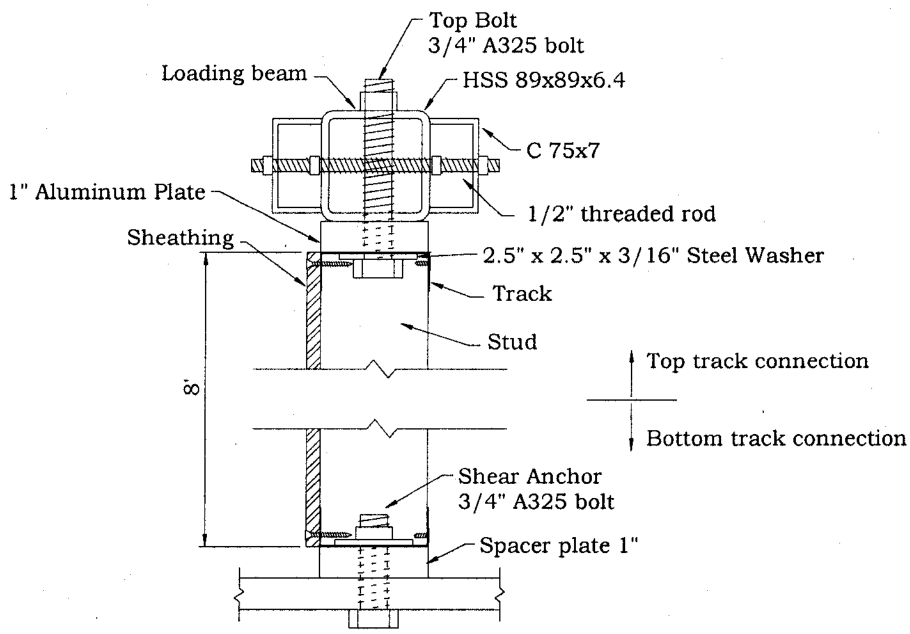

Figure 3-6: Top and Bottom Shear Wall Connection to the Testing Frame

In total, 12 Linear Variable Differential Transducers (LVDT), five load cells and an accelerometer (for cyclic tests only) were needed in the monitoring of the response of a 4'x8' shear wall. Nine of the twelve LVDTs were positioned directly on the wall as shown in Figure 3-8 and another was built-in to the actuator. The remaining two LVDTs were placed on lateral braces on each side of the wall to monitor the out-of-plane movement. The load applied to the shear wall specimen was measured using the 250 kN main load cell which was mounted in line with the actuator (Figure 3-2). An accelerometer was attached adjacent to the main load cell. Measurements from load cells that were placed at each hold-down and shear anchor location were found to be erroneous and therefore were not considered.

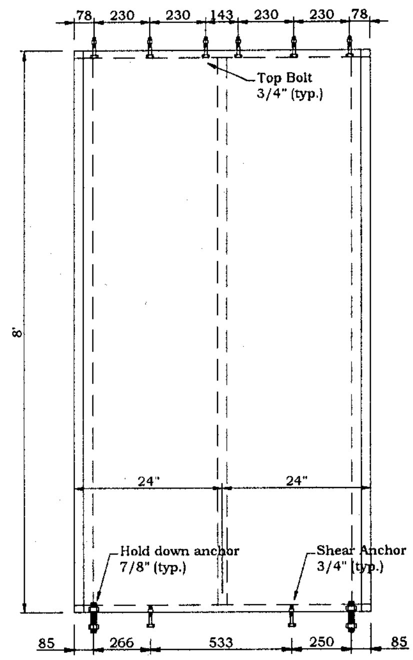

Figure 3-7: Hold-downs, Shear Anchors and Top Bolt Locations on a 4' Shear Wall

Measurement devices (LVDTs, load cells and accelerometer) were then connected to Vishay® scanners (Model 5100B) which in turn were connected to a computer running the Vishay® System 5000 StrainSmart software. Data were either recorded at 2 scans per second for monotonic tests or at 50 scans per second for cyclic tests.

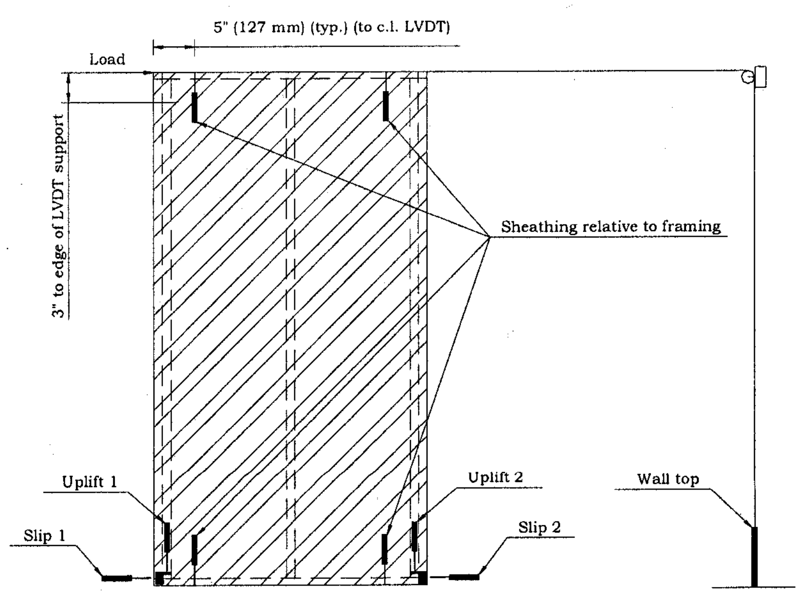

Figure 3-8: Positioning of LVDTs for 4'x8' wall specimen

3.3 *COMPARATIVE TESTS TO DETERMINE CYCLIC PROTOCOL*

The loading protocol can affect the performance of a test wall, and hence influence the design values obtained from test results. This being said, it is important that the loading protocol reflects as much as possible the expected demand on a light gauge steel frame / wood panel shear wall in a design level earthquake. In order to select the best suited cyclic protocol amongst those itemized in Chapter 2, the author pre-selected two protocols (Serrette-SPD (2002) and CUREE) that have been recently used in other shear wall research programs. The suitability and applicability of these two cyclic protocols for steel frame / wood panel shear walls was identified by using them in the testing of nominally identical wall specimens (3A,B,C and 4A,B,C). A comparison of the measured response of the test walls was then completed. The criteria for selecting the protocol to be used for the remainder of cyclic tests were based on the energy demand imposed on the specimens, the general scientific background of the protocols and a comparison between the monotonic response and the cyclic response, which are expected to be similar, as discussed in Chapter 2.

3.3.1 PROTOCOLS USED IN THE COMPARATIVE TESTING PROGRAM

In the comparative testing program the SPD reversed cyclic protocol that was adapted by Serrette (2002) was applied to tests 3-A,B,C, and the CUREE Ordinary Ground Motions reversed cyclic protocol (Krawinkler *et al.*, 2000) (see Section 2.2.5) was applied to tests 4-A,B,C. Since both protocols require the results of prior tests to determine the displacement history, test series 1 (A,B,C) and 2-A were carried out beforehand. A typical shear wall configuration was used for testing, i.e. a 4' x 8' (1220 mm x 2440 mm) wall sheathed with Canadian Softwood Plywood (CSP) and fastened with sheathing screws spaced at 4" (101.6 mm) along the panel perimeter and at 12" (304.8 mm) in the panel interior.

In order to utilize the Serrette-SPD protocol with the steel frame / wood panel shear wall specimens described above, the first major event (FME) had to be determined. To do so, a shear wall specimen (Test 2-A) was subjected to a special reversed cyclic protocol with which the displacement level associated with the first change in limit state could be identified, i.e. the displacement at which a 5% decrease in the capacity was observed between the first and third cycle at the same displacement level. This protocol consisted of multiple series of three identical displacement cycles starting at an amplitude of 2.5 mm. The displacement amplitude for each subsequent series was increased by 2.5 mm (Figure 3-9). Following the execution of this small cycles protocol, a FME of 20 mm (0.79") was identified and used in the development of the Serrette-SPD protocol. Table 3-4 and Figure 3-10 illustrate the displacement history of the Serrette-SPD protocol that was applied to tests 3-A,B,C. Note that in Table 3-4, the "actuator input" column differs from the "target" displacements because of corrections that are made to account for the uplift and slip of the specimen (Section 3.4.1), as well as the vertical movement of the actuator. A linear relationship between the "actuator input" and "target" displacement was obtained from the monotonic test data. The tests were displacement controlled at a frequency of 0.5 Hz, changing to 0.25 Hz after 350% of FME.

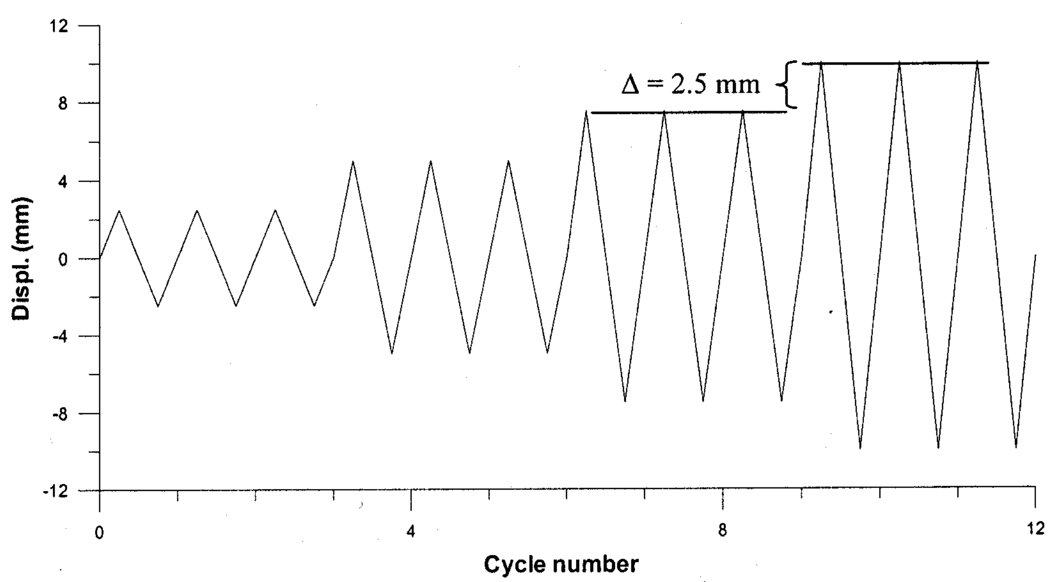

Figure 3-9 : Displacement time history for Test 2A for FME determination of SPD loading protocol

Table 3-4 : Sequence of displacements used for the Serrette-SPD (2002) reversed cyclic loading protocol (Tests 3-A,B,C)

FME =	20.0mm	Screw Pattern:	102/305 mm

	Target (corr.)	Actuator Input	
Displ. (% FME)	mm	mm	No. Of cycles
25%	5.0	7.04	3
50%	10.0	13.38	3
75%	15.0	19.27	3
100%	20.0	25.16	3
125%	25.0	31.18	3
150%	30.0	36.96	3
175%	35.0	42.62	3
200%	40.0	48.33	3
225%	45.0	54.07	3
250%	50.0	60.08	3
275%	55.0	65.82	3
300%	60.0	71.43	3
325%	65.0	76.92	3
350%	70.0	82.35	3
375%	75.0	87.76	3
400%	80.0	93.08	3
425%	85.0	99.03	3
450%	90.0	104.40	3

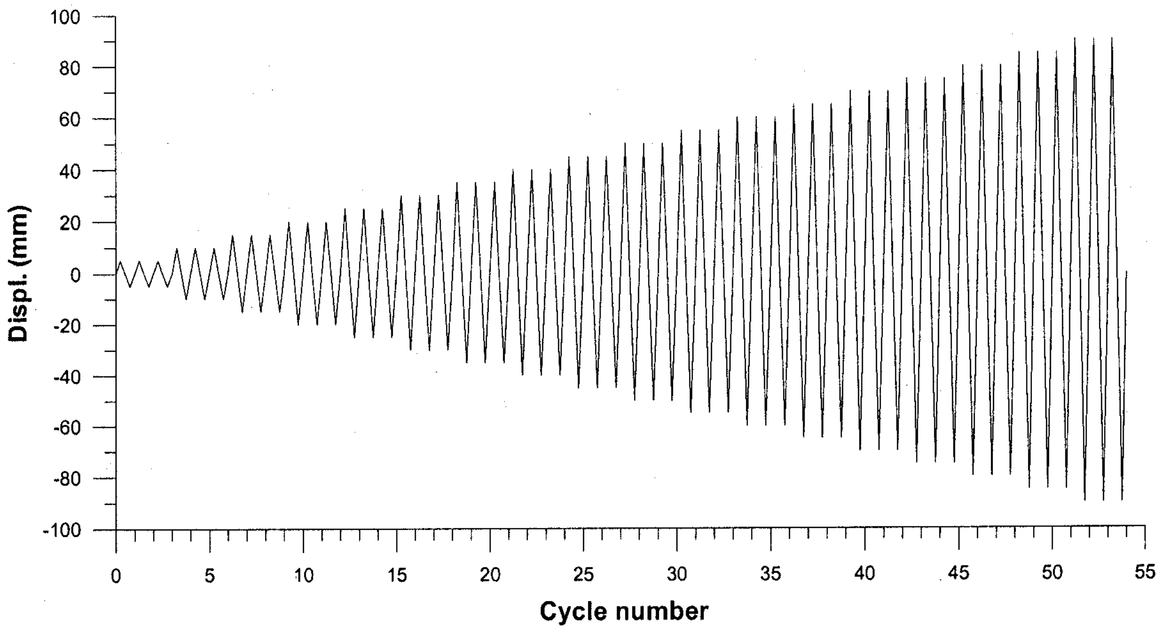

Figure 3-10 : Displacement history for Serrette-SPD (2002) reversed cyclic loading protocol with FME = 20mm (0.79")

The second reversed cyclic protocol considered for the comparative testing program was the CUREE Ordinary Ground Motions (Basic Loading History) protocol developed by Krawinkler *et al.* (2000) and presented in Section 2.2.5. Prior testing was also needed to evaluate the reference displacement (Δ). In this case the results of the monotonic tests were sufficient (tests 1A,B,C) to establish a value for the reference displacement. Table 3-5 and Figure 3-11 illustrate the displacement history of the protocol used for tests 4-A,B,C. The CUREE protocol is also displacement controlled and the frequency used was 0.5 Hz.

Table 3-5 : Sequence of displacements for the CUREE reversed cyclic loading protocol (Tests 4-A,B,C)

$\Delta=0.6*\Delta_m$ =	46.78mm	Screw Pattern:	102/305 mm

	Target (corr.)	Actuator Input	
Displ.	mm	mm	No. Of cycles
0.050 Δ	2.339	3.824	6
0.075 Δ	3.509	5.590	1
0.056 Δ	2.632	4.270	6
0.100 Δ	4.678	7.278	1
0.075 Δ	3.509	5.590	6
0.200 Δ	9.357	13.241	1
0.150 Δ	7.018	10.418	3
0.300 Δ	14.035	18.835	1
0.225 Δ	10.526	14.658	3
0.400 Δ	18.713	24.405	1
0.300 Δ	14.035	18.835	2
0.700 Δ	32.748	40.980	1
0.525 Δ	24.561	31.587	2
1.000 Δ	46.783	57.318	1
0.750 Δ	35.088	43.668	2
1.500 Δ	70.175	84.002	1
1.125 Δ	52.631	64.251	2

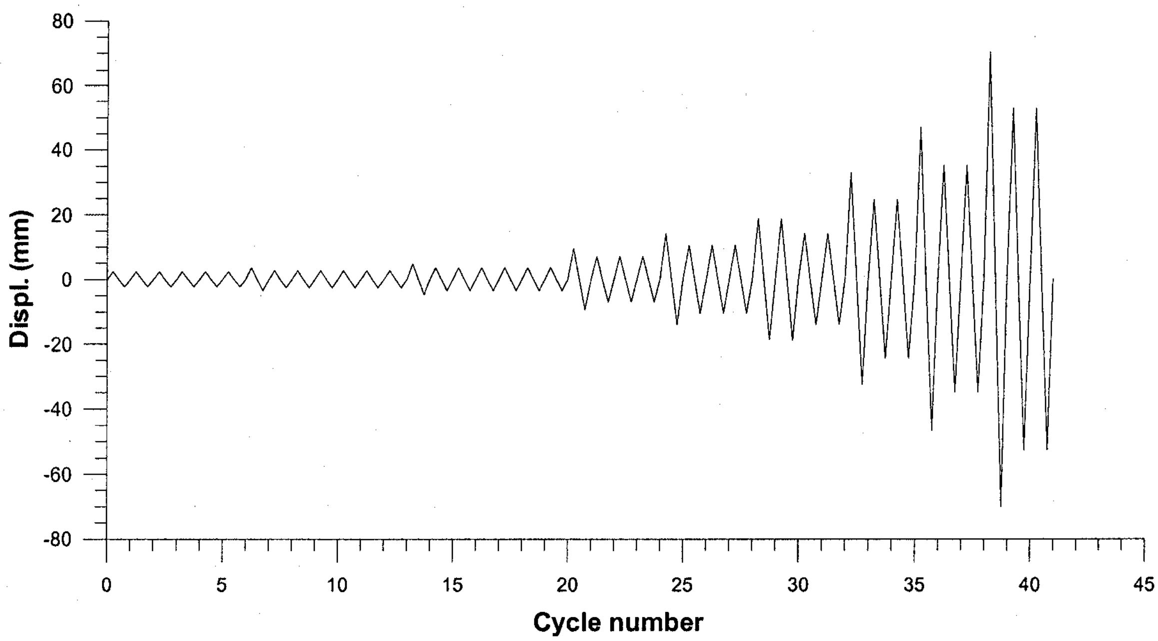

Figure 3-11 : Displacement history for the CUREE reversed cyclic protocol with Δ=46.78 mm (1.84")

3.3.2 COMPARISON OF MEASURED CYCLIC RESPONSE

Figures 3-12 and 3-13 present typical responses obtained for both the Serrette-SPD and CUREE cyclic protocols. The monotonic load-deformation curve from a nominally identical specimen is superimposed in order to appreciate the difference in shear resistance and displacement level. From Figure 3-12 the difference in capacity between the Serrette-SPD and monotonic protocols is evident. The monotonic response reaches a significantly higher shear capacity as the corrected displacement extends above 40 mm. The displacement at which the ultimate shear resistance occurs is also larger for the monotonic response. In the case of the CUREE tests (Figure 3-13), a better match of the monotonic response with respect to the cyclic load-deformation curve is observed, that is both the ultimate capacity and corresponding displacement are comparable.

Table 3-6 contains a listing of monotonic and cyclic (Serrette-SPD and CUREE) test results and expresses the differences in percentage. As for the dissipated energy, a direct comparison with the monotonic test is not possible due to the repeated cycles of the Serrette-SPD and CUREE protocols compared to a single excursion in the case of the monotonic test. It is however possible to compare the energy under the backbone curves for the cyclic tests with the energy dissipated by the monotonic tests (see Table 3-6, Backbone Energy column). For this interpretation of energy comparisons, the CUREE protocol results are comparable to the monotonic results.

The total dissipated energy for the specimens tested with the Serrette-SPD protocol is 2.5 times greater than the dissipated energy for the shear walls loaded with the CUREE protocol. In a similar comparison of the SPD and CUREE protocols on wood framed shear walls, Gatto and Uang (2002) also noticed that the SPD protocol lead to a much higher quantity of dissipated energy (2.1 times greater) than the CUREE loading protocol, and therefore concluded that the SPD loading protocol lead to an exaggerated amount of dissipated energy when compared with a real seismic event (Gatto and Uang, 2002; Karacabeyli and Ceccotti, 1998; Rose, 1998).

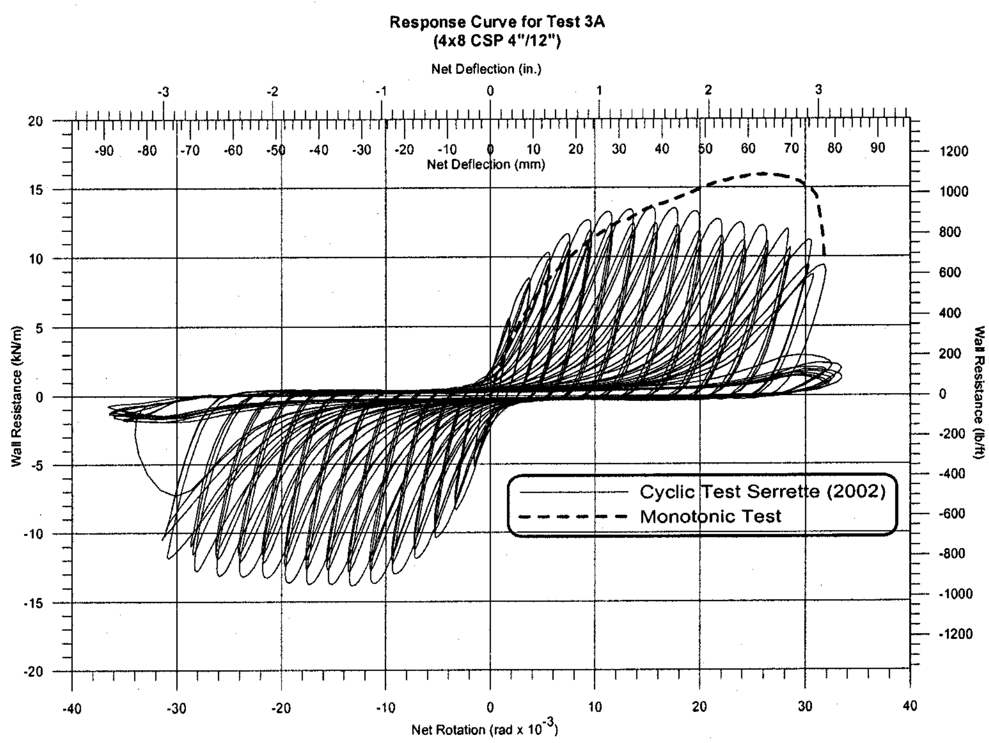

Figure 3-12 : Typical responses of specimen loaded with Serrette-SPD (2002) and monotonic protocols

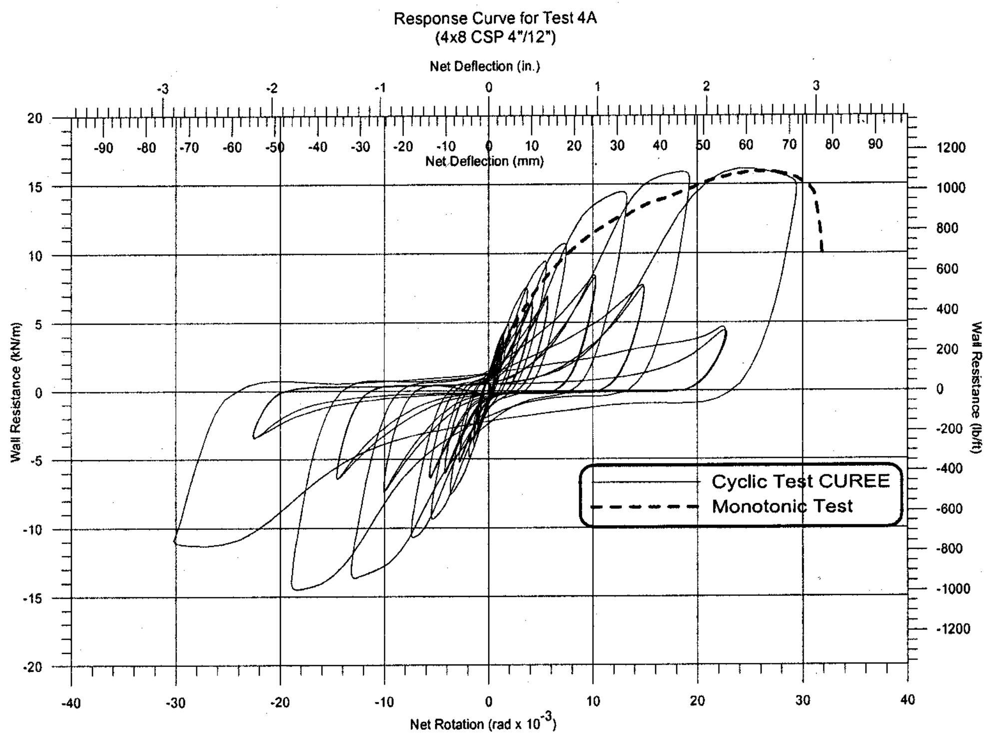

Figure 3-13 : Typical responses of specimen loaded with CUREE and monotonic protocols

Table 3-6 : Comparison of characteristics obtained from monotonic and cyclic tests

Shear wall test results									
Specimen	Max. Wall Resistance +ve cycle (S_{u+}) kN/m	Max. Wall Resistance -ve cycle (S_{u-}) kN/m	Mono vs Cyclic %	Disp. At S_u +ve cycle ($\Delta_{net,u+}$) mm	Disp. At S_u -ve cycle ($\Delta_{net,u-}$) mm	Mono vs Cyclic %	Energy Dissipation (E) Joules	Backbone Energy (E_+) Joules	Mono vs Cyclic %
Monotonic (Test Group 1)	16.6			60.6			1200	1200	
SPD (Test Group 3)	13.9	-14.0	**16%**	40.0	-37.4	**36%**	12229	1010	**16%**
CUREE (Test Group 4)	17.5	-15.3	**1%**	56.8	-44.0	**17%**	4941	1211	**1%**

3.3.3 CYCLIC PROTOCOL SELECTION

Following the comparative analysis, the CUREE Ordinary Ground Motions (Basic Loading History) was selected as the reversed cyclic protocol to be used in the scope of this research. This also includes the shear wall tests by Branston (2004) and Chen (2004). Even though both protocols share many similarities like their type of control (displacement control) and symmetrical reversed amplitudes, the CUREE protocol was found to be more suitable for the testing of steel frame / wood panel shear wall specimens for three main reasons:

1. The CUREE protocol was developed from the results of non-linear dynamic time history analyses of wood frame shear wall structures, and hence, in comparison to the Serrette-SPD protocol, was considered to be more representative of the demand that would be imposed on the steel frame / wood panel shear wall building component during an earthquake on the west coast of the North American continent. It is assumed that the overall resistance vs. deflection hysteretic behaviour of a light gauge steel framed shear wall is very similar to that of an all wood wall, mainly because of the important role that the wood sheathing and its connections play in the overall shear wall behaviour;
2. The CUREE protocol uses an estimate of the post ultimate failure load ($0.8S_u$) of a shear wall (which is easily obtained from a simple monotonic test) in order to develop its loading history, compared with a first major event (FME) displacement level for the Serrette-SPD protocol. Because of the highly non-linear behaviour observed in the response, it is very difficult to determine the FME (Salenikovich and Dolan, 2003; Karacabeyli and Ceccotti, 1996; Heine, 2001);
3. The cyclic responses obtained with the CUREE protocol, when compared to the monotonic load-deformation curves, showed a certain correlation in terms of resistance and displacement at which the walls failed, which is in accordance with the findings of Ceccotti (1995) and Daudeville et al. (1998). Since the determination of the loading history for the CUREE protocol is derived from the peak capacity which is in turn determined by a monotonic test, it is therefore of importance that the monotonic response matches the backbone curve of the reversed cyclic response

The CUREE Ordinary Ground Motions reversed cyclic protocol was therefore selected to be applied to all the subsequent test walls reported here and in Branston (2004) and Chen (2004). All reversed cyclic tests were run in displacement control at a rate of 0.5 Hz, which was slowed to 0.25 Hz for large displacements in some cases due to the limitations in the hydraulic oil supply. The specific CUREE protocols for each of the tests completed by the author can be found in Appendix 'A'.

3.4 *MONOTONIC PROTOCOL*

Each shear wall configuration included at least three monotonic tests, which served two purposes. Firstly, by loading the wall in only one direction and at a very low pace, it simulated a static wind load condition. Secondly, it was necessary to conduct the monotonic tests in order to determine the CUREE protocol for ordinary ground motions.

The displacement controlled monotonic protocol used in this research program was first introduced by Serrette *et al.* (1996, 1997, 2002). It differs from the usual static one-directional ramp test in that the permanent set at 12.5 mm and 38 mm is evaluated. These values represent storey drift values of h/200 (0.5%) and h/64 (1.5%), respectively. The rate of loading was constant 7.5 mm per minute. At the permanent set levels of displacement the actuator movement was reversed until a zero load was reached. At this point loading in the initial direction recommenced. After the second permanent set was measured, the loading continued until a significant drop in the wall resistance was observed. Figure 3-14 presents a typical monotonic resistance vs. deflection curve for a monotonic test.

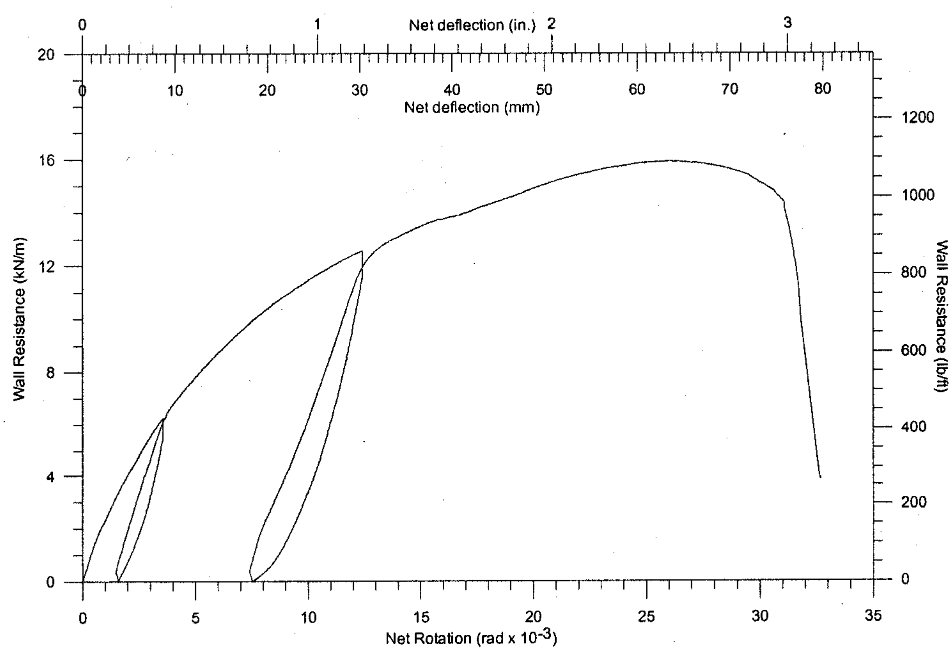

Figure 3-14: Typical Resistance vs. Deflection Curve for a Monotonic Test (Test 1A)

3.5 *Test Results*

3.5.1 Data Adjustments

Once a wall had been subjected to either the monotonic or the CUREE reversed cyclic protocol, interpretation and analysis of the results could then be completed. It was, however, first necessary to make modifications to the raw data in order to obtain useful parameters such as the stiffness of the wall, the ultimate shear resistance and the corresponding displacement. These modifications affected the top of the wall in-plane displacement of both cyclic and monotonic tests and the wall resistance for cyclic tests only.

The recorded top of the wall displacement included unwanted contributions from the slip at the base of the wall (rigid body translation) and uplift of both ends of the wall (rigid body rotation). The corrected net top of the wall displacement was defined by Equation 3-1 and the corresponding parameters are illustrated in Figure 3-15.

$$\Delta_{net} = \Delta_{walltop} - \left[\left(\frac{\Delta_{baseslip\_1} + \Delta_{baseslip\_2}}{2}\right)\right] - \left[\left(\Delta_{uplift\_1} - \Delta_{uplift\_2}\right) \times \frac{H}{L}\right] \qquad \textbf{(3-1)}$$

Inertia forces due to the weight of the loading beam and load cell were estimated based on the recorded accelerations for each cyclic test. Equation 3-2 was used to deduct these inertia forces from the measured load cell values in order to obtain the corrected shear wall resistance.

$$S' = S \pm \left(\frac{a \times g \times m}{1000 \times L}\right) \qquad \textbf{(3-2)}$$

Where:

S' = Corrected shear wall resistance (kN/m)
S = Measured shear wall resistance per unit length (Equation 3-3) (kN/m)
a = Measured acceleration of the top of the wall (g)
g = Gravitational acceleration (9.81 m/s^2)
m = Mass (200 kg for the 4' loading beam)
L= Length of the wall (4'=1220 mm)

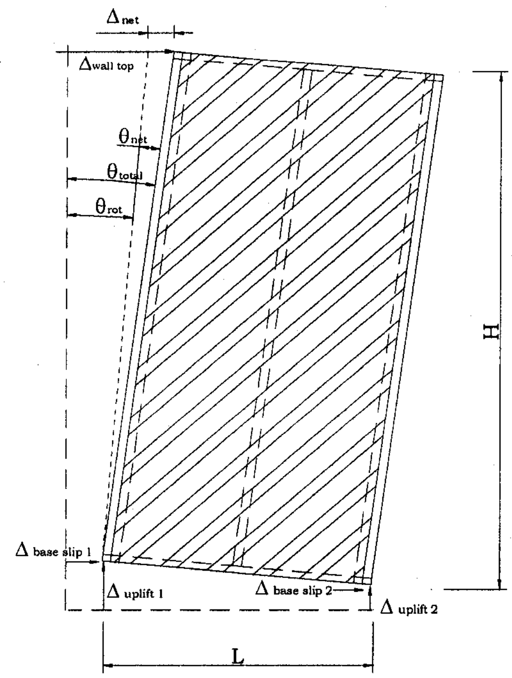

Figure 3-15: Deformed Configuration of a Loaded Shear Wall

The measured wall resistance is normally expressed as a shear force per unit length (shear flow) as shown by the following equation:

$$S = {}^{F}\!/_{L} \tag{3-3}$$

3.5.2 PRESENTATION OF TEST RESULTS

General results obtained from the test specimens of Groups 1 to 6 are shown in Table 3-7 (monotonic tests) and Table 3-8 (cyclic tests). All displacement measurements and wall resistance values (cyclic tests only) have been modified following the correction method described in Section 3.5.1. A comprehensive listing of all shear wall test results, including graphs, test data sheets and test observations, can be found in Branston *et al.* (2004).

Note that the wall capacities of the second set of tests of Group 1 (D,E,F) are substantially higher than those from the first suite (1-A,B,C). A probable explanation is that in the second set of tests (1-D,E,F) the plywood panels originated from a different mill (Richmond Plywood Corporation, also referred to as RichPly, mill number BC 858) than the panels of the first set of specimens where the plywood was from Alberta Plywood (mill number AB 244) (Figure 3-3). Chen (2004) also observed a considerable increase in shear wall capacity when similar wall configurations were constructed with plywood panels from Mill BC858 compared with those from Mill AB244. It was reported that the species type found in the AB244 panels was primarily spruce, whereas the BC 858 plywood contained Douglas fir face and back layers and a mixture of Hemlock / Amabilis fir for the inner plies. Douglas fir possesses significantly greater compression and shear resistance compared with spruce, as listed in the Wood Handbook (Forest Product Laboratory, 1999), which explains the higher measured shear resistance of walls 1D,E,F. Although the shear capacity differed greatly between walls 1A,B,C and 1D,E,F, a result of the makeup of the CSP plywood panels, the displacement levels reached were comparable at both the $0.4S_u$ and $0.8S_u$ load levels, which indicates that although the deflection capacities were not overly affected by the different wood species (Table 3-7) the shear stiffness was (Table 3-9). Furthermore, if a comparison of the average test results between the 1D,E,F and 5A,B,C,D (DFP) series is made, a similarity between the maximum wall resistance (S_u = 23.75 kN/m vs. S_u = 23.79 kN/m) and energy dissipation (E = 1664 J vs. E = 1619 J) is evident (Table 3-7). This supports the finding that the CSP plywood used for tests 1D,E,F was in fact composed of Douglas fir plies.

Tables 3-7 and 3-8 also present the moisture content of the wood panel of the tested shear walls determined according to the APA Test Method P-6 (APA PRP-108, 2001). After testing each shear wall, two 76 mm diameter (3") panel samples were cut and weighed immediately to obtain the initial weight (W_w) of the specimens. They were then placed in a drying oven at approximately 93°C ($\approx$200°F) for 24 hours and the oven-dry weight (W_d) was then obtained. The moisture content (MC) was determined using Equation 3-4.

$$MC = \frac{(W_w - W_d)}{W_d} x100 \qquad \textbf{(3-4)}$$

Where:

MC = Moisture content of specimen (%)
W_w = Initial weight of specimen (g)
W_d = Oven-dry weight of specimen (g)

Table 3-7 : Monotonic Shear Wall Test Results (Corrected Values)

Test	Panel Type	Fastener Schedule (mm)	Moisture Content (APA P-6)	Maximum Wall Resistance (S_u) kN/m	Displ. at S_u ($\Delta_{net,u}$) mm	Displ. at 0.4 S_u ($\Delta_{net,0.4u}$) mm	Displ. at 0.8 S_u ($\Delta_{net,0.8u}$) mm	Rotation at S_u ($\theta_{net,u}$) rad	Rotation at 0.8 S_u ($\theta_{net,0.8u}$) rad	Energy Dissipation (E) Joules
1A	CSP	102 / 305	5.75%	15.94	63.12	9.14	76.73	0.0259	0.0315	1137
1B	CSP	102 / 305	5.46%	17.09	60.16	9.39	79.71	0.0247	0.0327	1253
1C	CSP	102 / 305	5.68%	16.76	58.56	8.13	77.57	0.0240	0.0318	1209
AVERAGE	**CSP**	**102 / 305**	**5.63%**	**16.60**	**60.61**	**8.89**	**78.00**	**0.0249**	**0.0320**	**1200**
1D	CSP Richply	102 / 305	5.91%	27.40	61.48	9.39	74.12	0.0252	0.0304	1833
1E	CSP Richply	102 / 305	6.53%	22.01	60.88	9.32	82.29	0.0250	0.0337	1642
1F	CSP Richply	102 / 305	5.95%	21.83	57.12	8.33	75.28	0.0234	0.0309	1518
AVERAGE	**CSP Richply**	**102 / 305**	**6.13%**	**23.75**	**59.83**	**9.01**	**77.23**	**0.0245**	**0.032**	**1664**
5A	DFP	102 / 305	6.99%	21.09	62.20	7.83	76.63	0.0255	0.0314	1502
5B	DFP	102 / 305	6.13%	25.67	58.30	9.26	71.35	0.0239	0.0293	1621
5C	DFP	102 / 305	6.44%	23.91	62.07	10.55	79.69	0.0255	0.0327	1717
5D	DFP	102 / 305	7.02%	24.48	59.90	9.91	74.34	0.0246	0.0305	1636
AVERAGE	**DFP**	**102 / 305**	**6.65%**	**23.79**	**60.62**	**9.39**	**75.50**	**0.0249**	**0.0310**	**1619**

Table 3-8: Reversed Cyclic Shear Wall Test Results (Corrected Values)

Test	Panel Type	Fastener Schedule (mm)	Moisture Content (APA P-6)	Maximum Wall Resistance ($S_{u'+}$) (positive cycle) kN/m	Displacement at $S_{u'+}$ ($\Delta_{net\ u+}$) mm	Rotation at $S_{u'+}$ ($\theta_{net\ u+}$) rad	Maximum Wall Resistance ($S_{u'-}$) (negative cycle) kN/m	Displacement at $S_{u'-}$ ($\Delta_{net\ u-}$) mm	Rotation at $S_{u'-}$ ($\theta_{net\ u-}$) rad	Total Energy Dissipation, E Joules
3A	CSP	102 / 305	5.95%	13.58	37.27	0.0153	-13.84	-32.03	-0.0131	12795
3B	CSP	102 / 305	5.85%	14.36	37.92	0.0156	-14.41	-38.57	-0.0158	11822
3C	CSP	102 / 305	5.63%	13.85	44.27	0.0182	-13.84	-41.47	-0.0170	12071
AVERAGE	**CSP**	**102 / 305**	**5.81%**	**13.93**	**39.82**	**0.0163**	**-14.03**	**-37.36**	**-0.0153**	**12229** [1]
4A	CSP	102 / 305	5.27%	16.13	58.25	0.0239	-14.51	-44.98	-0.0184	4888
4B	CSP	102 / 305	6.12%	17.63	55.15	0.0226	-15.15	-44.59	-0.0183	5028
4C	CSP	102 / 305	5.35%	18.66	56.89	0.0233	-16.26	-42.48	-0.0174	4909
AVERAGE	**CSP**	**102 / 305**	**5.58%**	**17.47**	**56.76**	**0.0233**	**-15.31**	**-44.02**	**-0.0181**	**4942** [2]
6A	DFP	102 / 305	6.74%	22.55	61.44	0.0252	-19.90	-44.00	-0.0180	6718
6B	DFP	102 / 305	6.34%	22.94	56.79	0.0233	-19.32	-45.37	-0.0186	6408
6C	DFP	102 / 305	6.39%	22.26	57.97	0.0238	-19.59	-43.21	-0.0177	6473
AVERAGE	**DFP**	**102 / 305**	**6.49%**	**22.58**	**58.73**	**0.0241**	**-19.60**	**-44.19**	**-0.0181**	**6533** [2]

Note: Test 2-A is not shown because it was used for derivation of Group 3 – Serrette-SPD (2002) loading protocol only and not for design purposes

[1] Serrette-SPD (2002) loading protocol

[2] CUREE loading protocol.

3.5.3 FAILURE MODES

In general, the observed failure modes of the test specimens involved the wood sheathing to steel frame screwed connectors. Figure 3-16 represents a typical sheathing connection submitted to a cyclic shear loading regime. A monotonic loading could be represented by [a] and [b] in Figure 3-16.

Prior to loading, the wood sheathing and the light gauge steel stud are tightly held together by the screw (Fig. 3-16 [a]). At the onset of loading, on the first positive excursion or in the case of a monotonic loading, the screw tilts around the steel layer as this boundary is the stiffest. By tilting, the screw head and its threaded shank cause local inelastic crushing of the wood sheathing. As well, the hole in the light gauge steel stud enlarges slightly (Fig. 3-16 [b]). Tension in the screw increases but at the loading level applied to a typical shear wall, the screw does not yield in tension nor does it pull out from the steel framing member. Figure 3-16 [c] illustrates the equivalent phenomenon when loaded in the opposite direction as would occur in a cyclic test. It is often the case that the head of the sheathing screw pulls through the wood panel at final failure of the shear wall (Figure 3-16 [d]).

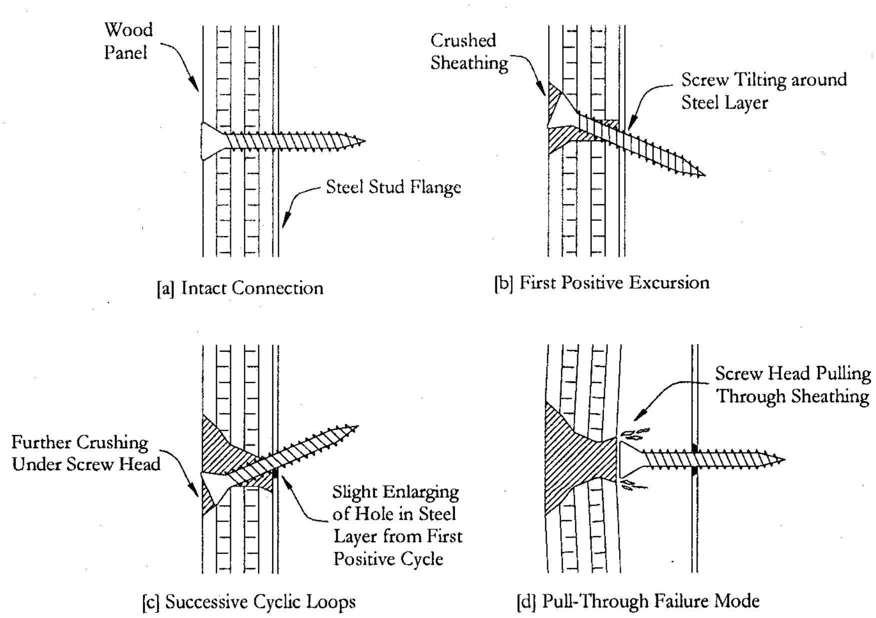

Figure 3-16 : Loading Sequence of a Steel Frame / Wood Panel Shear Wall Connection

Four main categories of sheathing connection failure modes and their combinations were observed:

1. **Pull-Through sheathing (PT) (Figure 3-16 [d] and 3-17)**
   With the screw tilting and rocking around the steel flange as seen in Figure 3-16, the wood is crushed and the screw hole in the wood is therefore enlarged until the bearing resistance of the remaining wood is exceeded and the screw head suddenly pulls through the sheathing.

2. **Partial Pull-Through (PPT) (Figure 3-18)**
   Partial pull-through occurred in a similar manner to the previous case except that the tension forces exerted on the screw head by the wood pulling out were partially resisted by the bearing capacity of some plies of the panel. It resulted in the screw head being embedded within the thickness of the wood panel at the end of the loading sequence.

3. **Tear-Out of Sheathing (TO) (Figure 3-19)**
   Wood sheathing tear-out occurred at the panel edges and especially at the corners where the differential movement of the steel frame and the wood panel was at the maximum. The in-plane movement of the sheathing relative to the framing members creates tension and shear forces in the screw and since the wood bearing capacity is lower than these forces, the screw head tears out of the side or corner of the panel. Typically the plies which are loaded perpendicular to the direction of grain will split, whereas the other plies will experience a plug shear failure mode.

Figure 3-17: Pull-Through Failure (PT)

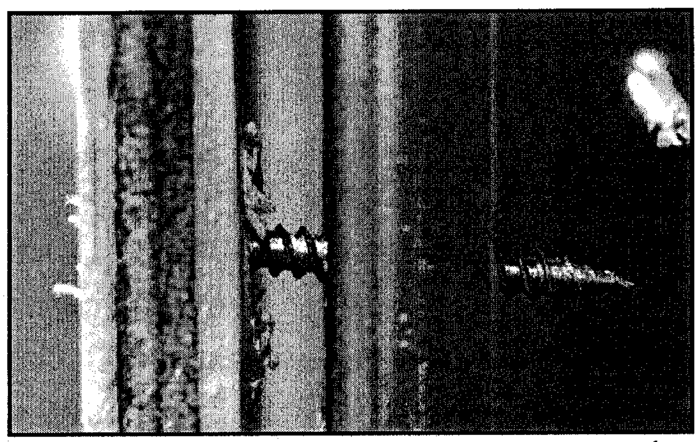

Figure 3-18: Partial Pull-Through Failure (PPT)

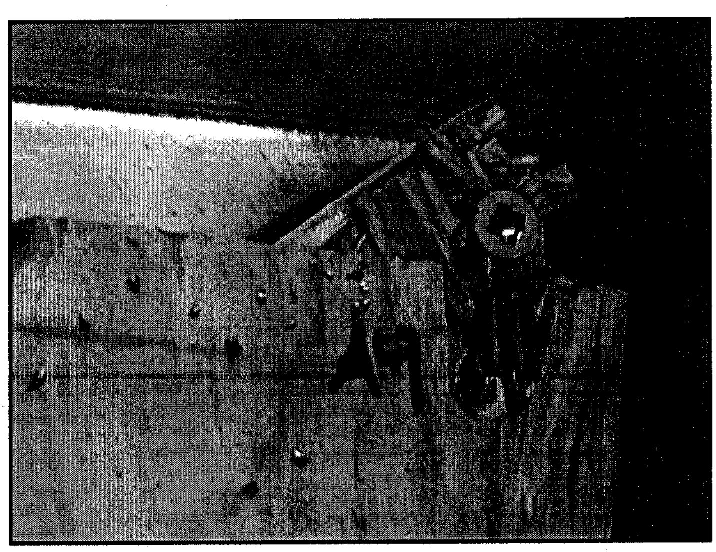

Figure 3-19: Tear-Out of Sheathing at a corner (TO)

4. **Wood Bearing Failure (WB) (Figure 3-20)**

   Wood bearing failure is characterized by the failure of one or several plies of the plywood panel. While some plies remain intact, the capacity of a connection exhibiting a wood bearing failure is greatly reduced due to the damage (plug shear failure) to the inner plies. The wood bearing failure typically precedes another more severe type of failure such as tear-out or pull-through. Plug shear failure of the inner plies can be observed in Figure 3-20.

Figure 3-20: Wood Bearing Failure (WB)

In contrast to nailed wood frame shear walls, where the fastener may be pulled out from the lumber studs or when the nail itself bends, in no test did the screw fasteners pull out of the flange of the steel framing nor did they bend to any visible degree. Furthermore, the anchorage connections such as hold-downs and shear anchor bolts, as well as the steel-to-steel screw connections, did not experience any substantial damage. In a few cases, sheathing fasteners connecting the wood panel with two layers of steel (principally the four corner screws) failed by shear (Figure 3-21). This failure mode occurred when the screw shank was restrained from tilting by both layers of steel causing the fastener to be loaded predominantly in shear instead of in tension, as would occur if the screw were able to tilt freely. In the case of cyclic tests, fatigue may also have affected the overall resistance of the fastener.

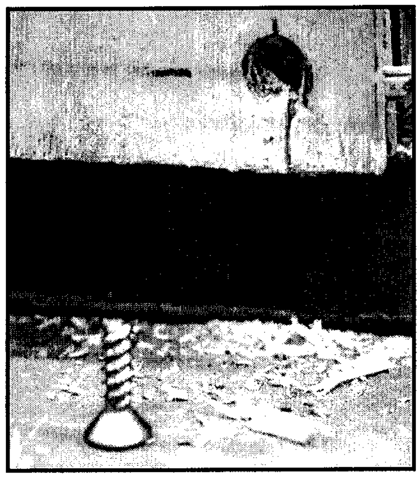

Figure 3-21: Shear Failure of a Corner Fastener

Towards the end of a test, a sudden drop in shear capacity generally occurred as a result of the unzipping of a row of sheathing screws pulling through the wood panel along the top or bottom tracks, as well as along perimeter studs (Figure 3-22). This indicated that the load in the screws along this edge was distributed in a uniform manner and that the fasteners failed in a rapid chain reaction. Essentially, the more highly loaded corner connections failed first, which caused the load on the shear wall to be shared by fewer sheathing connections overall. Once the resistance of each connection was exceeded one by one, a quick chain reaction or unzipping of the row of fasteners took place.

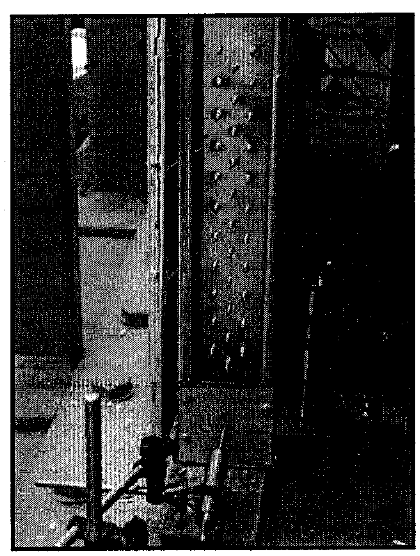

Figure 3-22: Unzipping of a row of screws

3.6 *PRESENTATION OF DESIGN PARAMETERS*

The research described in this thesis was carried out in combination with the work completed by Branston (2004) and Chen (2004). Branston adapted the Equivalent Energy Elastic-Plastic (EEEP) analysis approach such that it could be used to determine the recommended design parameters for the wall specimens detailed herein. The measured resistance vs. deflection behaviour of a steel frame / wood panel shear wall is quite non-linear, which is difficult to duplicate in terms of design parameters. However, it was assumed that the behaviour observed during testing could be represented by the EEEP curve based on the energy dissipation capability. This data interpretation method was selected because it provides basic strength and stiffness information that can be used for design; it gives a measure of the ductility inherent in the shear wall which is needed to define a force modification factor for seismic design; it can be applied irrespective of the loading protocol implemented, and because it has historically been used for the analysis of other structural systems that have exhibited a non-linear resistance vs. deflection behaviour (Branston, 2004). Since a complete description of the EEEP analysis approach can be found in Branston only a summary is provided in this Section.

3.6.1 EQUIVALENT ENERGY ELASTIC-PLASTIC (EEEP) ANALYSIS METHOD

In order to identify the important design parameters of a steel frame / wood panel shear wall, e.g. stiffness, ductility, nominal yield capacity, etc, it is necessary that the response be analysed using a standard methodology that accounts for the wall behaviour. Branston (2004) summarized 13 interpretation techniques of shear wall response, of which the Equivalent Energy Elastic-Plastic (EEEP) analysis method was selected to be implemented in this body of research.

The Equivalent Energy Elastic-Plastic (EEEP) method is based on the hypothesis that the dissipated energy of a tested shear wall can be represented by a perfectly bi-linear curve (Figure 3-23), which depicts a linear elastic behaviour before yielding and then perfectly plastic behaviour until failure of the system.

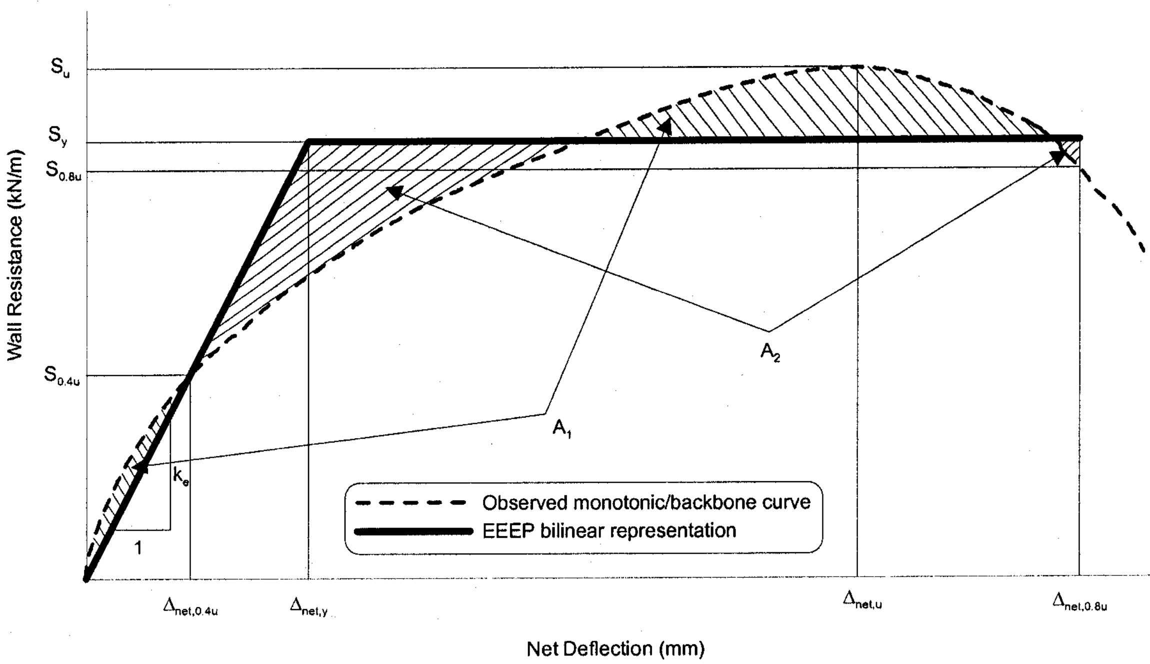

Figure 3-23 : EEEP model (Park, 1989; Salenikovich *et al.*, 2000)

The test response curve, represented by a dotted line in Figure 3-23, is either the resistance vs. deflection curve obtained from a monotonic test (without the unloading portions of the protocol described in Figure 2-1) or the backbone curve of a specimen tested with the CUREE reversed cyclic loading protocol. The backbone curve used in this body of research is described as the curve linking the peak resistance and / or the resistance attained at the maximum displacement for each primary cycle (Figure 3-24).

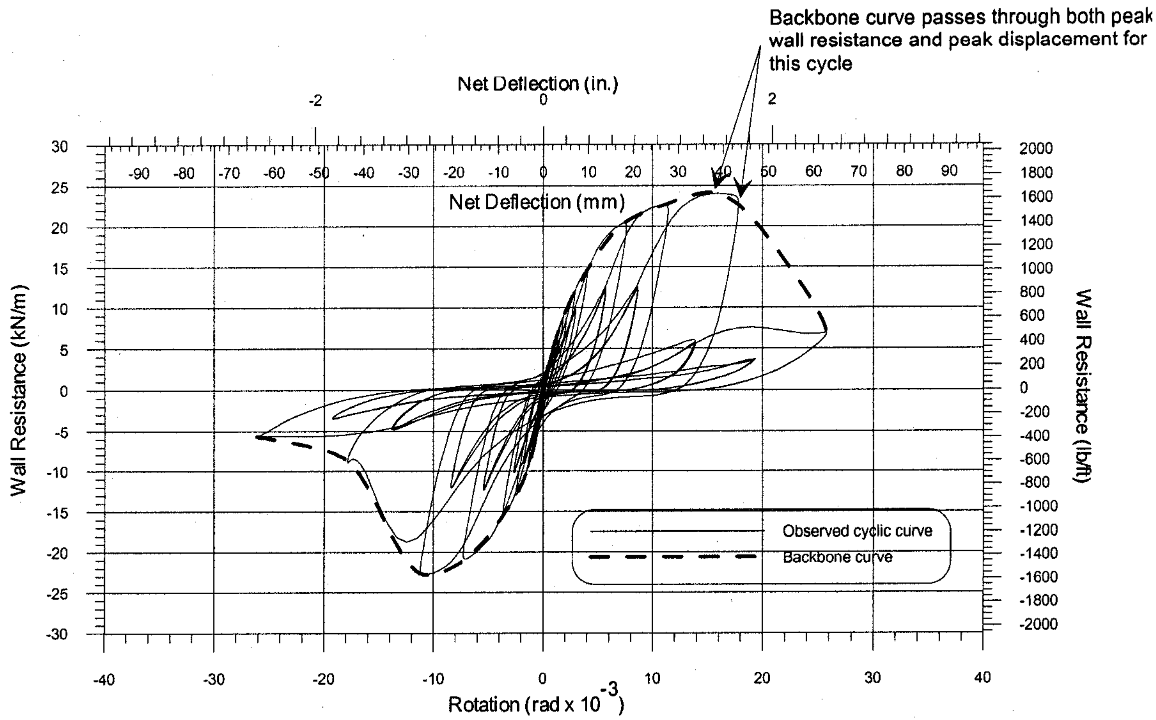

Figure 3-24 : Typical backbone curve of a CUREE reversed cyclic hysteresis response

3.6.2 DESIGN CHARACTERISTICS CALCULATIONS

The theory behind the general EEEP model is that the perfectly elastic-plastic bi-linear curve is equal in terms of energy dissipation capability to either the monotonic or cyclic test. This energy balance can be achieved by equating the area under the bi-linear curve with the area enclosed by the monotonic / backbone or similarly A_1=A_2 in Figure 3-23. It is assumed that the deformation corresponding to a post ultimate load of $0.8S_u$, $\Delta_{net,0.8u}$, represents the maximum deformation that the wall can reach and still possess a shear resistance. For this reason the $\Delta_{net,0.8u}$ was identified as the limit of the equivalent area calculation. This definition can be mathematically expressed by:

$$A_{EEEP} = \frac{\Delta_{net,y} \times S_y}{2} + (\Delta_{net,0.8u} - \Delta_{net,y}) \times S_y = A \qquad \textbf{(3-5)}$$

The EEEP analysis procedure defines the elastic portion of the bi-linear curve as a straight line from the origin through the $0.4S_u$ - $\Delta_{net,0.4u}$ point and up to the intersection with the plastic portion of the curve (S_y , $\Delta_{net,y}$).

The elastic stiffness k_e, is therefore defined by:

$$k_e = \frac{0.4S_u}{\Delta_{net,0.4u}} = \frac{S_y}{\Delta_{net,y}} \quad \text{or} \quad \Delta_{net,y} = \frac{S_y}{k_e} \tag{3-6}$$

To obtain an equal area, or energy balance, the nominal yield resistance (S_y) is adjusted as follows:

Rewriting (3-5) using (3-6):

$$A_{EEEP} = A = \frac{S_y^{\ 2}}{2\times k_e} + \Delta_{net,0.8u} \times S_y - \frac{S_y^{\ 2}}{k_e} \tag{3-7}$$

Simplifying:

$$-\frac{S_y^{\ 2}}{2\times k_e} + \Delta_{net,0.8u} \times S_y - A = 0 \tag{3-8}$$

A quadratic formula of the form $ax^2 + bx + c = 0$ is obtained, with $x = S_y$.

$$\frac{-b \pm \sqrt{b^2 - 4ac}}{2a} \quad \text{with } a = -\frac{1}{2k_e},\ b = \Delta_{net,0.8u} \text{ and } c = -A \tag{3-9}$$

Solving (3-8) using (3-9), we obtain:

$$S_y = \frac{-\Delta_{net,0.8u} \pm \sqrt{\Delta_{net,0.8u}^{\ 2} - \frac{2A}{k_e}}}{-\frac{1}{k_e}} \tag{3-10}$$

Where:

S_y = Wall resistance at yield, [force per unit length]
S_u = Ultimate wall resistance, [force per unit length]

A = Calculated area under monotonic response curve or backbone curve up to failure ($\Delta_{net,0.8u}$), [force]
k_e = Unit elastic stiffness, [force per displacement]

$\Delta_{net,0.8u}$ = Displacement at post-peak wall resistance of $0.8S_u$
$\Delta_{net,y}$ = Displacement at yield wall resistance S_y

A limitation on the maximum inelastic lateral displacement of a shear wall may affect the general EEEP analysis procedure. According to the 2005 NBCC *(NRCC, 2004)*, for seismic design the maximum acceptable inelastic inter-storey drift is equal to 2.5% of the storey height, i.e. 61 mm for a 2440 mm (8') high wall. In the general EEEP analysis method the equivalent energy calculation is carried out up to the post-peak displacement at 0.8 S_u ($\Delta_{net,0.8u}$). This results in two different cases in which the inelastic inter-storey drift limit may influence the calculation of design parameters for light gauge steel frame / wood panel shear walls; Case I: 61 mm < $\Delta_{net,u}$ (Fig. 3-25) and Case II: $\Delta_{net,u}$ < 61 mm < $\Delta_{net,0.8u}$ (Fig. 3-26). The general case is utilized when the seismic drift limitation prescribed by the 2005 National Building Code of Canada is above the failure displacement of the wall, $\Delta_{net,0.8u}$.

In Case I, the seismic drift limit is incorporated into the analysis in an attempt to maintain the structural integrity of a building during a design level earthquake. The inelastic drift limit is assumed to represent the upper bound on the useable portion of a wall's resistance vs. deflection behaviour. For this reason the general calculation procedure for the EEEP curve is modified. The elastic part of the curve remains as is, while the plastic portion of the curve is adjusted based on the 61 mm deflection limit. As found for the general method the areas, A_1 and A_2, are set equal to establish the value of S_y (Fig. 3-25).

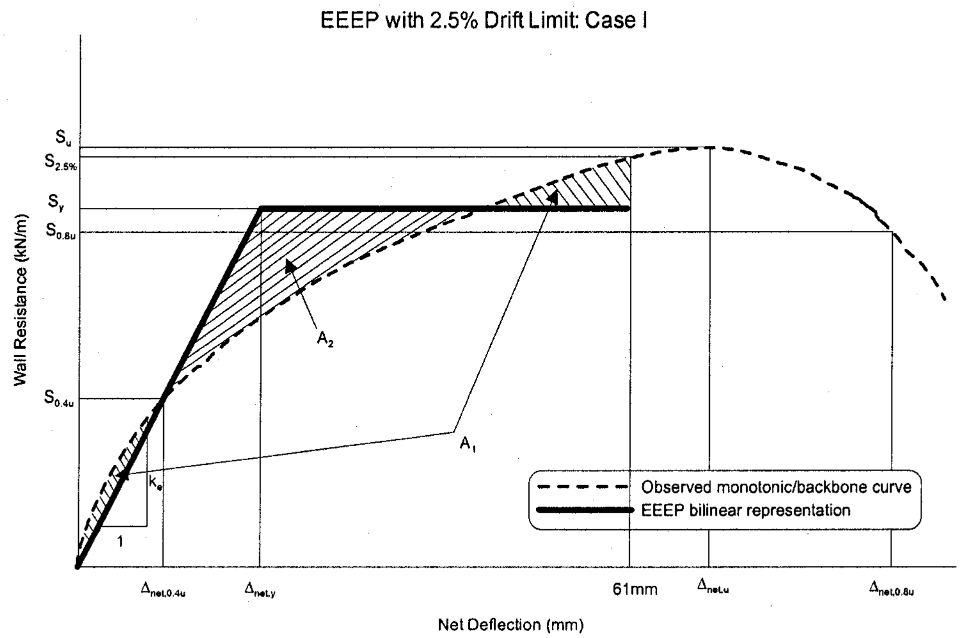

Figure 3-25 : EEEP design curve with imposed 2.5 % drift limit (Case I) (Branston, 2004)

In Case II, walls are able to attain their ultimate shear capacity prior to reaching the 2.5% inter-storey drift limit. However, $\Delta_{net,0.8u}$ occurs at a deflection that exceeds the 61 mm drift limit. In this instance the test results show that the wall is able to develop its ultimate shear capacity prior to reaching a deflection of 61 mm. Hence, the approach taken was to not adjust the area balance based on the seismic drift limit. The resulting EEEP curve is shown in Figure 3-26, for which all values are derived as per the general approach, Equations 3-5 to 3-10.

Since more than one hundred shear walls were tested in the laboratory, the author developed a spreadsheet using Visual Basic™ macros in order to diminish the calculation time and minimize the possibility of errors. An overview of the Spreadsheet is presented in Appendix B. Besides allowing the user to determine the elastic stiffness and the nominal wall resistance at yield (S_y), it was also possible to obtain values of the ductility ratio (μ) and the energy dissipation (E). Refer to Chapter 4 for the ductility calculations.

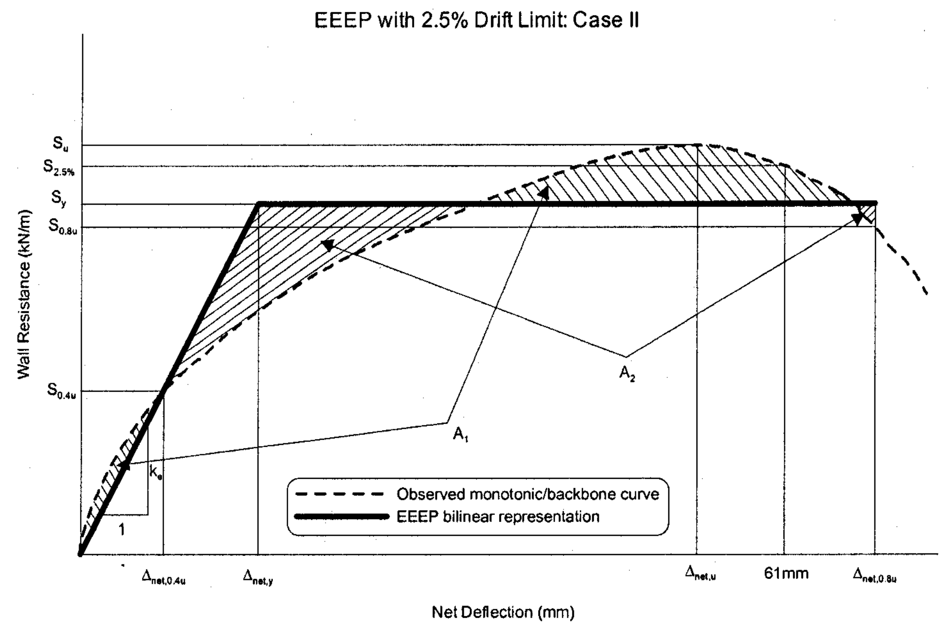

Figure 3-26 : EEEP design curve with imposed 2.5 % drift limit (Case II) (Branston, 2004)

EEEP curves superimposed on the measured shear wall response are shown for a typical monotonic and reversed cyclic test in Figures 3-27 and 3-28, respectively.

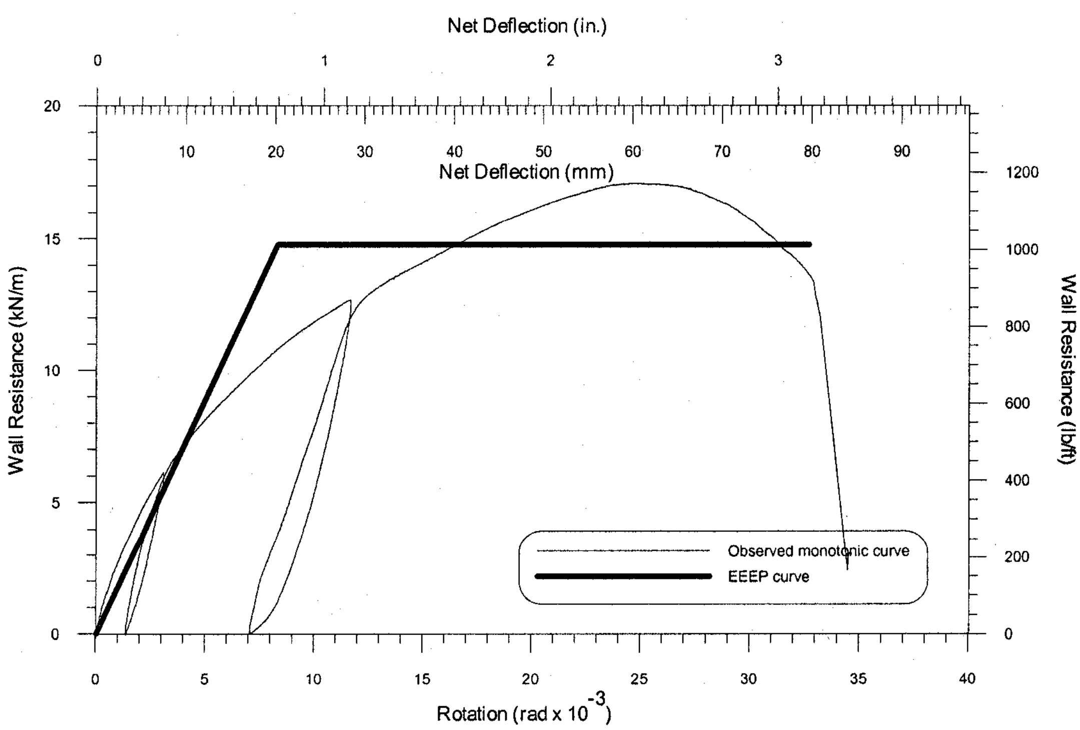

Figure 3-27 : EEEP Curve for monotonic test 1-B (4'x8' – CSP - 4"/12")

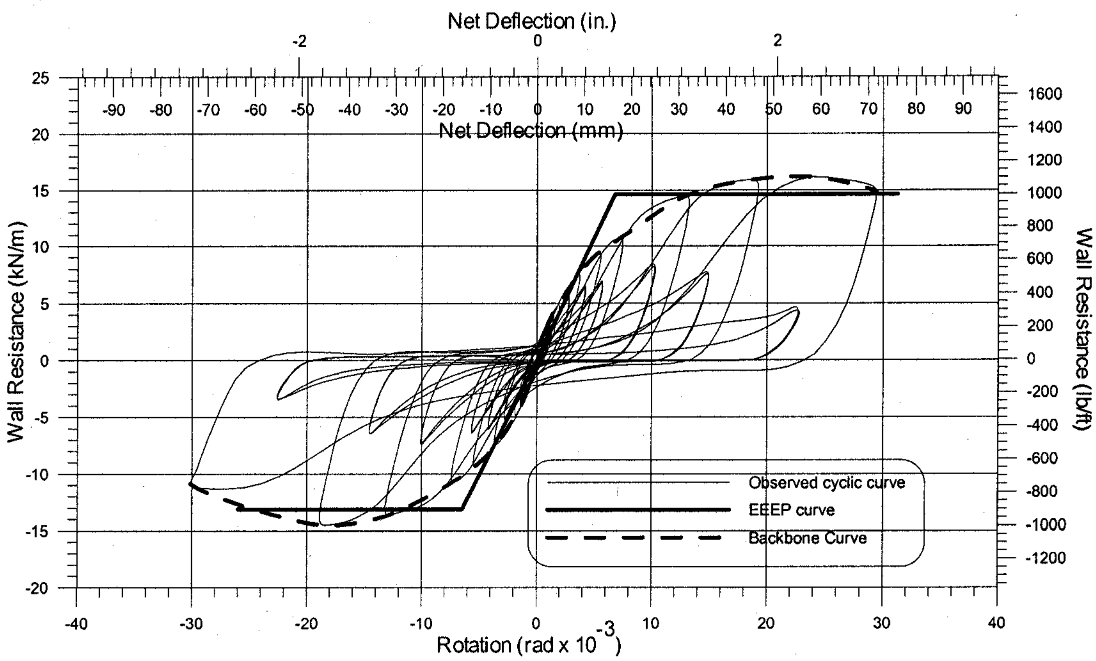

Figure 3-28 : EEEP Curve for Reversed Cyclic Test 4A (4'x8' – CSP – 4"/12")

Tables 3-9, 3-10 and 3-11 display the EEEP derived design values resulting from monotonic and reversed cyclic tests respectively. All test data, graphs, results and observation sheets are assembled in a stand-alone document (Branston *et al., 2004).* Furthermore, the final design value recommendations, which are based on the 109 shear wall specimens tested during the Summer of 2003, are provided by Branston (2004).

Table 3-9: Design values from monotonic tests

Test	Panel Type	Fastener Schedule (mm)	Displ. at 0.4 S_u ($\Delta_{net,0.4u}$) mm	Yield Load (S_y) kN/m	Displ. at S_y ($\Delta_{net,y}$) mm	Stiffness (k_e) kN/mm	Rotation at S_y ($\theta_{net,y}$) rad	Ductility (μ) rad	Energy Dissipation (E) Joules
1A	CSP	102 / 305	9.14	13.43	19.25	0.85	0.0079	3.17	841
1B	CSP	102 / 305	9.39	14.77	20.27	0.89	0.0083	3.93	1253
1C	CSP	102 / 305	8.13	14.41	17.47	1.01	0.0072	4.44	1209
AVERAGE	**CSP**	**102 / 305**	**8.89**	**14.20**	**19.00**	**0.92**	**0.0078**	**3.85**	**1101**
1D	CSP Richply	102 / 305	9.39	22.46	19.24	1.42	0.0079	3.17	1406
1E	CSP Richply	102 / 305	9.32	18.59	19.68	1.15	0.0081	4.18	1642
1F	CSP Richply	102 / 305	8.33	18.78	17.92	1.28	0.0073	4.20	1518
AVERAGE	**CSP Richply**	**102 / 305**	**9.01**	**19.94**	**18.95**	**1.28**	**0.0078**	**4.19**	**1522**
5A	DFP	102 / 305	7.83	17.51	16.24	1.31	0.0067	3.75	1128
5B	DFP	102 / 305	9.26	21.58	19.46	1.35	0.0080	3.67	1621
5C	DFP	102 / 305	10.55	19.73	21.76	1.11	0.0089	2.80	1204
5D	DFP	102 / 305	9.91	21.08	21.34	1.20	0.0088	3.48	1636
AVERAGE	**DFP**	**102 / 305**	**9.39**	**19.98**	**19.70**	**1.24**	**0.0081**	**3.43**	**1398**

Table 3-10 : Design values from reversed cyclic tests (positive cycles)

Test	Panel Type	Fastener Schedule (mm)	Yield Load (S_{y+}) kN/m	Displ. at S_{y+} ($\Delta_{net,y+}$) mm	Elastic Stiffness (k_{e+}) kN/mm	Rotation at S_{y+} ($\theta_{net,y+}$) rad	Ductility (μ)	Energy[1] Dissipation (E) Joules
3A	CSP	102 / 305	15.09	9.34	1.62	0.0038	8.02	1060
3B	CSP	102 / 305	15.84	9.72	1.63	0.0040	6.41	910
3C	CSP	102 / 305	15.08	13.62	1.11	0.0056	5.66	1060
AVERAGE	**CSP**	**102 / 305**	**15.34**	**10.89**	**1.45**	**0.0045**	**6.70**	**1010**
4A	CSP	102 / 305	14.63	16.55	1.08	0.0068	4.61	1211
4B	CSP	102 / 305	15.61	13.29	1.43	0.0055	5.26	1204
4C	CSP	102 / 305	16.19	14.75	1.34	0.0060	4.68	1217
AVERAGE	**CSP**	**102 / 305**	**15.48**	**14.86**	**1.28**	**0.0061**	**4.85**	**1211**
6A	DFP	102 / 305	18.79	16.88	1.36	0.0069	3.61	1203
6B	DFP	102 / 305	19.37	16.67	1.42	0.0068	4.16	1442
6C	DFP	102 / 305	19.23	15.11	1.55	0.0062	4.85	1541
AVERAGE	**DFP**	**102 / 305**	**19.13**	**16.22**	**1.44**	**0.0067**	**4.21**	**1395**

[1] Energy calculation based on area below backbone curve

Table 3-11 : Design values from reversed cyclic tests (negative cycles)

Test	Panel Type	Fastener Schedule (mm)	Yield Load (S_{y-}) kN/m	Displ. at S_{y-} ($\Delta_{net,y-}$) mm	Stiffness (k_{e-}) kN/mm	Rotation at S_{y-} ($\theta_{net,y-}$) rad	Ductility (μ)	Energy [1] Dissipation (E) Joules
3A	CSP	102 / 305	-15.89	-11.54	1.38	-0.0047	6.4	1081
3B	CSP	102 / 305	-15.81	-10.79	1.46	-0.0044	5.96	931
3C	CSP	102 / 305	-15.16	-10.11	1.5	-0.0041	6.8	967
AVERAGE	**CSP**	**102 / 305**	**-15.62**	**-10.81**	**1.45**	**-0.0044**	**6.39**	**993**
4A	CSP	102 / 305	-13.12	-15.82	1.01	-0.0065	4.01	889
4B	CSP	102 / 305	-13.64	-18.67	0.89	-0.0077	3.52	937
4C	CSP	102 / 305	-14.19	-14.18	1.22	-0.0058	3.95	846
AVERAGE	**CSP**	**102 / 305**	**-13.65**	**-16.22**	**1.04**	**-0.0067**	**3.83**	**891**
6A	DFP	102 / 305	-17.56	-15.66	1.37	-0.0064	3.98	1168
6B	DFP	102 / 305	-16.60	-14.82	1.37	-0.0061	3.93	1028
6C	DFP	102 / 305	-17.55	-15.90	1.35	-0.0065	4.34	1309
AVERAGE	**DFP**	**102 / 305**	**-17.24**	**-15.46**	**1.36**	**-0.0063**	**4.08**	**1168**

[1] Energy calculation based on area below backbone curve

3.7 *Ancillary Testing of Materials*

Included in the scope of this research was the determination by testing of the relevant material properties for the steel and wood components of the shear wall specimens. The ancillary testing program provided values for the ultimate shear strength and shear modulus (G) of the CSP, DFP and OSB wood sheathing, as well as the yield and ultimate tensile stress, modulus of elasticity (E) and the percentage of elongation of the steel studs and tracks.

3.7.1 Shear Properties of Wood Sheathing Panels

Determination of the shear modulus (G) and ultimate shear strength of the wood sheathing panels was necessary to verify that the sheathing used for the walls had properties similar to those listed by the CSA O86 Engineering Design in Wood Standard (2001). Moreover, these material properties were required for the analytical predictions of the shear wall capacity carried out by Chen (2004).

3.7.1.1 Test Set-Up and Procedure

In order to determine the abovementioned properties, Sections 130 to 136 of ASTM Standard D1037 (1999) were used. These sections describe the edgewise shear test, which consists of a 254 x 90mm (10" x 3½") wood specimen clamped between two pairs of steel loading rails, as shown in Figures 3-29 (a) and (b). The interior face of the rails was serrated to provide a gripping surface to the wood test pieces. Each specimen was tightly bolted between the rails to prevent slipping and was then loaded in compression at a rate of 0.5 mm per minute using an MTS® Sintech 30/G universal testing machine equipped with a 150 kN load cell. Figure 3-29 (c) shows the back side of a test specimen where the LVDTs were positioned. One LVDT measured the direct displacement in line with the test piece and another was used to evaluate the cross-head displacement of the test machine. For all tests, data was recorded at 2 Hz with the same data acquisition system as used for the shear wall tests.

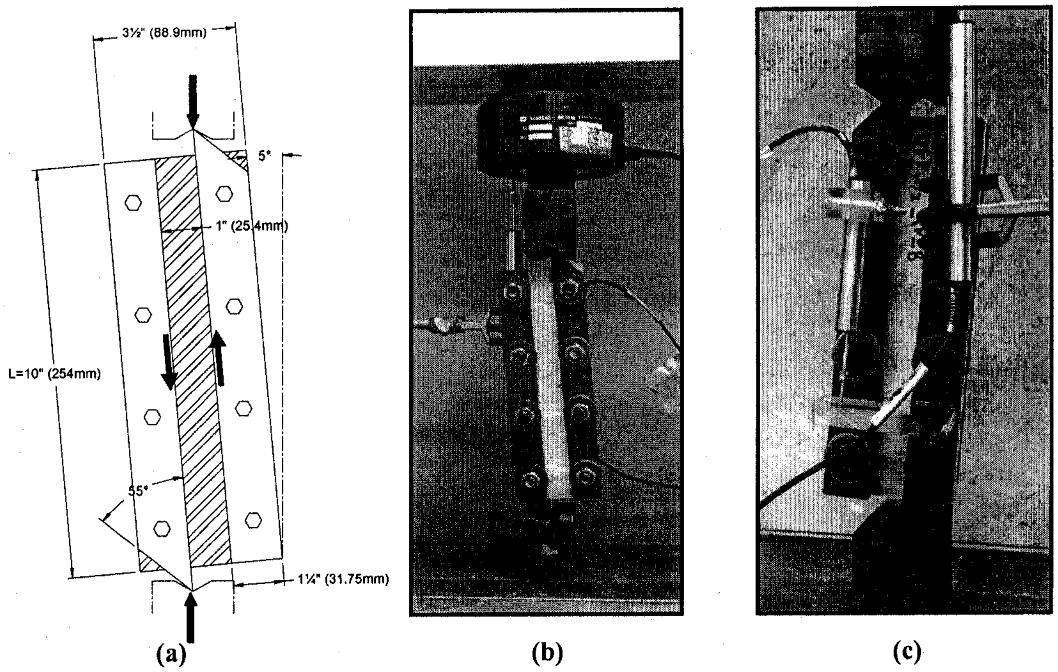

Figure 3-29: (a) Detail of Loading Rails; (b) General View of Wood Panel Specimen; (c) Positioning of two LVDTs on Specimen

The edgewise shear strength and the shear modulus (modulus of rigidity) were calculated using the equations

$$v_p = \frac{P_{\max}}{L \cdot t} \qquad \textbf{(3-11)}$$

$$G = \frac{P \times b}{L \times t \times r} \times F \qquad \textbf{(3-12)}$$

Where:

v_p = Edgewise shear strength (MPa);
P_{max} = Maximum compressive load (N);
G = Shear modulus (modulus of rigidity) (MPa);
P = Compressive load (N);
b = Width of portion of the specimen in shear (mm) (b = 25.4 mm in this case);
L = Length of specimen (mm);
t = Average thickness of shear area (mm);
r = In-line displacement at load P (mm);
F = Multiplication factor to compensate nonuniform stress distribution in small specimens. F = 1.19 (ASTM D2719, 1994)

3.7.1.2 Experimental Test Program Matrix

In total, 48 specimens were tested as listed in Table 3-12. As required by the ASTM D1037 Standard, half of the specimens were tested with their long dimension parallel to the long dimension of the 1220 x 2440 mm (4' x 8') panel and the other half with their long dimension perpendicular to the long dimension of the same panel to account for the direction dependent properties of the wood sheathing. In order to evaluate the influence of the panel thickness on its intrinsic properties, thickness were not limited to 12.5 mm (1/2") Plywood and 11 mm (7/16") OSB as used for the construction of the shear wall specimens tested in this thesis. Thickness ranging from 9.5 mm (3/8") to 15.9 mm (5/8") were included in the testing program.

Table 3-12: Shear Properties of Panel Ancillary Test Matrix

Test Name	Wood Type	Nominal Thickness	Test Orientation	
			PL[1]	PP[2]
DFP_3/8_PL_A,B,C	DFP	9.5mm (3/8")	x	
DFP_3/8_PP_A,B,C	DFP	9.5mm (3/8")		x
DFP_1/2_PL_A,B,C	DFP	12.7mm (1/2")	x	
DFP_1/2_PP_A,B,C	DFP	12.7mm (1/2")		x
DFP_5/8_PL_A,B,C	DFP	15.9mm (5/8")	x	
DFP_5/8_PP_A,B,C	DFP	15.9mm (5/8")		x
CSP_3/8_PL_A,B,C	CSP	9.5mm (3/8")	x	
CSP_3/8_PP_A,B,C	CSP	9.5mm (3/8")		x
CSP_1/2_PL_A,B,C	CSP	12.7mm (1/2")	x	
CSP_1/2_PP_A,B,C	CSP	12.7mm (1/2")		x
CSP_5/8_PL_A,B,C	CSP	15.9mm (5/8")	x	
CSP_5/8_PP_A,B,C	CSP	15.9mm (5/8")		x
RichPly_1/2_PL_A,B,C	CSP RichPly	12.7mm (1/2")	x	
RichPly_1/2_PP_A,B,C	CSP RichPly	12.7mm (1/2")		x
OSB_7/16_PL_A,B,C	OSB	11.1mm (7/16")	x	
OSB_7/16_PP_A,B,C.	OSB	11.1mm (7/16")		x

[1] Long dimension of the specimen **parallel** to the long dimension of the wood panel
[2] Long dimension of the specimen **perpendicular** to the long dimension of the wood panel

3.7.1.3 Test Results

Figure 3-30 represents a typical stress-strain curve of a wood sheathing panel specimen as determined using the edgewise shear standard method. The shear modulus was taken as an average of the values calculated with Equation 3-12 for the straight-line portion of the curve situated between 5% and 40% of the maximum shear strength value.

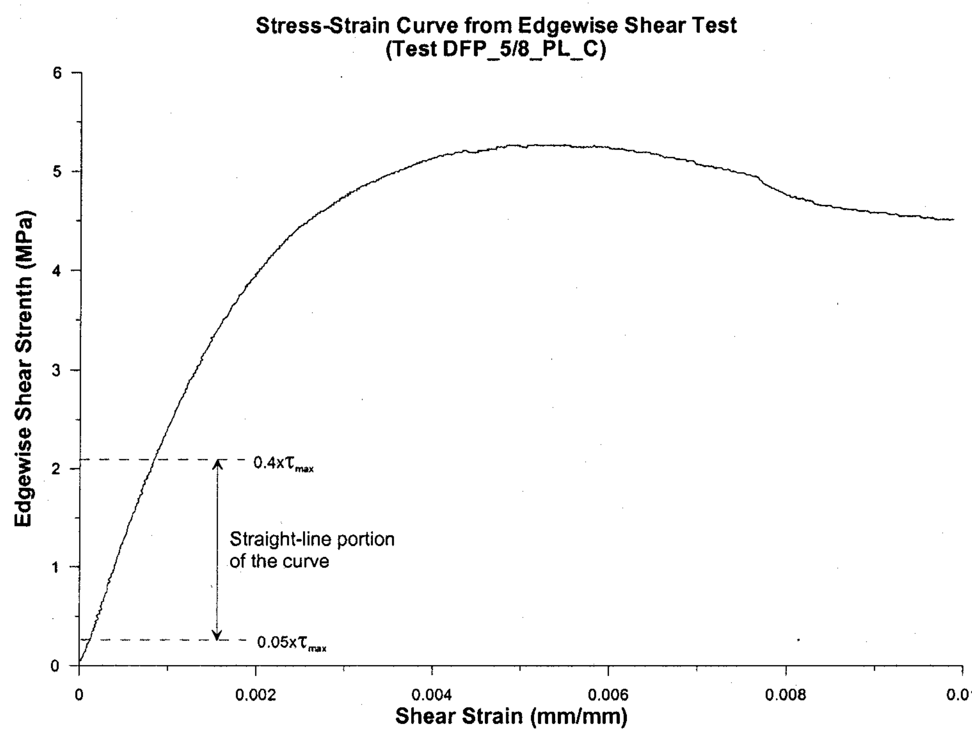

Figure 3-30: Typical Stress-Strain Curve for an Edgewise Shear Test of a 5/8" Plywood panel

An overview of the edgewise shear test results is presented in Table 3-13 for the 48 specimens. The direction of testing (parallel or perpendicular to the long dimension of the board) did not overly influence the shear modulus nor the shear strength, which has also been the case in studies by Suzuki *et al.* (2000) and Suzuki and Miyagawa (2003).

Table 3-13: Test Results for Edgewise Shear of Wood Sheathing Panels (average values)

Test Series	Thickness (mm)	Shear strength (v_p) (MPa)	Shear Modulus (G) (MPa)	CoV (%)	G/v_p
DFP_3/8_PL_A,B,C	8.86	5.52	327	20.9%	59
DFP_3/8_PP_A,B,C	8.81	5.48	463	22.7%	85
	PL vs PP	***-0.8%***	***29.5%***		
DFP_1/2_PL_A,B,C	12.62	4.86	838	29.7%	172
DFP_1/2_PP_A,B,C	12.47	5.14	434	35.4%	84
	PL vs PP	***5.7%***	***-48.2%***		
DFP_5/8_PL_A,B,C	16.41	5.11	281	6.4%	55
DFP_5/8_PP_A,B,C	16.20	4.84	274	9.3%	57
	PL vs PP	***-5.3%***	***-2.7%***		
CSP_3/8_PL_A,B,C	9.20	4.52	327	11.6%	72
CSP_3/8_PP_A,B,C	9.19	5.00	293	16.2%	59
	PL vs PP	***10.7%***	***-10.3%***		
CSP_1/2_PL_A,B,C	11.63	3.92	322	16.1%	82
CSP_1/2_PP_A,B,C	11.48	4.95	284	10.3%	57
	PL vs PP	***26.3%***	***-11.7%***		
CSP_5/8_PL_A,B,C	15.32	5.31	299	8.2%	56
CSP_5/8_PP_A,B,C	15.02	5.87	310	9.7%	53
	PL vs PP	***10.6%***	***3.3%***		
Richply_1/2_PL_A,B,C	11.67	5.48	371	18.4%	68
Richply_1/2_PP_A,B,C	11.70	5.50	313	11.4%	57
	PL vs PP	***0.3%***	***-15.5%***		
OSB_7/16_PL_A,B,C	11.26	9.05	473	10.4%	52
OSB_7/16_PP_A,B,C	11.03	9.14	530	16.1%	58
	PL vs PP	***1.0%***	***10.9%***		

In general, the test results show that the OSB has the highest shear modulus and shear strength when compared to the other wood panel types. This behaviour can be explained by the degree of strand alignment and the amount of adhesive used in the fabrication of OSB. Except for the DFP 1/2", the ratio of the shear modulus to shear strength (G/v_p) is consistent (≈ 60) for all of the wood panels, which indicates that in spite of the difference in nominal capacity the panels have a maximum shear strength proportional to their rigidity (Figure 3-31). The testing method used for the DFP 1/2" groups was found to be erroneous and results were therefore not considered in the analysis but are presented nevertheless.

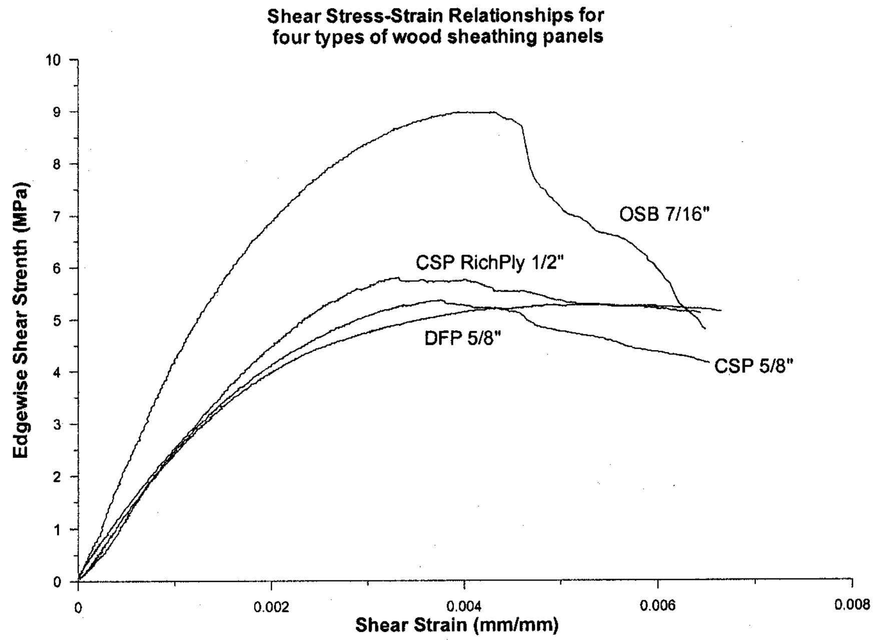

Figure 3-31: Superimposed Typical Shear Stress-Strain Curves for Different Wood Panel Types

3.7.1.4 Comparison with CSA O86 Panel Shear Values

The shear-through-thickness strength and modulus values for wood sheathing panels included in the CSA O86 Standard (2001) originate from research conducted by Smith (1974) and Parasin and Stieda (1985) and are the 5th percentile standard deviation values. Since wood components can largely be affected by their condition of loading and their environment in general, the abovementioned researchers recommended the application of various modification factors to account for the change in condition between the controlled testing environment and the real application for these wood sheathing panels. Modification factors that take into account the load duration, the factor of safety, an adjustment for inner veneer species and the moisture content can all be applied. Therefore the characteristic plywood shear strength values obtained experimentally have been divided by a suitable factor to adjust the values from short term to normal duration of load, i.e. a loading period not exceeding 10 years.

Thus the shear-through-thickness strength values obtained in the scope of this research have been divided by 2, a factor found to be suitable to account mainly for the duration of the load and other safety factors (Parasin and Stieda, 1985). The corrected shear strength values are presented in Table 3-14, as well as the CSA O86 (2001) values. Note that only the average values of the parallel and perpendicular tests are shown in accordance with CSA O86. The shear-through-thickness rigidity (B_v) is also presented as the shear modulus multiplied by the real thickness of the tested specimens. The edgewise shear strength (v_p) are in compliance with the design standard values but the shear modulus (G) values differ significantly from the CSA O86 standards values. This discrepancy can be explained by the fact that the standard test method ASTM D1037 is not meant for measuring the shear modulus but rather for measuring solely the edgewise shear strength (v_p) for the reasons explained in the next section.

Table 3-14: Experimentally Obtained Shear Properties and CSA O86 Shear Properties

Test Series	v_p (086) (MPa)	v_p (Exp) (MPa)	v_p (Exp Corr)[1] (MPa)	Difference (%)	G (086) (MPa)	G (Exp) (MPa)	Difference (%)	B_v (086)[2] (N/mm)	B_v (Exp) (N/mm)	Difference (%)
DFP 3/8	2.53	5.50	2.75	8.7%	579	395	31.8%	5500	3485	36.6%
DFP 1/2	2.40	5.00	2.50	4.2%	552	636	15.3%	6900	7998	15.9%
DFP 5/8	2.32	4.97	2.49	7.2%	542	277	48.8%	8400	4619	45.0%
CSP 3/8	2.42	4.76	2.38	1.6%	453	310	31.6%	4300	2847	33.8%
CSP 1/2	2.40	4.44	2.22	7.5%	456	303	33.6%	5700	3500	38.6%
CSP 5/8	2.45	5.59	2.79	14.1%	458	304	33.5%	7100	4619	34.9%
Richply 1/2	2.40	5.49	2.75	14.4%	456	342	24.9%	5700	4000	29.8%
OSB 7/16	4.18	9.09	4.55	8.8%	1000	501	49.9%	11000	5585	49.2%

[1] Load Modification Factor of 2 applied to experimentally obtained shear strength to account for short duration of the test and safety;
[2] $B_v = G \times t$ = Shear-through-thickness rigidity

3.7.1.5 Applicability of Edgewise Shear Method

Although the ASTM D1037 edgewise shear method is said to be suitable (Suzuki *et al.*, 2000; Suzuki and Miyagama, 2003) to evaluate the shear properties of wood panels, the two rail shear or large panel shear test methods (ASTM D2719, 1994) are recommended by many researchers (Smith 1974, Parasin and Stieda 1985, Biblis 2001), as well as by the Forintek Wood Products Research Institute (2004).

The true gauge length present in the Edgewise Shear section of the ASTM D1037 test method is difficult to estimate because the serrated rails restrain the deformation of the exterior layers and with the small distance between rails, the error is significant and the true value of the shear modulus (G) remains unknown.

The increased specimen size used in the two rail shear or large panel shear test methods (ASTM D2719) diminishes the effects of nonuniform shear stress distribution at shear area edges. It is therefore suggested that for future testing of the shear properties of wood sheathing panels the ASTM D2719 method be followed.

3.7.2 TENSILE PROPERTIES OF STEEL STUDS AND TRACKS

Also part of the ancillary testing program was the determination of the tensile material properties of the light gauge steel studs and tracks. Branston (2004) and Chen (2004) carried out six coupon tests following the ASTM A370 (2002) test standard. Coupons were tested at a cross-head speed of 0.5 mm per minute in the elastic range and an increased rate of 4 mm per minute once plastic behaviour was observed. A 50 mm gauge length extensometer was used to measure the strain. The stress was calculated by dividing the applied tension by the cross-sectional area of the base metal. Material properties for the light gauge steel studs and tracks are reported in Table 3-15.

Table 3-15: Measured Light Gauge Steel Properties

Member	Specimen	Base Metal Thickness (mm)	Yield Stress (F_y) (MPa)	Ultimate Stress (F_u) (MPa)	F_u/F_y	Modulus of Elasticity (E) (MPa)	% Elong
Stud (AVG)	1.12mm 230 MPa	1.09	250.9	335.2	1.34	197667	38.5%
Track (AVG)	1.12mm 230 MPa	1.08	272.1	343.7	1.26	203667	41.6%

The two steels met the North American Specification for the Design of Cold-Formed Steel Structural Members (AISI, 2001) requirements for $F_u/F_y \geq 1.08$ and elongation of at least 10 % of the 50 mm gauge length. In all cases the measured yield stress exceeded the specified minimum strength (230 MPa) by a significant amount. The steel exhibited a sharp yielding behaviour with a yield plateau before strain hardening occurred prior to failure.

CHAPTER 4

SEISMIC FORCE MODIFICATION FACTORS FOR STEEL FRAME / WOOD PANEL SHEAR WALLS

4.1 INTRODUCTION

The National Building Code of Canada (NBCC) has evolved tremendously over the past half century in terms of seismic design provisions. Although the first fragments of seismic regulations appeared in 1941 (Heidebrecht, 2003), it took another 50 years and a major earthquake in Mexico (1985) before the appearance, in the 1990 edition of the NBCC (NRCC, 1990), of a design concept that relies on seismic force modification factors[1] . The seismic force modification factor used in modern design codes reflects the ability of a structure to sustain its load carrying capacity and to dissipate energy through inelastic behaviour while being cyclically loaded by an earthquake. In effect, the designer relies on the inelastic behaviour and the overstrength of the structure in order to obtain a more economic design. A detailed description of the use of the seismic force modification factor in the 1995 (NRCC, 1995), and 2005 National Building Codes of Canada is contained in the following sections.

---

[1] The term "Seismic force modification factor" will be used throughout the text. Other researchers have called it: force reduction factor, response modification factor, system performance factor, behaviour factor ("q" in Europe) (Fulop and Dubina, 2002), action reduction factor (Ceccotti and Karacabeyli, 2000), strength reduction factor (Miranda and Bertero, 1994), structural coefficient (Ceccotti and Vignoli, 1989).

4.2 Comparison of Seismic Provisions for NBCC 1995 and NBCC 2005

Building codes evolve with the continuing improvement in the knowledge of the earth's seismicity, the lessons drawn from the performance of buildings in past earthquakes and the results from earthquake engineering research programs. The proposed 2005 draft edition of the NBCC contains several major changes in the provisions for seismic loading and design when compared to the 1995 edition. These include: an updated hazard map, a change in the return period of the design earthquake, explicit recognition of higher mode effects, building irregularity considerations, method of dynamic analysis and the delineation of the overstrength and ductility effects (Heidebrecht, 2003).

The latter proposed adjustment concerns the seismic force modification factors which are incorporated in the determination of the base shear used for design. In the 1995 NBCC, the base shear equation was expressed as:

$$V = \frac{V_e}{R} \times U \qquad \textbf{(4-1)}$$

where V_e is the equivalent lateral force at the base corresponding to an elastic response, R is the force modification factor and U is a calibration factor (U=0.6). The force V_e is determined from:

$$V_e = v \times S \times I \times F \times W \qquad \textbf{(4-2)}$$

where:

- v = zonal velocity ratio (determined at 10% in 50 years probability of exceedance);
- S = Seismic response factor (depends on period of structure and ratio Z_a/Z_v);
- I = Building importance factor (1.0 – 1.5);
- F = Foundation or site factor (1.0 – 2.0);
- W = Dead load including 25% of design snow load.

The seismic force modification factor, R in Equation 4-1, reflected only the ability of a structure to dissipate energy through inelastic deformation. Hence, the R-factor was based solely on the level of ductility of the seismic force resisting system (SFRS) observed during experimental testing and real earthquake events, as well as the results obtained by representative computer analyses. It varied from 1.0 for an unreinforced masonry wall to 4.0 for a ductile moment-resisting frame. The calibration factor (U) represented a level of protection based on experience and was generally interpreted as an implicit recognition of the presence of overstrength in a structure, although its value was identical (0.6) for all SFRS type and materials (steel, concrete, timber).

With experience gained by viewing the performance of buildings in past earthquakes and an increasing interest and capability in the dynamic analysis of structures, recent model building codes tend to consider the significant contribution of overstrength present within different structural systems. The 2005 NBCC contains a modified seismic base shear equation, in which an overstrength-related force modification factor is included.

$$V = \frac{S_{(T)} M_V I_E W}{R_d R_o} \tag{4-3}$$

where:

- $S_{(T)}$ = Design spectral response acceleration (determined at 2% in 50 years probability of exceedance);
- M_v = Factor to account for higher mode effect on base shear;
- I_E = Earthquake importance factor of the structure;
- W = Dead load including 25% of design snow load;
- R_d = Ductility-related force modification factor that reflects the ability of a structure to dissipate energy through inelastic behaviour;
- R_o = Overstrength-related force modification factor that accounts for the dependable portion of reserve strength in a structure.

The relation:

$$V_e = S_{(T)} M_v I_E W \tag{4-4}$$

can also be established (Heidebrecht, 2003; Humar and Mahgoub, 2003) so the design seismic base shear equation can also be expressed as:

$$V = \frac{V_e}{R_d R_o} \tag{4-5}$$

Figure 4-1 shows the reduced elastic force that accounts for both the inelastic behaviour and the overstrength of the seismic force resisting system.

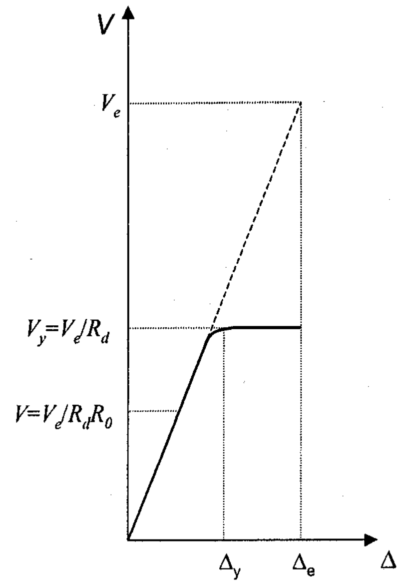

Figure 4-1: Resulting Reduced Design Force, V (From Mitchell *et al.*, 2003)

4.3 Conceptual Background and Definitions

4.3.1 Ductility

Park (1989) defines the concept of ductility as:

> *"The ability of a structure to undergo large amplitude cyclic deformations in the inelastic range without a substantial reduction in strength"*

Physically, the ductility ratio μ is defined by:

$$\mu = \frac{\Delta_{\max}}{\Delta_y} \qquad \textbf{(4-6)}$$

where Δ_{max} is the maximum displacement taken from any non-linear model or response from a test specimen and Δ_y is the yield displacement based on an idealized bilinear force-displacement curve.

From the elastic acceleration spectrum presented in Figure 4-2, three distinct sections of the spectrum and their respective assumptions for ductility definition are illustrated.

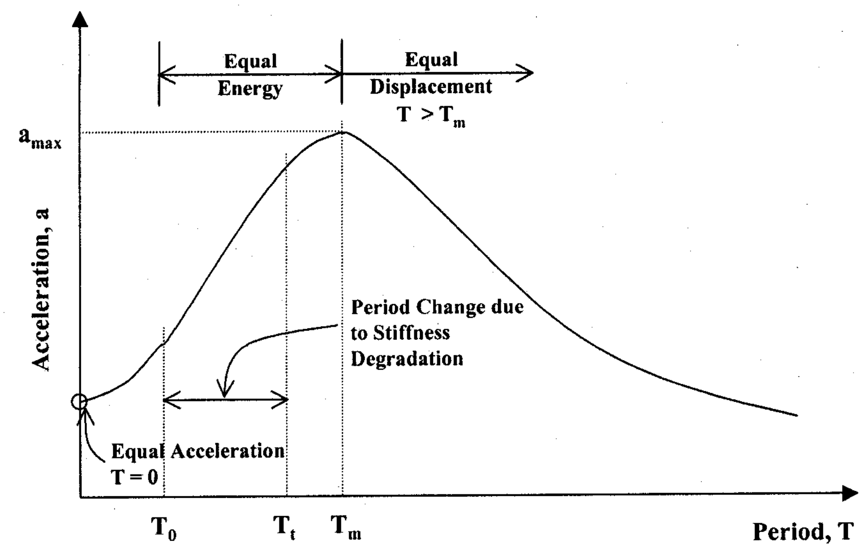

Figure 4-2: Elastic Acceleration Spectrum (Adapted from Paulay and Priestley (1992))

Newmark and Hall (1982) derived the relationship between the ductility ratio (μ) and the ductility-related force modification factor (R_d) depending on the period of a structure (Equations 4-7 to 4-9). These equations represent the three sections of the Elastic Acceleration Spectrum illustrated in Figure 4-2.

$R_d = \mu$	for T>0.5 sec	**(4-7)**
$R_d = \sqrt{2\mu - 1}$	for 0.1<T<0.5 sec	**(4-8)**
$R_d = 1$	for T<0.03 sec	**(4-9)**

These equations rely, respectively, on the equal displacement, equal energy and equal acceleration assumptions as illustrated in Figure 4-3.

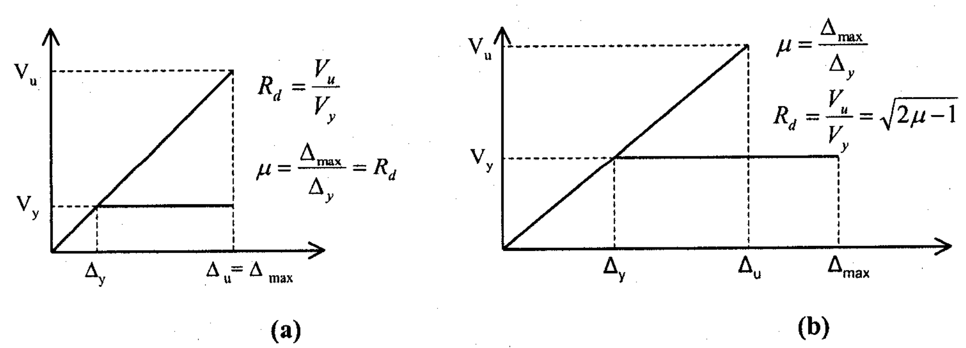

Figure 4-3: (a) Equal Displacement Theory; (b) Equal Energy Theory (From Gad *et al.*, 1999a)

The equal displacement principle (Figure 4-3 (a)) assumes that for a given earthquake, the perfectly elastic system and the equivalent elastic-plastic bilinear system have the same maximum lateral deflection. This principle, or Newmark's assumption, applies to structures with long periods (>0.5 sec). The NBCC seismic provisions have been developed by applying the equal displacement assumption for simplicity in defining the force modification factor, as demonstrated in Clause 4.1.9.2 (2) of the 1995 NBCC (NRCC, 1995):

> *"Lateral deflections obtained from an elastic analysis using the loads given (...) shall be multiplied by R to give realistic values of anticipated deflections"*

and in Clause 4.1.8.13 (2) of the 2005 NBCC draft (NRCC, 2004):

> *"Lateral deflections obtained from a linear elastic analysis using the methods given (...) and incorporating the effects of torsion, including accidental torsional moments, shall be multiplied by R_dR_o/I_E to give realistic values of anticipated deflections."*

However, if a system is stiffer, and therefore has a much shorter natural period than the dominant period of the acceleration spectrum, the equal displacement assumption can no longer be used. Stewart (1987) and Dolan (1989) observed that when a stiff system yields, its period becomes longer as a result of partial damage (e.g. loosening of the joints) and can enter in a quasi-resonance state as it approaches T_m on the acceleration spectrum (Filiatrault, 2002). For such systems, which also have a relatively short period of vibration (between 0.1 and 0.5 sec), the equal energy principle applies. This principle, illustrated in Figure 4-3 (b), states that the strain energy of an inelastic system must be equal to the strain energy of the corresponding elastic system. Or in more graphical terms, the area of the triangle representing the elastic system is set equal to the area under the bilinear curve:

$$\frac{V_u \cdot \Delta_u}{2} = V_y(\Delta_{max} - \Delta_y) + \frac{V_y \cdot \Delta_y}{2} \tag{4-10}$$

Using similar triangles, the following expression is obtained:

$$\frac{V_y}{\Delta_y} = \frac{V_u}{\Delta_u} \text{ or } \Delta_u = \frac{V_u \cdot \Delta_y}{V_y} \tag{4-11}$$

Equation 4-11 is substituted in Equation 4-10:

$$\frac{V_u \cdot V_u \cdot \Delta_y}{2 \cdot V_y} = V_y \left(\frac{\Delta_y}{2} + \left(\Delta_{\max} - \Delta_y \right) \right) \tag{4-12}$$

Simplifying 4-12 we find:

$$\left(V_u\right)^2 = \left(V_y\right)^2 \left(2 \cdot \frac{\Delta_{\max}}{\Delta_y} - 1 \right) = \left(V_y\right)^2 \left(2\mu - 1\right) \tag{4-13}$$

Or,

$$R_d = \frac{V_u}{V_y} = \sqrt{2\mu - 1} \tag{4-14}$$

Gad and Duffield (2000) found that the ductility ratio (μ) can vary considerably depending on the definition of yield and ultimate displacement. The selection of a suitable approach for the evaluation of yield and ultimate displacement is therefore crucial in the development of a seismic design procedure. Branston (2004) reviewed numerous techniques in order to facilitate the interpretation of test data for the highly non-linear steel frame / wood panel shear wall specimens. As mentioned in Chapter 3, the Equivalent Energy Elastic-Plastic (EEEP) model was implemented in this body of research in order to determine the design values of interest, such as the equivalent elastic wall stiffness, the yield wall resistance and the ductility. Figure 4-4 shows the bilinear curve obtained after applying the EEEP model.

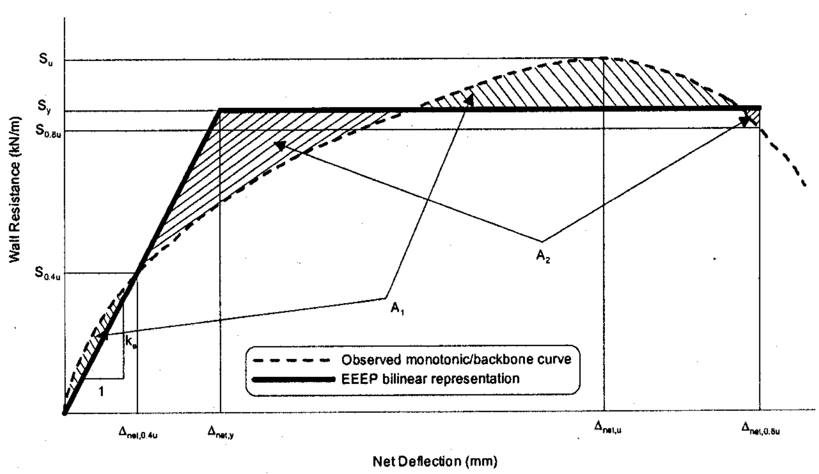

Figure 4-4: EEEP model (Park, 1989; Salenikovich *et al.*, 2000)

Applying the EEEP notation used for this research project to Equation 4-6, the following expression is obtained for the ductility ratio:

$$\mu = \frac{\Delta_{net,0.8u}}{\Delta_{net,y}} \qquad \textbf{(4-15)}$$

Ductility ratios for 108 tests[2] and the corresponding ductility-related force modification factors were calculated according to the equal energy method (Figure 4-3 (b)) and are presented in Section 4.4.1.

4.4 EVALUATION OF THE FORCE MODIFICATION FACTORS FROM EXPERIMENTAL DATA

4.4.1 DETERMINING THE DUCTILITY-RELATED FORCE MODIFICATION FACTOR (R_D)

As stated in Section 4.3.1, the determination of the ductility-related force modification factor (R_d) depends on the selected assumption for the displacement of an inelastic system (equal displacement or equal energy theories, Figure 4-3). Because the selection of an approach depends on the natural period of the SFRS, it is important to know what would be the expected natural period for low rise structures, in which light framed shear walls are usually used. Table 4-1 summarises the natural periods found from past experiments and calculation estimates for light-framed buildings.

[2] As mentioned in Chapter 3, a total of 109 specimens were actually tested, however test number 2 was only used for the determination of the FME in the definition of the SPD protocol, and was therefore not analysed.

Table 4-1: Summary of Findings for Natural Periods for Light-Framed Buildings

Building Type	Natural Period T_n (sec)	Reference
One, one and a half, and two storey North American residential house	0.06 to 0.25	Soltis *et al.* (1981)
Two and three storey North American residential house	0.14 to 0.32	Sugiyama (1984)
Residential House	0.25	Gad *et al.* (1999a)
Low rise wood frame structure	0.05 to 0.1	Foliente and Zacher (1994)
Residential houses (Univ. of BC code estimate)	0.18	Folz and Filiatrault (2001a)
Typical 8'x4' shear wall (NBCC 1995 estimate)	0.20	Zhao (2002)

The consistently low natural periods found in the literature suggest that the equal-energy approach should be used since $T_n < 0.5$ sec. Equation 4-8 can therefore be applied to the ductility ratio found with the EEEP approach and values for R_d can be derived. Table 4-2 presents the ductility and R_d values for the 108 tests carried out during the summer 2003 experimental testing program (Branston *et al.*, 2004, Branston, 2004; Chen, 2004) while Table 4-3 presents some statistical information by category of walls (wood panel type, wall length, fastener spacing and loading regime). The equal-displacement approach (Figure 4-3 (a)) to determine R_d is also represented in the table as is the ductility since, according to this theory, $\mu = \Delta_{\max}/\Delta_y = R_d$. The lowest value of the two, $R_d = \sqrt{2\mu - 1}$, was taken as R_d in order to obtain a conservative estimate of the ductility related force modification factor.

Table 4-2: Ductility and R_d Values for all 108 tests

Test ID	Wall Length	Sheathing	Fastener Schedule	Ductility (μ)	R_d[1]
1A	4	CSP	4/12	3.17	*[2] 2.31
1B	4	CSP	4/12	3.93	2.62
1C	4	CSP	4/12	4.44	2.81
1-A,B,C	**4**	**CSP**	**4/12**	**3.85**	**2.59**
1D	4	CSP	4/12	3.17	* 2.31
1E	4	CSP	4/12	4.18	2.71
1F	4	CSP	4/12	4.20	2.72
1-D,E,F	**4**	**CSP**	**4/12**	**3.85**	**2.59**
3A	4	CSP	4/12	7.21	3.66
3B	4	CSP	4/12	6.19	3.37
3C	4	CSP	4/12	6.23	3.39
3-A,B,C	**4**	**CSP**	**4/12**	**6.54**	**3.48**
4A	4	CSP	4/12	4.31	2.76
4B	4	CSP	4/12	4.39	2.79
4C	4	CSP	4/12	4.32	2.76
4-A,B,C	**4**	**CSP**	**4/12**	**4.34**	**2.77**
5A	4	DFP	4/12	3.75	* 2.55
5B	4	DFP	4/12	3.67	2.52
5C	4	DFP	4/12	2.80	* 2.14
5D	4	DFP	4/12	3.48	2.44
5-A,B,C,D	**4**	**DFP**	**4/12**	**3.63**	**2.50**
6A	4	DFP	4/12	3.80	* 2.57
6B	4	DFP	4/12	4.05	2.66
6C	4	DFP	4/12	4.60	2.86
6-A,B,C	**4**	**DFP**	**4/12**	**4.15**	**2.70**
7A	4	CSP	6/12	4.98	2.99
7B	4	CSP	6/12	5.68	3.22
7C	4	CSP	6/12	4.89	2.96
7-A,B,C	**4**	**CSP**	**6/12**	**5.18**	**3.06**
8A	4	CSP	6/12	5.74	3.24
8B	4	CSP	6/12	5.35	3.11
8C	4	CSP	6/12	5.61	3.20
8-A,B,C	**4**	**CSP**	**6/12**	**5.56**	**3.18**
9A	4	CSP	3/12	3.23	* 2.34
9B	4	CSP	3/12	3.17	2.31
9C	4	CSP	3/12	3.39	2.40
9-A,B,C	**4**	**CSP**	**3/12**	**3.26**	**2.35**
10A	4	CSP	3/12	3.81	2.57
10B	4	CSP	3/12	3.59	2.48
10C	4	CSP	3/12	2.90	2.19
10-A,B,C	**4**	**CSP**	**3/12**	**3.43**	**2.42**
11A	4	DFP	6/12	4.47	2.82
11B	4	DFP	6/12	4.65	2.88
11C	4	DFP	6/12	4.04	2.66
11-A,B,C	**4**	**DFP**	**6/12**	**4.39**	**2.79**
12A	4	DFP	6/12	5.76	3.24
12B	4	DFP	6/12	4.74	2.91
12C	4	DFP	6/12	4.73	2.91
12-A,B,C	**4**	**DFP**	**6/12**	**5.07**	**3.02**
13A	4	DFP	3/12	3.13	2.29
13B	4	DFP	3/12	3.45	2.43
13C	4	DFP	3/12	3.35	2.39
13-A,B,C	**4**	**DFP**	**3/12**	**3.31**	**2.37**
14A	4	DFP	3/12	3.83	2.58
14B	4	DFP	3/12	3.43	2.42
14C	4	DFP	3/12	4.14	2.70
14D	4	DFP	3/12	3.74	2.54
14-A,B,C,D	**4**	**DFP**	**3/12**	**3.78**	**2.56**
15A	2	CSP	6/12	3.58	* 2.48
15B	2	CSP	6/12	2.94	* 2.21
15C	2	CSP	6/12	1.52	* 1.43
15-A,B,C	**2**	**CSP**	**6/12**	**2.68**	**2.09**
16A	2	CSP	6/12	3.71	* 2.53
16B	2	CSP	6/12	3.34	* 2.38
16C	2	CSP	6/12	3.79	* 2.57
16-A,B,C	**2**	**CSP**	**6/12**	**3.61**	**2.49**
17A	2	CSP	4/12	2.00	* 1.73
17B	2	CSP	4/12	2.01	* 1.74
17C	2	CSP	4/12	2.36	* 1.93
17-A,B,C	**2**	**CSP**	**4/12**	**2.12**	**1.80**

Test ID	Wall Length	Sheathing	Fastener Schedule	Ductility (μ)	R_d
18A	2	CSP	4/12	2.91	* 2.20
18B	2	CSP	4/12	2.82	* 2.15
18C	2	CSP	4/12	2.70	* 2.10
18-A,B,C	**2**	**CSP**	**4/12**	**2.81**	**2.15**
19B	2	OSB	6/12	3.68	* 2.52
19C	2	OSB	6/12	4.45	* 2.81
19-A,B,C	**2**	**OSB**	**6/12**	**4.07**	**2.67**
20A	2	OSB	6/12	5.14	* 3.05
20B	2	OSB	6/12	5.38	* 3.12
20C	2	OSB	6/12	5.79	* 3.25
20-A,B,C	**2**	**OSB**	**6/12**	**5.44**	**3.14**
21A	4	OSB	6/12	7.18	3.66
21B	4	OSB	6/12	5.88	3.28
21C	4	OSB	6/12	7.22	3.67
21-A,B,C	**4**	**OSB**	**6/12**	**6.76**	**3.54**
22A	4	OSB	6/12	6.80	3.55
22B	4	OSB	6/12	7.24	3.67
22C	4	OSB	6/12	5.83	3.26
22-A,B,C	**4**	**OSB**	**6/12**	**6.62**	**3.50**
23A	4	OSB	4/12	4.57	2.85
23B	4	OSB	4/12	4.65	2.88
23C	4	OSB	4/12	5.42	3.14
23-A,B,C	**4**	**OSB**	**4/12**	**4.88**	**2.96**
24A	4	OSB	4/12	4.09	2.68
24B	4	OSB	4/12	6.15	3.36
24C	4	OSB	4/12	4.78	2.92
24-A,B,C	**4**	**OSB**	**4/12**	**5.00**	**3.00**
25A	4	OSB	3/12	3.88	2.60
25B	4	OSB	3/12	3.10	2.28
25C	4	OSB	3/12	3.75	2.55
25-A,B,C	**4**	**OSB**	**3/12**	**3.58**	**2.48**
26A	4	OSB	3/12	4.69	2.89
26B	4	OSB	3/12	3.74	2.54
26C	4	OSB	3/12	4.99	3.00
26-A,B,C	**4**	**OSB**	**3/12**	**4.47**	**2.82**
27A	2	OSB	4/12	3.93	* 2.62
27B	2	OSB	4/12	3.83	* 2.58
27C	2	OSB	4/12	3.72	* 2.54
27-A,B,C	**2**	**OSB**	**4/12**	**3.83**	**2.58**
28A	2	OSB	4/12	5.09	* 3.03
28B	2	OSB	4/12	3.90	* 2.61
28C	2	OSB	4/12	3.88	* 2.60
28-A,B,C	**2**	**OSB**	**4/12**	**4.29**	**2.75**
29A	8	CSP	6/12	5.94	3.30
29B	8	CSP	6/12	5.49	3.16
29C	8	CSP	6/12	6.00	3.32
29-A,B,C	**8**	**CSP**	**6/12**	**5.81**	**3.26**
30A	8	CSP	6/12	4.97	2.99
30B	8	CSP	6/12	5.20	3.07
30C	8	CSP	6/12	4.52	2.83
30-A,B,C	**8**	**CSP**	**6/12**	**4.89**	**2.96**
31A	8	CSP	4/12	4.32	2.76
31B	8	CSP	4/12	4.54	2.84
31C	8	CSP	4/12	4.53	2.84
31D	8	CSP	4/12	4.11	2.69
31E	8	CSP	4/12	4.14	2.70
31F	8	CSP	4/12	3.40	2.41
31-A,B,C,D,E,F	**8**	**CSP**	**4/12**	**4.17**	**2.71**
32A	8	CSP	4/12	4.60	2.86
32B	8	CSP	4/12	3.99	2.64
32C	8	CSP	4/12	3.93	2.62
32-A,B,C	**8**	**CSP**	**4/12**	**4.17**	**2.71**
33A	8	CSP	3/12	3.19	* 2.32
33B	8	CSP	3/12	3.31	* 2.37
33C	8	CSP	3/12	3.08	* 2.27
33-A,B,C	**8**	**CSP**	**3/12**	**3.19**	**2.32**
34A	8	CSP	3/12	3.85	2.59
34B	8	CSP	3/12	3.74	2.55
34C	8	CSP	3/12	4.01	2.65
34D	8	CSP	3/12	3.96	2.63
34-A,B,C,D	**8**	**CSP**	**3/12**	**3.89**	**2.60**

[1] $R_d = \sqrt{2\mu - 1}$

[2] The asterisk (*) signifies that the 2.5% drift limit has been applied

Note: Groups with even ID numbers were tested cyclically using the CUREE protocol and groups with odd ID numbers were tested monotonically, except for Group 3 which was tested cyclically with the Serrette *et al.* (2002) protocol.

Table 4-3: Statistical Information on Ductility-Related Seismic Force modification Factor (R_d)

Categories	Average R_d	Standard Dev.	CoV
All 108 Walls	2.73	0.40	14.7%
CSP walls	2.64	0.43	16.4%
DFP walls	2.66	0.23	8.7%
OSB walls	2.93	0.38	12.8%
610 mm (2') walls	**2.44**	0.42	17.2%
1220 mm (4') walls	2.83	0.38	13.2%
2440 mm (8') walls	2.76	0.32	11.6%
1220 mm (4') and 2440 mm (8') walls	2.82	0.36	12.7%
76 / 305 mm Spacing	**2.49**	0.17	6.7%
102 / 305 mm Spacing	2.66	0.39	14.5%
152 / 305 mm Spacing	2.96	0.43	14.4%
Monotonic	2.62	0.42	16.0%
Cyclic	2.84	0.36	12.7%

As is shown in Tables 4-2 and 4-3, shear walls of 610 mm (2') in length were found to provide especially low values for ductility mainly because the great majority exceeded the NBCC limit for the inelastic drift for regular buildings (2.5% of the storey height). As stated in Chapter 3, a shear wall response controlled by the 2.5% drift limit exhibits a lower ductility ratio because the maximum displacement is lowered to 61 mm, instead of using the displacement at the 0.8 S_u post-ultimate load level. Also, the low ductility ratio of the 610 mm long walls (height to length ratio: 4:1) can be explained by their low stiffness, which gives a higher yield displacement in comparison with the longer walls that were tested. Branston (2004) recommends a maximum aspect ratio (height : length) of 2:1 for shear walls considered in the lateral resistance system of a low-rise building. Within this limit (shear walls of 1220 mm (4') and 2440 mm (8') in length for 2440 mm (8') of height), no noticeable difference in terms of ductility can be observed between similar configuration specimens, i.e. shear walls with the same sheathing panel type and same fastener schedule. The average R_d value for all 1220 mm (4') and 2440 mm (8') long walls combined is 2.82.

Miranda and Bertero (1994) noted that the ductility ratio depends not only on the characteristics of the evaluated system, but also on the ground motion input, or in a quasi-static test case, on the reversed cyclic testing protocol applied to the system. This is demonstrated by the difference in measured ductility between tests 1 A,B,C and tests 3 A,B,C of this research program (both groups had the same configuration but test series 1 was tested monotically and test series 3 was loaded with the Serrette (SPD) cyclic protocol). The specimens tested under the SPD cyclic protocol exhibited a ductility ratio 35% higher than that obtained for the monotonic tests. As mentioned in Chapter 3, one of the main criteria for the selection of an appropriate cyclic loading protocol is the similitude of the monotonic and cyclic responses. When the specimens loaded with the CUREE protocol were compared with those tested monotically, a quasi-negligible difference of 5% in the ductility ratio was observed.

The wood sheathing type seemed to influence the ductility of a shear wall, especially when the specimen was sheathed with OSB ($\approx$11% increase). On the other hand, no significant difference was observed in terms of ductility between specimens sheathed with CSP panels and those sheathed with DFP panels. The ductility increase in the case of specimens sheathed with OSB could be explained by the composition of these panels, which consist of oriented thin wood strands glued together which benefit from a reduction of imperfections due to their small size. Also, shear walls sheathed with OSB panels benefited from a higher initial stiffness, which gives a lower yield displacement (Δ_y) and following Equation 4-15 leads to a higher ductility ratio.

A ductility-related seismic force modification factor of 2.5 is recommended for the design of light gauge steel frame / wood panel shear walls using the 2005 National Building Code of Canada. This value has been selected to conservatively represent the ductility based test results provided in Tables 4-2 and 4-3. Given that the yield displacement of a test specimen is required to calculate the ductility, and that the ductility is relied on to determine R_d, it follows that the EEEP analysis approach (Branston, 2004) must be implemented in the determination of shear wall strength values for this value of the force modification factor to be valid.

4.4.2 Determining the Overstrength-Related Force Modification Factor (R_O)

The limit states design philosophy, as applied in Canada, dictates that a structure must be designed to have a factored resistance greater than the sum of the factored loads. However, it has been repeatedly shown that the reserve of strength due to conservative design values increases with the ductility and the redundancy of a structure (Nassar and Krawinkler, 1991; Paulay and Priestley, 1992; Mitchell *et al.*, 2003). Therefore, it is important for the designer to consider an overstrength factor for seismic design.

As stated in Equation 4.3, the proposed seismic base shear equation in the 2005 NBCC includes a parameter R_o to account for the built-in reserve of strength available within the SFRS and beyond the minimum resistance required by the code. Since numerous components contribute to this reserve of strength, the following equation was chosen to evaluate the overstrength-related force modification factor (Mitchell *et al.*, 2003):

$$R_o = R_{size} \cdot R_{\phi} \cdot R_{yield} \cdot R_{sh} \cdot R_{mech} \qquad \textbf{(4-16)}$$

where:

- R_{size} = Overstrength due to restricted choices for member sizes and dimension rounding;
- R_{Φ} = Overstrength due to the difference between nominal and factored resistances, or $1/\Phi$;
- R_{yield} = Ratio of probable yield strength to minimum specified yield strength;
- R_{sh} = Overstrength arising due to strain hardening;
- R_{mech} = Overstrength developed when a collapse mechanism is formed.

The factor R_{size} accounts for the fact that designers are usually restricted in their choice of member sizes and/or fastener spacings by the available standardised sections and rounding of dimensions. R_{Φ} relates the difference between the nominal and factored resistances, considering that it is appropriate to use nominal resistances in the design of structures for rare events such as earthquakes (return period of 2500 years in the case of the NBCC 2005). For the same reason, R_{yield} is the ratio of the actual to the minimum specified material strength because the latter is usually underestimated. If strain hardening is expected in the inelastic deformation of a structure, R_{sh} is to be evaluated. When yielding is to take place in a sequence rather than in all members at once, R_{mech} is to be included because this factor accounts for the additional resistance that can be exploited just before a collapse mechanism occurs. With these definitions in mind, numerical values for each of these factors can be derived from the empirical data obtained during the testing programme.

As found by Branston (2004), the resistance factor of a steel frame / wood panel shear wall is Φ=0.7 when the EEEP approach is utilized in the definition of a nominal design strength. R_{Φ} is therefore 1/0.7 = 1.43. As opposed to wood framed shear walls where strain hardening can occur due to the bending of the nails, the screw in a steel frame / wood panel shear wall does typically not bend because of its ability to tilt freely around the steel layer. Therefore, a value for R_{sh} of 1.0 was assumed. Also, because procedures are not yet established for the design of steel frame / wood panel structures in Canada, a value of 1.0 for R_{mech} was chosen. The R_{size} component was set to 1.05 to account for the fact that designers typically choose practical fastener spacings, which are in most instances smaller than that required to meet the calculated design loads. Finally, in order to determine the ratio of the actual to the minimum specified material strength the measured shear resistance, S_u, and nominal yield capacity, S_y, were relied on. Figure 4-5 shows graphically the overstrength that is associated with the nominal design values that are obtained using the EEEP analysis approach. Tables 4-4 and 4-5 present the individual overstrength ratios, S_u / S_y, for each shear wall test. The overall average of the monotonic and cyclic results leads to an R_{yield} factor of 1.22.

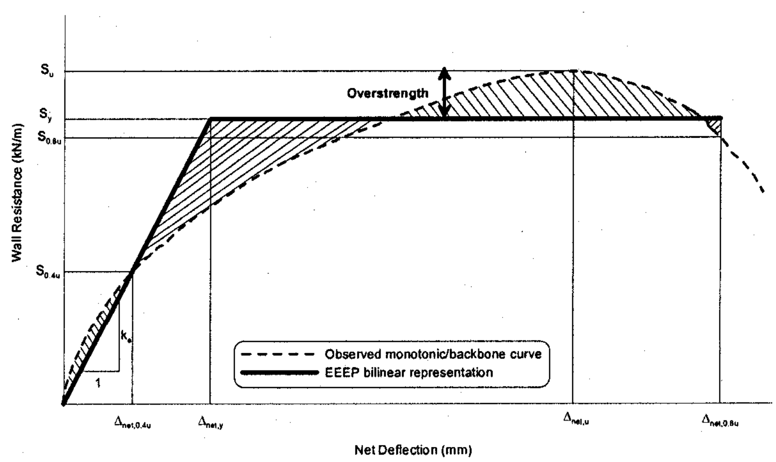

Figure 4-5: Ratio of the actual to the minimum specified shear strength

Table 4-4 : Overstrength inherent in design for monotonic test values (Branston, 2004)

Test N°	Length	Sheathing	Fastener Schedule	Ultimate Resistance (S_u) kN/m	Yield Load (S_y) kN/m	Overstrength S_u/S_y
1A	4	CSP	4/12	15.9	14.4	1.10
1B	4	CSP	4/12	17.1	14.4	1.19
1C	4	CSP	4/12	16.8	14.4	1.17
1-A,B,C	**4**	**CSP**	**4/12**	**16.6**	**14.4**	**1.15**
5A	4	DFP	4/12	21.1	19.1	1.10
5B	4	DFP	4/12	25.7	19.1	1.35
5C	4	DFP	4/12	23.9	19.1	1.25
5D	4	DFP	4/12	24.5	19.1	1.28
5-A,B,C,D	**4**	**DFP**	**4/12**	**23.8**	**19.1**	**1.25**
7A	4	CSP	6/12	12.0	10.6	1.13
7B	4	CSP	6/12	12.6	10.6	1.19
7C	4	CSP	6/12	13.6	10.6	1.28
7-A,B,C	**4**	**CSP**	**6/12**	**12.7**	**10.6**	**1.20**
9A	4	CSP	3/12	27.2	21.6	1.26
9B	4	CSP	3/12	23.5	21.6	1.09
9C	4	CSP	3/12	24.7	21.6	1.14
9-A,B,C	**4**	**CSP**	**3/12**	**25.1**	**21.6**	**1.16**
11A	4	DFP	6/12	15.8	12.9	1.22
11B	4	DFP	6/12	16.9	12.9	1.31
11C	4	DFP	6/12	15.3	12.9	1.19
11-A,B,C	**4**	**DFP**	**6/12**	**16.0**	**12.9**	**1.24**
13A	4	DFP	3/12	28.0	24.5	1.14
13B	4	DFP	3/12	30.8	24.5	1.26
13C	4	DFP	3/12	30.4	24.5	1.24
13-A,B,C	**4**	**DFP**	**3/12**	**29.7**	**24.5**	**1.21**
21A	4	OSB	6/12	13.4	11.0	1.22
21B	4	OSB	6/12	13.1	11.0	1.19
21C	4	OSB	6/12	13.3	11.0	1.21
21-A,B,C	**4**	**OSB**	**6/12**	**13.3**	**11.0**	**1.21**
23A	4	OSB	4/12	19.1	16.2	1.18
23B	4	OSB	4/12	20.3	16.2	1.25
23C	4	OSB	4/12	18.5	16.2	1.14
23-A,B,C	**4**	**OSB**	**4/12**	**19.3**	**16.2**	**1.19**
25A	4	OSB	3/12	23.7	20.6	1.15
25B	4	OSB	3/12	22.2	20.6	1.08
25C	4	OSB	3/12	24.7	20.6	1.20
25-A,B,C	**4**	**OSB**	**3/12**	**23.5**	**20.6**	**1.14**
29A	8	CSP	6/12	13.6	10.6	1.28
29B	8	CSP	6/12	13.8	10.6	1.30
29C	8	CSP	6/12	13.3	10.6	1.25
29-A,B,C	**8**	**CSP**	**6/12**	**13.6**	**10.6**	**1.28**
31A	8	CSP	4/12	21.9	14.4	1.52
31B	8	CSP	4/12	18.8	14.4	1.31
31C	8	CSP	4/12	19.8	14.4	1.38
31D	8	CSP	4/12	19.2	14.4	1.33
31E	8	CSP	4/12	22.6	14.4	1.57
31F	8	CSP	4/12	21.0	14.4	1.46
31-A,B,C,D,E,F	**8**	**CSP**	**4/12**	**20.6**	**14.4**	**1.43**
33A	8	CSP	3/12	26.1	21.6	1.21
33B	8	CSP	3/12	27.4	21.6	1.27
33C	8	CSP	3/12	25.6	21.6	1.19
33-A,B,C	**8**	**CSP**	**3/12**	**26.4**	**21.6**	**1.22**

Average	**1.24**
Standard Dev.	**0.08**
CoV	**6.1%**

Table 4-5 : Overstrength inherent in design for cyclic test values (Branston, 2004)

Test N°	Length	Sheathing	Fastener Schedule	Ultimate Resistance (S_u) kN/m	Yield Load (S_y) kN/m	Overstrength S_u/S_y
4A	4	CSP	4/12	16.1	14.4	1.12
4B	4	CSP	4/12	17.6	14.4	1.22
4C	4	CSP	4/12	18.7	14.4	1.30
4-A,B,C	**4**	**CSP**	**4/12**	**17.5**	**14.4**	**1.21**
6A	4	DFP	4/12	22.6	19.1	1.18
6B	4	DFP	4/12	22.9	19.1	1.20
6C	4	DFP	4/12	22.3	19.1	1.17
6-A,B,C	**4**	**DFP**	**4/12**	**22.6**	**19.1**	**1.18**
8A	4	CSP	6/12	12.0	10.6	1.13
8B	4	CSP	6/12	11.9	10.6	1.12
8C	4	CSP	6/12	11.8	10.6	1.11
8-A,B,C	**4**	**CSP**	**6/12**	**11.9**	**10.6**	**1.12**
10A	4	CSP	3/12	26.1	21.6	1.21
10B	4	CSP	3/12	26.9	21.6	1.25
10C	4	CSP	3/12	25.5	21.6	1.18
10-A,B,C	**4**	**CSP**	**3/12**	**26.2**	**21.6**	**1.21**
12A	4	DFP	6/12	13.5	12.9	1.05
12B	4	DFP	6/12	16.0	12.9	1.24
12C	4	DFP	6/12	14.4	12.9	1.12
12-A,B,C	**4**	**DFP**	**6/12**	**14.6**	**12.9**	**1.13**
14A	4	DFP	3/12	31.0	24.5	1.27
14B	4	DFP	3/12	29.0	24.5	1.18
14C	4	DFP	3/12	29.5	24.5	1.20
14D	4	DFP	3/12	29.1	24.5	1.19
14-A,B,C,D	**4**	**DFP**	**3/12**	**29.7**	**24.5**	**1.21**
22A	4	OSB	6/12	11.7	11.0	1.06
22B	4	OSB	6/12	11.9	11.0	1.08
22C	4	OSB	6/12	11.5	11.0	1.05
22-A,B,C	**4**	**OSB**	**6/12**	**11.7**	**11.0**	**1.06**
24A	4	OSB	4/12	17.0	16.2	1.05
24B	4	OSB	4/12	17.4	16.2	1.07
24C	4	OSB	4/12	17.2	16.2	1.06
24-A,B,C	**4**	**OSB**	**4/12**	**17.2**	**16.2**	**1.06**
26A	4	OSB	3/12	24.0	20.6	1.17
26B	4	OSB	3/12	22.6	20.6	1.10
26C	4	OSB	3/12	23.9	20.6	1.16
26-A,B,C	**4**	**OSB**	**3/12**	**23.5**	**20.6**	**1.14**
30A	8	CSP	6/12	13.5	10.6	1.27
30B	8	CSP	6/12	13.1	10.6	1.24
30C	8	CSP	6/12	13.4	10.6	1.26
30-A,B,C	**8**	**CSP**	**6/12**	**13.3**	**10.6**	**1.26**
32A	8	CSP	4/12	20.0	14.4	1.39
32B	8	CSP	4/12	20.7	14.4	1.44
32C	8	CSP	4/12	20.4	14.4	1.42
32-A,B,C	**8**	**CSP**	**4/12**	**20.4**	**14.4**	**1.41**
34A	8	CSP	3/12	26.8	21.6	1.24
34B	8	CSP	3/12	29.1	21.6	1.35
34C	8	CSP	3/12	28.0	21.6	1.30
34D	8	CSP	3/12	30.5	21.6	1.41
34-A,B,C,D	**8**	**CSP**	**3/12**	**28.6**	**21.6**	**1.32**

Average	**1.20**
Standard Dev.	**0.10**
CoV	**8.6%**

Table 4-6 provides a summary of the different numerical values of the overstrength-related force modification factor components, as well as a proposed R_o value of 1.8 for use in seismic design following the 2005 National Building Code of Canada. This value is largely dependent on the resistance factor and the overstrength. As noted for the ductility related force modification factor, the EEEP analysis approach (Branston, 2004) must be implemented in the determination of shear wall strength values for this value of the overstrength related force modification factor to be valid.

Table 4-6: Overstrength-related force modification factors for steel frame / wood panel shear walls

Calculation of R_o						Proposed
R_{size}	R_Φ	R_{yield}	R_{sh}	R_{mech}	R_o	R_o (NBCC)
1.05	1.43	1.22	1.0	1.0	1.83	**1.8**

4.5 PARTIAL CONCLUSIONS

Values for the ductility-related and overstrength-related force modification factors are proposed in this Chapter. By using the equal energy assumption to determine the ductility of a system composed of steel frame / wood panel shear walls, a value of 2.5 for R_d is suggested with limitation in terms of aspect ratio (max 2:1). The recommended overstrength-related force modification factor (R_o) is set to 1.8. The NBCC 2005 (NRCC, 2004) assigns an R_d value of 3.0 and an R_o value of 1.7 for nailed shear walls with wood-based panels (Mitchell *et al.*, 2003). The proposed values for steel framed/wood panel shear walls presented in this study seem therefore realistic knowing that wood framed and steel framed shear walls behave similarly when submitted to seismic loading.

Comparison with other model building codes such as the Uniform Building Code 1997 (UBC 1997) (ICBO, 1997) and the International Building Code 2003 (IBC 2003) (ICC, 2003) from the US is possible if the product of R_d and R_o is compared to the R-Factor values. It is assumed that the R-factors of these codes represent the system ductility and the structural over-strength factors combined. Table 4-7 lists the proposed reduction factor values presented in this Chapter and those used in the United States. Although a direct comparison is not possible due to the inconsistency in the R-Factor definitions from one building code to another, it can be observed that the proposed values are on the conservative side when compared with those from the US.

Table 4-7 : R-Factor values for steel frame/wood panel shear walls from different building codes

Proposed R_d	Proposed R_o	Proposed R_dR_o	UBC 1997 R Factor	IBC 2003 R factor
2.5	1.8	4.5	5.5	6.5

The proposed values included in this research are based on a limited sample of shear wall configurations. Further research is needed to verify these values if important design characteristics such as wall aspect ratio, panel thickness, fastener spacing, steel stud gauge, etc, are different from those contained in the scope of this study.

The proposed values, especially the ductility-related force modification factor, should be verified using the methodology for the assessment of force modification factors as expressed by Ceccotti and Karacabeyli (2000), which includes the following steps:

1. Full scale testing of shear wall specimens under monotonic and cyclic protocols;
2. Matching of an hysteresis model to the backbone curve;
3. Performing a non-linear time-history dynamic analysis under selected earthquake records in order to obtain the ultimate peak ground acceleration (PGA) at which the building reaches a near-collapse state;
4. Comparing the obtained PGA values to the code maximum values to assess the suitability of the hypothetical force modification factor;
5. Performing shake-table tests to ensure the appropriateness of the design methodology.

Furthermore, the Canadian National Committee on Earthquake Engineering (CANCEE), whose responsibility is to provide recommendations for the development of the seismic design aspects of Part 4 of the National Building Code of Canada, requires that force modification factors be justified accordingly. Firstly, this includes an evaluation of R_d and R_o based on the results of physical tests. The adequate seismic performance of representative buildings designed with the test based force modification factors must then be confirmed with the use of non-linear time-history dynamic analyses. Finally, proof of performance through dynamic shake table testing or through an evaluation of structures that have been subjected to a significant earthquake is needed.

The author (Chapter 3), as well as Branston (2004) and Chen (2004), have presented the results of full-scale testing as required by Step 1. Step 2, as defined by Ceccotti and Karacabeyli, is presented in Chapter 5 where a hysteresis model is suggested for the various wall types that were tested. It is recommended that Steps 3, 4 and 5 should eventually be carried out to confirm the recommended force modification factors, or to propose new values.

CHAPTER 5

HYSTERETIC MODELING OF STEEL FRAME / WOOD PANEL SHEAR WALLS

5.1 INTRODUCTION

To a large extent our knowledge of the behaviour of light framed shear walls subjected to seismic loads comes from full-scale experiments with limited theoretical considerations. These testing programs are generally very expensive and labour intensive. Therefore, the development of numerical methods and computer modeling is important in order to understand, predict and mimic the response of the system subjected to earthquake ground motions and eventually to provide a better comprehension of the complex structural behaviour.

Computer modeling and 3-D dynamic analyses are commonly used in the design of steel and reinforced concrete structures due to the always increasing availability of commercial advanced structural analysis software. Nowadays, a personal computer equipped with the appropriate software can solve complex finite element problems or time-history analyses within a reasonable computing time. However, for the design of light framed structures, such as found in residential houses and low-rise buildings, very limited dynamic and seismic force analyses have traditionally been carried out mainly because the commercial structural analysis software packages are not very efficient in their modeling (Filiatrault *et al.*, 2000). The need for computer analysis is becoming more obvious when we realize that lateral force resisting systems within such buildings can be very intricate (CUREE, 2002). The intrinsic characteristics of shear walls, such as non-linearity, a large number of redundant components, high variability in the strength and stiffness properties of wood components and their connections, etc, make analyses with commercial software less accurate than the equivalent analyses for steel or concrete buildings.

Included in this chapter is a description of these intrinsic characteristics, an overview of the different available hysteretic models, a review of available computer software and recommendations for the use of a hysteretic rule-and-software combination adapted to run inelastic time-history analyses for buildings with steel frame / wood panel shear walls as a lateral-force-resisting system.

5.2 Characteristics of Steel Frame / Wood Panel Shear Wall Hysteresis

Every seismic force resisting system (SFRS) loaded in shear exhibits hysteretic behaviour of its load-deformation curve. In part, factors that influence the hysteresis loops can be attributed to external variables such as the load protocol and the rate of loading (ref. Chapter 2), as well as material and structural characteristics of the SFRS itself. For instance, steel, concrete and wood shear walls do not necessarily behave similarly when loaded cyclically.

The load-deformation hysteresis curve of a typical 1220 x 2440 mm (4' x 8') steel frame / wood panel shear wall is shown in Figure 5-1. From this figure, we can visually appreciate the asymmetrical "butterfly" shape characterized by the narrowing of the wall resistance amplitude near the origin. These cycles are mainly characterised by the minimal energy dissipation in the second and fourth quadrants of the graph (Ceccotti and Vignoli, 1989).

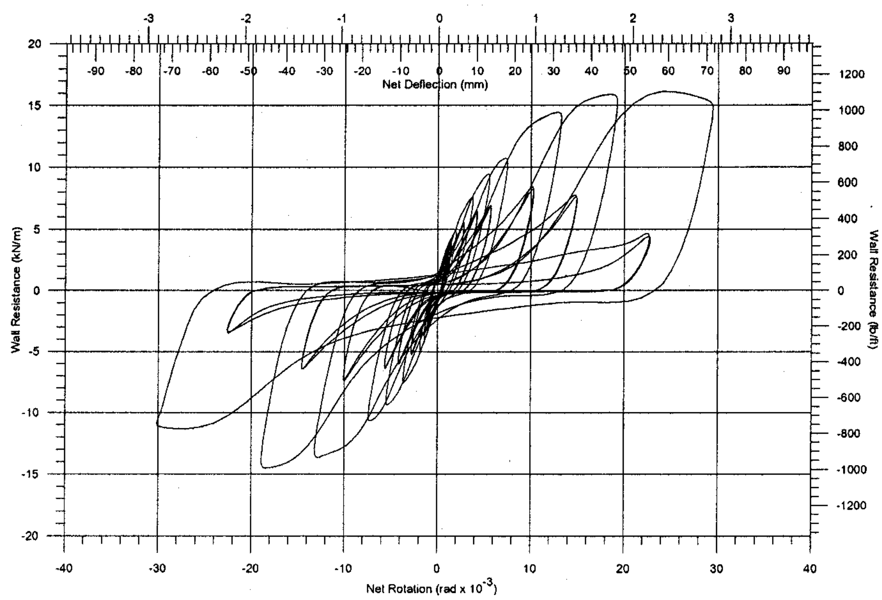

Figure 5-1 Typical Load-Deformation Hysteresis Curve of a Tested Shear Wall

Many researchers (Dowrick, 1986; Stewart, 1987; Dolan, 1989; Filiatrault, 1990; Salenikovich *et al.*, 2000; Richard *et al.*, 2001) have shown in previous studies that the global force-deformation response of a wood frame shear wall is in many ways identical and fully attributable to that of the individual sheathing-to-framing connectors. In a wood frame shear wall nail connections are typically used, whereas in a steel frame / wood panel shear wall screw fasteners are common. Therefore, in a wood frame wall the wood bearing deformation and nail bending contribute to the behaviour of the connection; however, in a steel frame / wood panel wall the wood plays a more important role because the screw does not exhibit any extensive amount of bending deformation.

Wood panel shear walls are therefore extensively influenced by their load history and plastic deformation at the connection level. Memory effect, as it is often called, occurs when the load-deformation relation of a cycle is directly influenced by the displacement and load level of the previous cycle. This particular characteristic makes modeling of panel to frame connections under cyclic loading significantly more complex than the modeling of a monotonic loading case.

The most prominent characteristics of a shear wall hysteresis curve are: highly non-linear behaviour from the onset of loading, progressive loss of lateral stiffness in each loading cycle (will be referred to as stiffness degradation), degradation of strength when cyclically loaded at the same displacement level (strength degradation) and pinched hysteresis loops.

5.2.1 NON-LINEARITY

Unlike other SFRSs constituted of material such as steel or concrete, where the behaviour is linear at low strain, wood panel shear walls exhibit highly non-linear behaviour of the load-displacement hysteresis curve even at very low displacement levels (as shown in Figure 5-2). This feature is mainly due to the fact that the wall is a complex structure including steel studs, wood sheathing, hold downs and connectors. As mentioned in Chapter 2, this inelastic load-displacement relationship hinders the determination of a distinct yield point. The non-linear behaviour of the shear wall can be explained by a close look at the behaviour of a single sheathing-to-framing connector under loading, as shown in Figure 3-16.

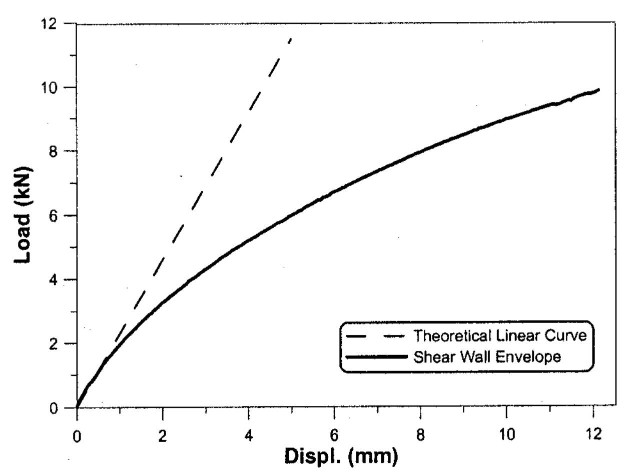

Figure 5-2 Non-linear Force-Displacement Relationship for a Typical Shear Wall at Low Loading

5.2.2 STIFFNESS DEGRADATION

The tendency for the effective stiffness of the wall over successive loops to decrease, as described by Dinehart and Shenton III (1998) and van de Lindt and Walz (2003), is expressed as the slope of the virtual straight line between the positive and the negative excursion peaks of a hysteresis loop (see Equation 5-1).

$$k_E = \frac{F_p^{i+1} - F_p^i}{x_p^{i+1} - x_p^i} \quad \textbf{(5-1)}$$

In Equation 5-1, F_p represents the peak force and x_p the corresponding displacement. This characteristic is particularly present in light-framed structures such as the steel frame / wood panel shear walls under study. The stiffness degradation results in a reduction of the amount of dissipated energy, i.e. the area of a degraded hysteresis loop is smaller than if there were no degradation. Knowledge of this characteristic is crucial such that an over estimation of the wall stiffness and ability to dissipate energy is avoided in design. An example of stiffness degradation for a typical 1220 x 2440 mm (4' x 8') steel frame / wood panel shear wall is shown in Figure 5-3 where the effective stiffness is plotted as a function of the hysteresis loop number. In the final stages of the loading protocol, a near zero stiffness is observed due to the failure of an extensive section of screw connections (generally unzipping of a complete edge of the wall, see Figure 3-22).

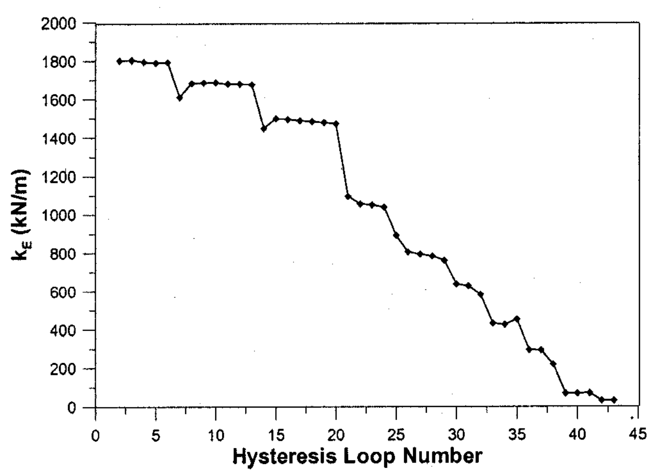

Figure 5-3 Effective Stiffness vs Hysteresis Loop Number

5.2.3 STRENGTH DEGRADATION

The strength degradation phenomenon can be easily pictured as the difference in capacity of a structure when cyclically loaded to the same displacement level. At the fastener scale, the formation of play around the screw head during the first excursion in a given direction results in a lower capacity for successive loops at the same displacement level simply because we can expect less resistance from the crushed wood around the fastener.

Although strength degradation is a noticeable feature of a shear wall hysteresis force-deformation curve (see Figure 5-4), it is considered by many researchers (Stewart, 1987; Ceccotti and Vignoli, 1989; Dolan, 1989; van de Lindt and Walz, 2003) to play a lesser role than the other characteristics such as stiffness degradation and pinching in the response of a shear wall. Therefore, it was not considered in most of the hysteretic models under study.

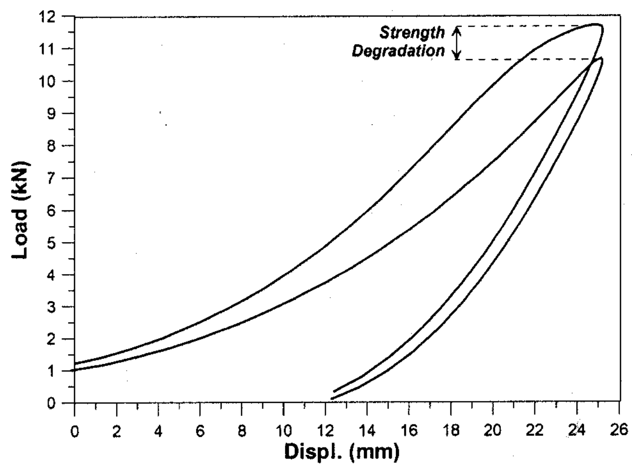

Figure 5-4 Strength Degradation Representation Between Two Successive Loops

5.2.4 PINCHING

Probably the most prominent feature of a steel frame / wood panel shear wall hysteresis curve is the pinching effect. Pinching is caused by the loss of stiffness at the connection level, where a gap or slot is formed around the screw head when the wood fibres are crushed. With each reversed displacement of the structure, the resistance is greatly reduced as the fasteners move freely through the slot until contact with the wood is reinstated and a gain in stiffness is re-established. When moving through the gap, the screw is free to tilt without wood support around its head and the contact between the shank's threads and the thin layer of steel provides a residual resistance to the applied load. The reduced but existing friction that remains between the screw and the edges of the slot in the wood sheathing also contributes to the remaining resistance. This residual resistance can be observed to be quite constant even after consecutive loops as shown in Figure 5-5 where the intercept load is represented. Pinched hysteresis loops are therefore a consequence of the stiffness degradation described above.

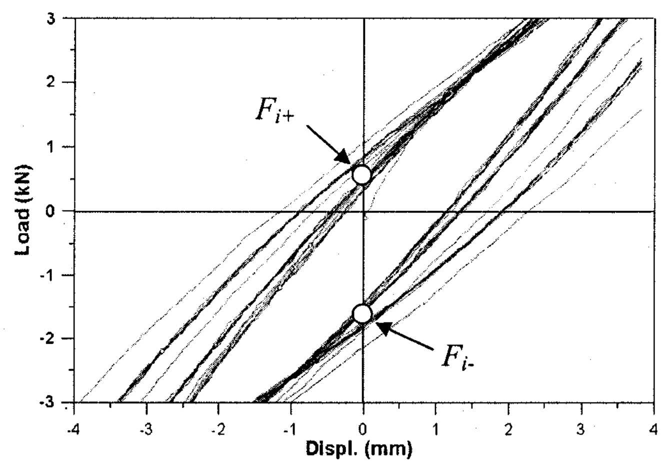

Figure 5-5 Intercept Force at Zero Displacement

Figure 5-6 illustrates the different levels of pinching that may be observed. At very low displacement levels, pinching is not yet visible because of the low damage inflicted to the wood (see Figure 5-6 (a)). With increasing displacement, inflection points appear and consequently the area enclosed within the loop, which is a direct measure of seismic energy dissipation due to hysteresis, diminishes (Figure 5-6 (b) and (c)). Thus, neglecting pinching in development of a shear wall model would lead to an overestimation of dissipated energy and would yield to unconservative response estimates.

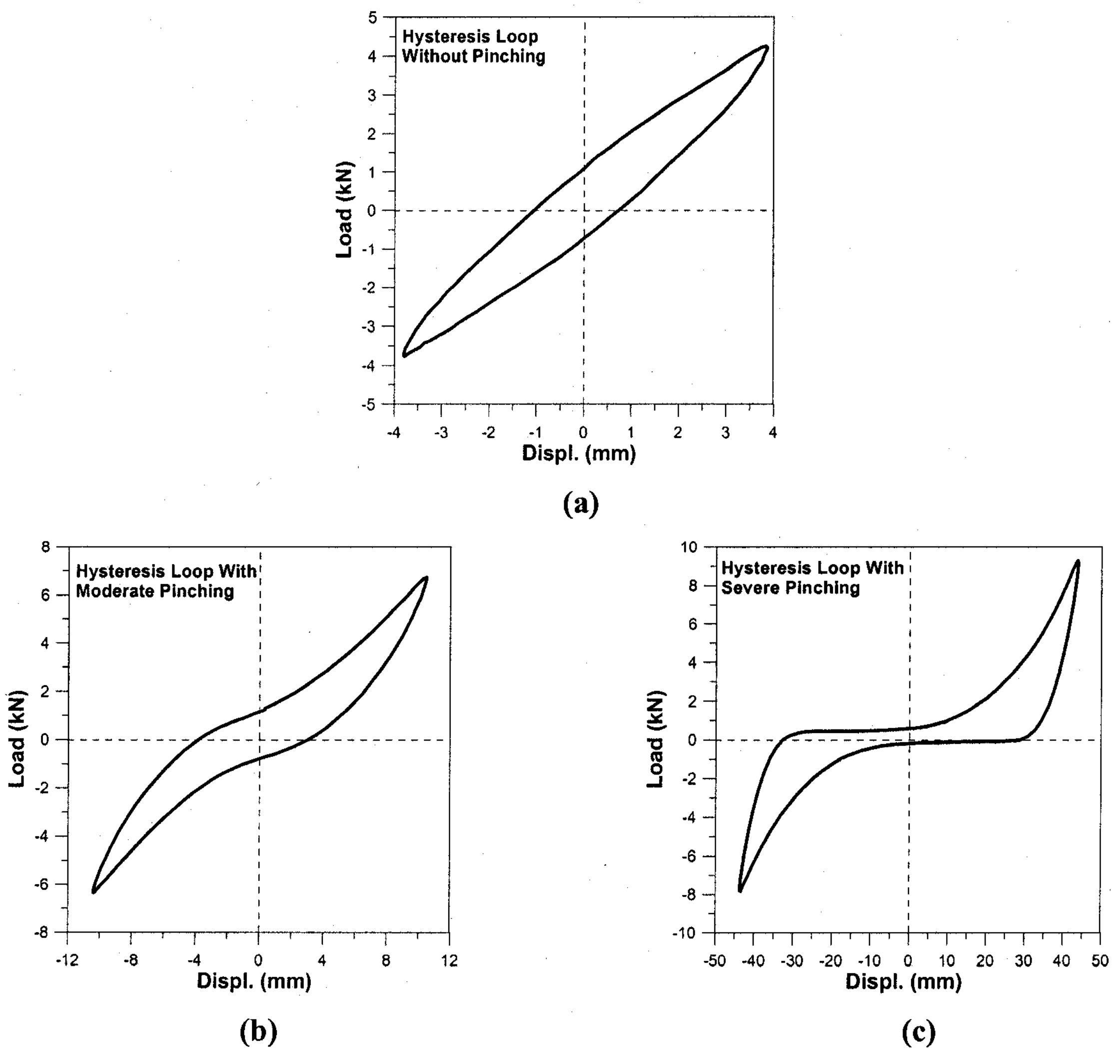

Figure 5-6 Evolution of Pinched Hysteresis Loops with Increased Displacement Level

5.3 REVIEW OF EXISTING HYSTERESIS MODELS

Historically, the trend to replicate or mimic the seismic response of structures became popular with the availability and enhanced performance of computing devices and software. As mentioned previously, the lack of theoretical research has to be filled to study the dynamic behaviour of light framed structures such as wood panel shear walls to assess their performance and safety towards seismic design. As for now, this type of structure is treated unfavourably by stringent prescriptive code requirements, and therefore put at a disadvantage when compared with other usual construction materials such as structural steel or reinforced concrete (Foliente, 1995).

Due to the relatively recent use of light gauge steel studs in the shear wall industry, no hysteretic models have been developed for them exclusively. However, the general behaviour of a steel frame / wood panel shear wall is in many points similar to walls made from wood framing members (Rogers *et al.*, 2004). The origins of hysteretic modeling for wood structures go back to the early 1980s, where researchers and mathematicians derived formulas for sheathing fastener forces (van de Lindt, 2004). Since then, modeling has evolved in different areas: from finite element modeling (FEM) of fasteners to non-linear time-history analyses of single degree of freedom (SDOF) models and recently cyclic analysis models.

For the purposes of this research, a selection of models is reviewed in this section and their application to the shear wall configuration that is under study is evaluated. Focus is made on their ability to model or mimic the characteristics itemised in Section 5.2.

5.3.1 The Bouc-Wen-Baber-Noori (BWBN) Model (1986)

The BWBN model was initiated by Bouc (1967) who developed one of the first closed-form mathematical hysteresis models for structures in general. In the following decades, many researchers improved the basic model to integrate stiffness degradation, strength degradation and pinching, and hence make this model of interest for wood structures design. Foliente (1995) modified the pinching equation and tested its applicability to wood systems.

This model draws its sources from a "black-box approach" (Heine, 2001) which refers to the simplification of a complex system in an equivalent structure consisting of a mass (m) connected to an elastic spring (k), a viscous damper (c) and a hysteretic element ($z(t)$ Figure 5-7). To calibrate the system and its various components, empirical data are necessary but extrapolation is permitted. The BWBN model is therefore valid for a wide range of system configurations.

That being said, the model is restricted in its application by some important shortcomings. Firstly, pinching effect, especially for wood structures, is exclusively controlled by the displacement level, and not by the dissipated energy as assumed by the model (Heine, 2001; Foliente, 1995).

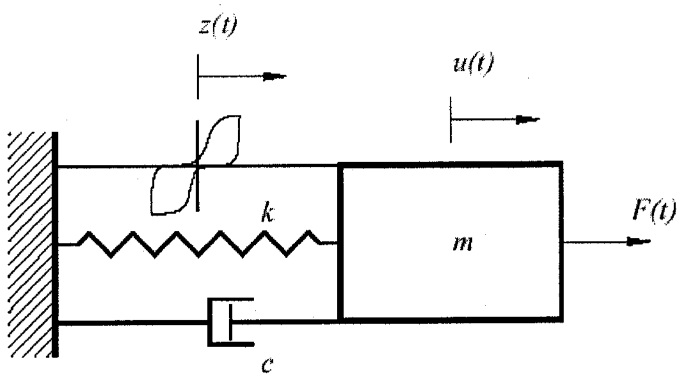

Figure 5-7 "Black-box" Representation of a SDOF System (Baber and Noori [1986])

5.3.2 STEWART (1987)

Stewart carried out research on plywood sheathed shear walls at the University of Canterbury, in New Zealand, and developed a hysteretic model especially for this type of structure to be used in a non-linear time history computer analysis program. The hysteretic approximation consists of a series of straight-line segments calibrated by various parameters. The model is a single degree-of-freedom (SDOF) lumped parameter model able to predict the seismic response of wood shear walls. The general shape of the model is shown in Figure 5-8 and the calibration parameters are itemised in Table 5-1.

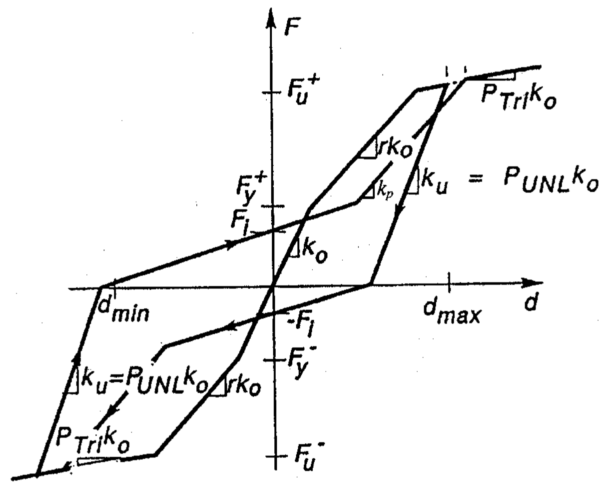

Figure 5-8 Stewart Degrading Hysteresis (Carr, 2000)

Table 5-1 : Stewart Hysteresis Model Calibration Parameters

Parameter	Description	Units
k_0	Initial Wall Stiffness	N/mm
F_u	Ultimate Force (>0.0)	N
F_y	Yield Force (>0.0)	N
r	Bi-Linear Factor beyond yield force	-
F_i	Intercept Force (>0.0)	N
P_{Tri}	Tri-Linear factor beyond ultimate force	-
P_{UNL}	Unloading Stiffness Factor (>1.0)	-
Gap_+	Initial Slackness, Positive Axis (>0.0)	mm
Gap_-	Initial Slackness, Negative Axis (<0.0)	mm
β (Beta)	Softening Factor (1.0)	-
α (Alpha)	Reloading or Pinch Power Factor (1.0)	-

The Stewart Hysteresis model is included in the RUAUMOKO® Inelastic Dynamic Analysis software package and is described by Carr (2000) as :

"A model that allows for initial slackness as well as subsequent degradation of the stiffness as the nails enlarged the holes and withdrew themselves from the framework"

More specifically, the loading sequence of the model is as follows. Until a predefined yield point (F_y), the response force follows the initial stiffness (k_0). When the hysteretic force exceeds F_y, the stiffness is reduced by the bi-linear factor (r) and then by the tri-linear factor (P_{Tri}) if deemed necessary. Unloading stiffness is also adjusted from the initial wall stiffness by the unloading stiffness factor (P_{UNL}). Initial slackness (Gap_+, Gap_-) can be included, if necessary, in the first cycle to account for the possible shrinkage at joints or any possible deformation at supports (this is an important issue in the US west coast where it is common to use green lumber in construction). Re-loading after the first inelastic cycle results in stiffness degradation and pinching of the load-deflection hysteresis loops according to:

$$k_p = k_0 \left[\frac{\Delta_y}{(\beta - 1)\Delta_{\max}} \right]^{\alpha} \qquad \textbf{(5-2)}$$

In equation 5-2, Δ_y is the yield displacement, $\Delta_{\max}$ is the previous maximum deflection in the respective loading direction, α is the pinching parameter controlling the rate of stiffness degradation and β is a softening factor.

When used in a non-linear time history analysis, the deflection level at each time step is given from the expression:

$$M\ddot{y}(t) + c\dot{y}(t) + ky(t) = -M\ddot{y}_g(t) \qquad \textbf{(5-3)}$$

where M is the inertia mass, c is the viscous damping ratio, k is the updated wall stiffness depending on the position on the load-deflection model (Fig. 5-8) and $\ddot{y}_g(t)$ is the ground acceleration.

A set of history rules was used to develop this model that allows pinching and stiffness degradation but not strength degradation. However, as stated in Section 5.2.3, this latter characteristic is not predominant in the shear wall hysteresis response, especially when the cyclic protocol used has few cycles at a similar amplitude as found for the Stewart loading protocol (Fig. 5-9). As seen in Chapter 2, previous investigations by Karacabeyli and Ceccotti (1998) and Gatto and Uang (2002) demonstrated that during a real earthquake, the probability of successive displacements reaching the same level is relatively low, hence a non-recurrent cyclic protocol as used by Stewart is realistic to assess the seismic response of a structure.

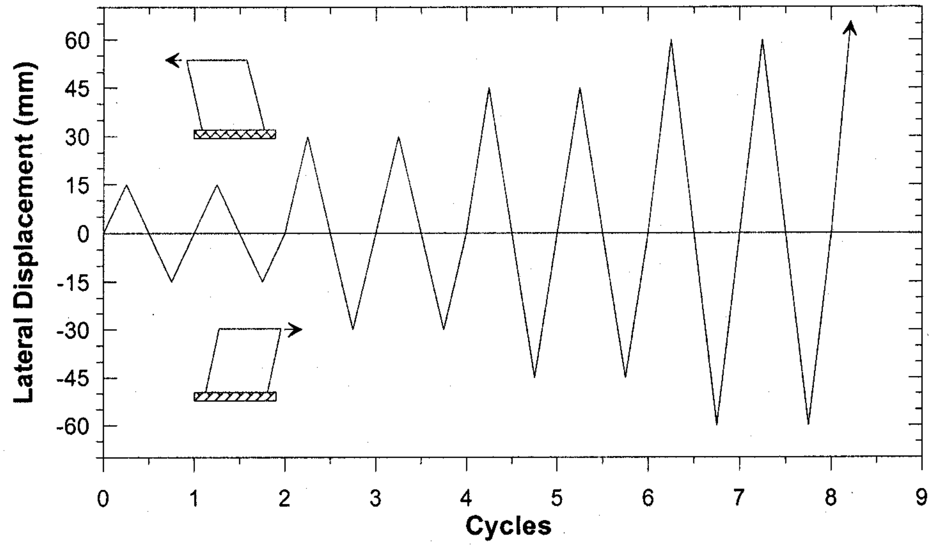

Figure 5-9 Stewart Cyclic Protocol

5.3.3 FLORENCE (1989)

The proposed model introduced by Ceccotti and Vignoli (1989) from the University of Florence is able to mimic stiffness degradation and pinching but once again, does not model strength degradation (Figure 5-10).

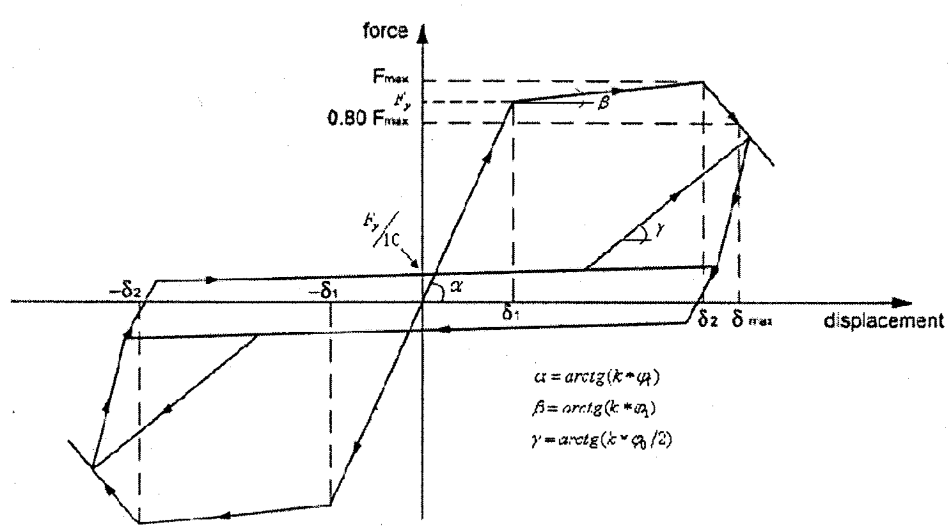

Figure 5-10 Florence Hysteresis Model (adapted from Ceccotti and Karacabeyli 2002)

According to Ceccotti *et al.* (2000), since the model is piece-linear and because it must be calibrated to test data, it is not extremely precise with regards to load estimates. However, from an energy point of view, the results are satisfactory.

Similarities exist between the Stewart and the Florence models; both of which are built from straight-line segments that require empirical full-scale testing data and used within a SDOF model. The cycle description is also quite similar: the load path is linear until the yield force is attained, then it bifurcates at an angle β until it reaches F_{max}, and then unloads.

However, the Florence model requires less calibration parameters (Table 5-2) than the Stewart model, which increases the difficulty of fitting experimental hystereses with modeled responses. For instance, the intercept load is set to 10% of the yield force, which is restrictive, considering that this value might not be universal for all structures. Also, the unloading stiffness of each cycle is the same as the initial elastic stiffness, which is not necessarily the case for all configurations.

Table 5-2 : Florence Hysteresis Model Calibration Parameters

Parameter	Description	Units
F_{max}	Maximum Force	N
F_y	Yielding Force	N
$0.8\ F_{max}$	Near-Collapse criterion	N
$F_y/10$	Intercept Force	N
α	Angle in the Elastic Phase	rad
$k^*\phi_0$	Initial Elastic Stiffness	N/mm
β	Angle in the Yielded Phase	rad
$k^*\phi_1$	Stiffness in Yielding Phase	N/mm
γ	Angle of Following Degraded Cycles	rad
$k^*\phi_0/2$	Stiffness Degradation for Following cycles	N/mm

Although the Florence pinching hysteresis model was originally developed to fit glue-laminated timber portal hystereses, modifications have been made to the model over the years (Ceccotti *et al.* 1994) such that it can be used for modeling all types of degrading structures. The model is now available in the time history dynamic analysis program DRAIN® (Prakash and Powell, 1993).

5.3.4 DOLAN (1989)

Dolan (1989) used a finite element approach to model the cyclic response of timber shear walls sheathed with plywood. Two different hysteresis responses were developed: one for the entire wall (Fig. 5-11) and one for a single sheathing-to-framing connector (Fig. 5-12). The model representing the response of an entire wall (Fig. 5-11) is based on six linear segments approximating the hysteresis. For this model, Dolan used a SDOF system consisting of a mass and a hysteretic spring, but omitted the viscous damper. The parameters necessary to calibrate the entire wall model are described in Table 5-3.

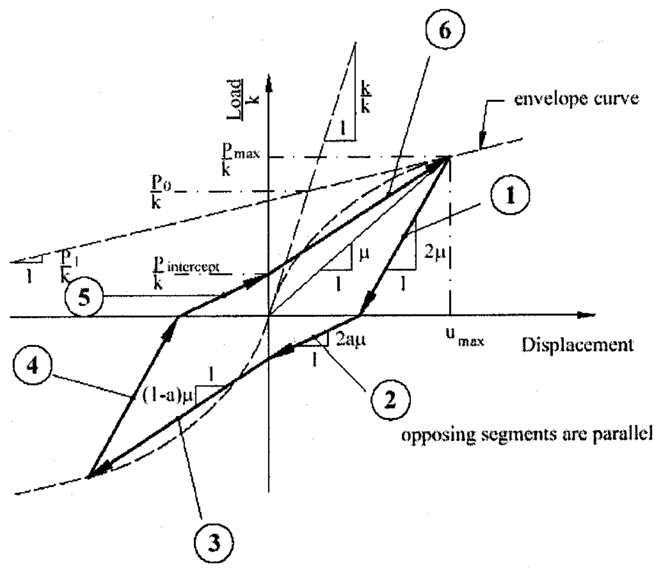

Figure 5-11 Dolan's Model of a Timber Shear Wall (Heine, 2001)

Dolan also developed another model that mimicked more specifically the behaviour of a single sheathing-to-framing connector (Fig. 5-12). According to Dolan (1989), the fasteners are not exposed to the same level of excitation or loading and consequently, the general response of the system can be affected by the energy dissipation of the individual fastener. This more sophisticated hysteresis model can better estimate the real hysteretic response of a shear wall but needs to be solved numerically by finite element methods and can therefore be computationally more demanding than the SDOF models seen previously.

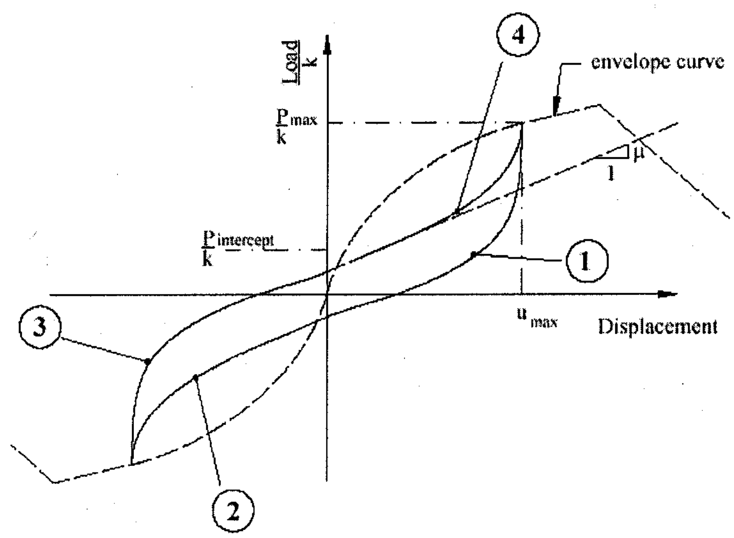

Figure 5-12 Dolan's Model of a Sheathing-to-Framing Connector Element (Heine, 2001)

Table 5-3 : Dolan Model Calibration Parameters

Parameter	Description	Units
k	Initial Wall Stiffness	N/mm
a	Ratio of Peak Hysteretic Load to Load at Intercept	-
μ	Slope of Line Passing through Origin and Peak Hysteretic Load	N/mm
P_0	Slope of Asymptote	N/mm
P_{max}	Peak Hysteretic Load per Cycle	N
$P_{intercept}$	Intercept Load	N
μ_{max}	Maximum Displacement per Cycle	mm

5.3.5 FOLZ AND FILIATRAULT [CASHEW] MODEL (2001)

Folz and Filiatrault (2001a) noted that in the past few years, there has been a proliferation of experimental research programs in the field of wood shear walls loaded cyclically in addition to monotonic testing. Most hysteretic models are theoretically developed and then refined and recalibrated using test data. CUREE (the Consortium of Universities for Research on Earthquake Engineering) introduced a new loading protocol (Krawinkler *et* *al.* 2001), as presented in Chapter 2, and a new cyclic analysis hysteresis model that was verified and calibrated on their specific loading protocol.

Folz and Filiatrault considered the response of a single connector under monotonic loading using the model proposed by Foschi (1977) and modified it to account for cyclic loading (Figure 5-13).

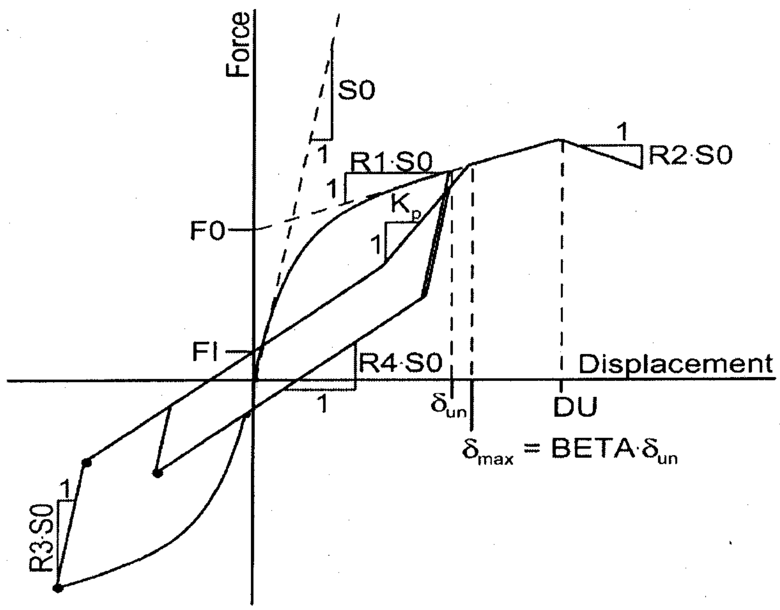

Figure 5-13 Folz and Filiatrault [CASHEW] Connector Hysteresis Model (2001*a*)

As a result, the sheathing-to-framing connector hysteresis model shown in Figure 5-13 can be applied to the entire wall response if properly calibrated (Table 5-4).

Table 5-4 : Folz and Filiatrault [CASHEW] Model Parameters

Parameter	Description	Units
F_0	Intercept Connector Strength for the Asymptotic Line of the Envelope Curve	N
F_I	Intercept Connector Strength at the Origin	N
D_U	Connector Displacement at Ultimate Load	mm
K_P	Stiffness of the Degraded Cycles	N/mm
S_0	Initial Connector Stiffness	N/mm
R_1	Stiffness Ratio of the Asymptotic Line to the Connector Envelope Curve	-
R_2	Stiffness Ratio of the Descending Branch of the Connector Envelope Curve	-
R_3	Stiffness Ratio of the Unloading Branch of the Connector Envelope Curve	-
R_4	Stiffness Ratio of the Pinching Branch for the connector	-
α and β	Stiffness Degradation Connector Parameters	-

Unlike the other models reviewed in this chapter, a particular feature of the model by Folz and Filiatrault is the lack of a linear portion of the load-deformation curve, even at a low displacement level. This characteristic is due to the modeling of the racking response by the following relationship:

$$F=\begin{cases} sgn(\delta)\cdot(F_0+R_1S_0|\delta|)\cdot[1-exp(-S_0|\delta|/F_0)], & |\delta|\leq|\delta_{max}| \\ sgn(\delta)\cdot F_U+R_2S_0[\delta-sgn(\delta)\cdot\delta_{max}], & |\delta_{max}|<|\delta|\leq|D_U| \\ 0, & |\delta|>|D_U| \end{cases} \tag{5.4}$$

In Figure 5-13, the first excursion is modeled by Equation 5.4 as in a monotonic loading until unloading occurs with a $R_3 \cdot S_0$ slope. Under continued unloading, the path then follows a $R_4 \cdot S_0$ slope corresponding to a pinched behaviour due to slackness created around the fastener's head. On the return loop, the load path passes through the zero-displacement at an intercept force F_I and reloads at a slope $R_4 \cdot S_0$. Continued reloading follows a slope K_P corresponding to degrading stiffness and evaluated by:

$$K_P = S_0\left(\frac{\delta_0}{\delta_{MAX}}\right)^{\alpha} \tag{5.5}$$

with $\delta_0=(F_0/S_0)$ and α a hysteretic parameter determining the stiffness degradation degree.

A total of 10 parameters are required to calibrate this model; parameters that can be found either from visual evaluation of a shear wall hysteresis or from the results of an analysis with the CASHEW® computer program developed by CUREE in 2001 (Folz and Filiatrault 2001), which was based on the SWAP® (Shear Wall Analysis Software) program by Filiatrault (1990). CASHEW® is generally used when full-scale testing data are not available but sheathing-to-framing tests have been completed. With the assumptions that a shear wall is composed of pin-connected rigid framing members, elastic shear deformable sheathing panels and non-linear sheathing-to-framing fasteners that follow the hysteretic model shown in Figure 5-13, an analysis can replicate either a static racking loading test (monotonic), a CUREE cyclic protocol loading test or any other cyclic protocol loading desired. Also, part of the CUREE-Caltech research program was the development of the dynamic analysis software SAWS® (Seismic Analysis of Woodframe Structures) (Folz and Filiatrault, 2002) that incorporates the CASHEW model as described in Section 5.4.3.

5.4 Computer Programs Review

The computing time and cost of inelastic static or dynamic time-history analyses contribute to a fair amount of the design budget if executed with commercial software packages, especially for wood or light-framed structures such as residential houses or low-rise buildings where the design funds are usually limited. Researchers have therefore developed programs that can execute an analysis for a fraction of the price, such as DRAIN® (University of California, Berkeley), RUAUMOKO® (University of Canterbury, New Zealand), SAWS® (University of California, San Diego), and many more. These three programs are reviewed in this section to evaluate their applicability to wood panel shear walls.

5.4.1 DRAIN Series of Computer Programs [2D, 2DX, 3DX] (1973)

The DRAIN software (Kannan and Powell, 1973) was first released in 1973 in its 2D version. It is a batch mode program, developed at the University of California at

Berkeley, capable of calculating the dynamic response of non-linear 2D (and later 3D with DRAIN-3DX) structures subjected to earthquake ground motions using the equilibrium method, and carried out by the finite-element method. A number of elements are available for modeling including springs, dampers, degrading stiffness elements, etc.

DRAIN programs also allow for creating, modifying and integrating elements into the software library if the designer is not satisfied with the embedded ones. Considering this option, Ceccotti and Vignoli (1989) have incorporated their hysteretic model (Section 5.3.3) into the DRAIN-2D element library in order to have an element that matches more closely the characteristics of woodframe structures. This element is now known as EC-7 within the DRAIN-2D and DRAIN-2DX programs.

Ceccotti *et al.* (2000) used the subroutine created especially for this element to perform a 3D inelastic time-history analysis on a studied building for which wall test data was available. It was noted that the analysis was not extremely precise in terms of displacements or load-carrying capacity. On the other hand, from an energy point of view, the model gave reasonable results within a 15% margin of the test information. The authors therefore concluded that the subroutine should not be used to assess design values and other absolute quantities such as the ductility or the force modification factors.

5.4.2 RUAUMOKO (1981)

Representing the god of earthquakes and volcanoes in the Maori mythology, RUAUMOKO was developed by Carr in 1981 to provide for a piece-wise dynamic elastic and inelastic analysis capability of structures subjected to earthquake ground motions or any other defined dynamic loads. RUAUMOKO permits the execution of several type of analyses, including static analysis, time-history analysis, dynamic analysis, monotonic pushover analysis, cyclic pushover analysis or various combinations. RUAUMOKO also includes over forty hysteretic rules for member behaviour modeling; some especially for steel structures, reinforced concrete members or timber structures.

Accordingly, the hysteretic rule included in RUAUMOKO that best fits the steel frame / wood panel shear wall type of structure is the Stewart model (see Section 5.3.2). As mentioned previously, the Stewart Degrading Stiffness Hysteretic Rule was specifically conceived for the modeling of timber framed shear walls sheathed in plywood nailed to the frame. Despite its initial restrictions to woodframe structures, it is said in the RUAUMOKO user manual (Carr, 2000) that because of its degrading stiffness and slackness characteristics, the Stewart model has been successfully applied to other materials and structural configurations, such as reinforced concrete compression members with plain reinforcement bars.

A number of post-processing programs are included in the RUAUMOKO® package to be able, for instance, to plot the required node and member results graphs (Dynaplot®), to produce an elastic response spectra for any earthquake acceleration (Spectra®), to reproduce an artificial earthquake acceleration time-history (Simqke®) or to match experimental loops to a hysteretic rule using the hysteresis rule exerciser Hysteres® (this program was used for the current research, refer to Section 5.5).

Isoda *et al.* (2002) used RUAUMOKO as part of Task 1.5.4 of the CUREE-Caltech Woodframe Project by modeling four index woodframe buildings into pancake models (i.e. no consideration of building height) simulating the 3D dynamic response of these structures through a degenerated 2D planar analysis. Shear walls were represented in the models as zero-length non-linear shear spring elements with the Stewart Model for hysteretic rule. This modeling approach was meant to evaluate the general seismic response of the buildings and not necessarily to model every single connection between the elements. Therefore, the pancake model was found to be an efficient and simple method to assess the general dynamic response of a building subjected to an earthquake event but not to determine the exact forces in the connections.

5.4.3 SAWS (2002)

As part of the CUREE-Caltech Woodframe Research Project, the Task 1.5.1 by Folz and Filiatrault (2002) was meant to develop an analysis program especially focused on woodframe structures. This software program, SAWS (Seismic Analysis of Woodframe Structures), is capable of predicting the global seismic response of a building as well as its dynamic characteristics such as frequency and damping ratio.

SAWS uses the CASHEW hysteretic rule (Section 5.3.5) to model the pinched hysteresis loops as well as stiffness and strength degradation typical to woodframe shear walls. The shear wall element is then modeled as a non-linear shear spring in the SAWS representation. Therefore, only three degrees-of-freedom per floor are required (U, V, θ) which limit the needed level of computing time and reduce to a single spring element the whole shear wall configuration. A limiting aspect of the SAWS program is its inability to incorporate any other hysteretic rule or even a modified CASHEW model.

As part of Task 1.1.1 of the CUREE-Caltech Research Project, two-storey woodframe houses were built and tested on a shake table to evaluate their dynamic response to earthquake ground motions (Fisher *et al.*, 2001). Empirical data from these full-scale tests were then used to estimate the adequacy of the analysis program to evaluate the seismic response of a woodframe house. The SAWS time-history analyses under-predicted the roof displacement and acceleration by nearly 20% when compared to full-scale test results. One of the factors explaining this difference is the assumption of a rigid diaphragm in the SAWS model. Although this is an advantage when it comes to computational time, considering that only 3 DOF per floor are modeled, the diaphragm does in reality exhibit some in-plane flexibility.

Because of its early stage of development, many limitations exist within the SAWS program. The complexity in modeling building irregularities, the either fully flexible or fully rigid diaphragms and the exclusion of p-delta effects due to a "pancake" model, which does not account for the building height, can introduce significant restrictions.

5.5 *Recent Hysteresis Modelling Studies of Steel Frame / Wood Panel Shear Walls*

<u>Fülöp and Dubina (2004b)</u>

Fülöp and Dubina determined that it is of importance to find a suitable hysteretic model in order to assess the structural performance of a steel frame / wood panel shear wall in case of an earthquake. Fülöp and Dubina used a simplified tri-linear hysteretic model (Figure 5-14) that is in many ways similar to the Stewart degrading hysteretic model presented in Section 5.3.2.

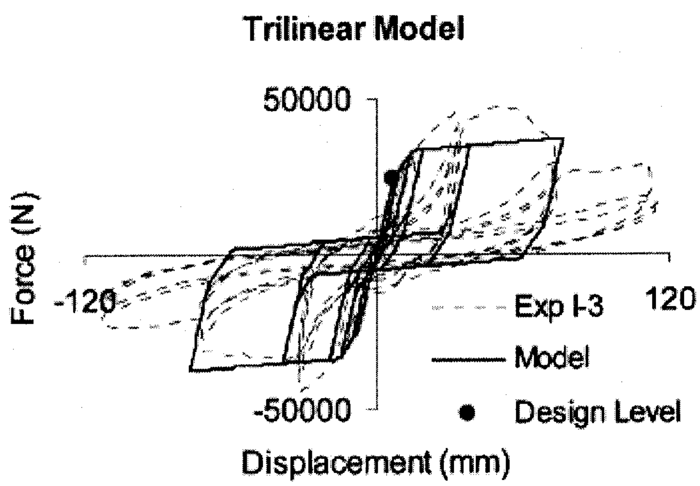

Figure 5-14 : Simplified tri-linear hysteretic model used by Fülöp and Dubina (2004b)

The simplified tri-linear model was introduced in Drain-3DX for non-linear time history analyses using a single degree of freedom representation to model shear wall elements.
The model used by Fülöp and Dubina is not capable of taking into account strength degradation due to repeated loading. It also depends on a large number of parameters that need to be taken from relevant experimental results. On the other hand, the model has very good capability in characterizing the response of the shear walls up to the maximum resistance loads in terms of pinching.

Della Corte *et al.* (2005)

In order to model the strong non-linearity and pinched hysteresis loops of a shear wall response, Della Corte *et al.* developed a refined mathematical model that could adequately capture these aspects of the structural system. The model, presented in Figure 5-15, does not allow for stiffness degradation or strength degradation. It is also said to be semi-empirical, i.e. some parameters can be theoretically deduced, but others need to be computed based on the results of experiments.

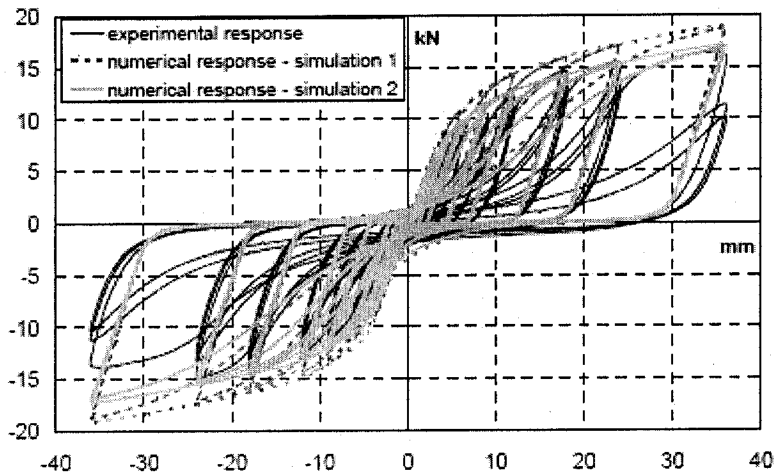

Figure 5-15 : Comparison of experimental and numerical simulation data (Della Corte *et al.*, 2005)

As can be observed in Figure 5-15, the model predicts quite accurately the shear strength at each displacement level if only the first loop is considered. As for the energy dissipated by the system, the model tends to underestimate it for small excursions and overestimate it for larger displacements.

5.6 *RECOMMENDATIONS FOR THE SELECTION OF A HYSTERETIC RULE AND ANALYSIS SOFTWARE*

Although steel frame / wood panel shear walls share some important response characteristics with wood frame shear walls, differences exist and have to be accounted for in the hysteretic loop matching. Table 5-5 presents some of the main advantages and disadvantages of the reviewed hysteretic rules.

A general constitutive model is generally sought because it is usually less dependent on full-scale experiments than empirical models, which are normally derived from unique structural configurations. In the case of the current research project, full-scale test data were available so this condition was not constraining.

A choice was made to use the combination RUAUMOKO / Stewart Degrading Stiffness Hysteretic Rule because of its versatility in modeling inelastic structures. Martin (2002) and Yang (2004) even applied this combination for steel roof deck diaphragms by modifying some of the calibration factors, namely α and β, to account for the different structure type and material. Given this experience, it is expected that the Stewart Model can be calibrated to adequately mimic steel frame / wood panel shear walls hysteresis.

Table 5-5 : Hysteretic Rule Comparison Table

Model Name	Advantages	Disadvantages
Bouc-Wen-Baber-Noori (BWBN)[1]	• Allows for stiffness and/or strength degradation as well as pinching • MDOF system • Separates the non linear from linear components • Independent from empirical model • Possibility to add other parameters if deemed necessary	• Needs further modification to be applicable in modelling general wood-system behaviour • Almost impossible to identify the parameters by trial and error • Not capable of tracing slack systems • Model very dependent on dissipated energy; can only predict systems that have similar energy demands as the one the model was calibrated to • No commercial software packages can assist with the fitting problem due to the difficulty in finding the appropriate input parameters
Stewart[2]	• From nailed sheathing to lumber connections • Widely used for wood shear walls research (e.g. CUREE) • Already integrated in RUAUMOKO as a hysteretic rule (#9) • Used a set of force-history rules to idealized pinching and stiffness degradation. • Include an initial slackness in the first loading cycle • Versatile and able to capture the detailed behaviour of a wood shear wall	• Does not include strength degradation • SDOF model and can only examine the overall wall response • Have to be calibrated for each wall configuration
Florence[3]	• To be used as a subroutine for DRAIN, a well known non-linear time-history analysis software • Column model more detailed (not necessarily pinned) • Panel elements have shear stiffness and are not necessarily rigid	• Does not include strength degradation • Tested and verified with glue-laminated timber portals only • Aim was not to match the experimental data exactly but to assess the general behaviour of the structural coefficient, q. • Model underestimates the energy dissipated during loading cycles • Proposed model is suited for providing quantitative information only
Dolan[4]	• Models for joints and shear walls exist • FEA Model that solves the steady state frequency response function for the entire wall	• Does not include strength degradation • Is case dependent, based on empirical research • Extensive mathematical manipulations required • Computationally demanding to model each connector within a shear wall
Folz and Filiatrault [CASHEW][5]	• Model based on modern cyclic protocol (CUREE) • CASHEW software helps determine the calibration parameters either from full-scale data or from connection tests • Included as the hysteretic rule in SAWS dynamic analysis program	• Restrictive assumptions made such as pin-connected elements • Is a mix of simple static analysis and full non-linear dynamic analysis • Model did not achieve good predictions for monotonic loading

1 Baber and Noori (1986)
2 Stewart (1987)
3 Ceccotti and Vignoli (1989)
4 Dolan (1989)
5 Folz and Filiatrault (2001)

5.6.1 HYSTERETIC LOOP MATCHING

Included in the RUAUMOKO package is a hysteresis rule exerciser called HYSTERES. This program is generally used to determine the loop calibration parameters for any hysteretic rule integrated in RUAUMOKO. For the purpose of this research, HYSTERES was used to calibrate the Stewart model by determining the parameters listed in Table 5-1.

As seen in Chapter 3, 16 different wall configurations were tested cyclically by Branston (2004), Chen (2004) and the author. One typical cyclic test from each group was chosen to be modeled with the help of HYSTERES. Among the 11 different parameters necessary for the Stewart model, some were taken directly from the experimental tests and some had to be evaluated using a parametric study (trial and error). For instance, the initial stiffness (k_0) and the ultimate force (F_u) were taken from the test data table (Branston *et al.*, 2004). Two other calibration factors were derived, namely the yield force (F_y) and the intercept force (F_i), with the use of calibration ratios. Based on a trial and error approach to find the ratios, Table 5-6 presents the range of suggested ratios for the steel frame / wood panel shear walls detailed in this research and the parameters Stewart used to calibrate his model to full-scale tests carried out on wood frame shear walls.

Table 5-6 : Suggested Ratios for Stewart Hysteresis Parameters

	F_u/F_y	F_i/F_y	β	α
Suggested [1]	1.50-1.86	0.09-0.18	1.07-1.10	0.23-0.45
Stewart [2]	1.5	0.25	1.09	0.38

[1] Suggested by the author for a steel frame / wood panel shear wall

[2] Values used by Stewart (1987) for wood frame / wood panel shear walls

The complete list of all parameters recommended for use in future modeling of the different wall configurations with RUAUMOKO is presented in Table 5-7. From this table, one can note that the softening factor (β) and the pinch power factor (α) for groups with similar screw patterns, with a few exceptions, are consistent. For example, 5 of the 6 groups with a screw pattern of 6"x12" have a β factor of 1.10 and an α factor of 0.41. The groups that do not have similar factors may exhibit unsymmetrical behaviour or other irregularities.

Table 5-7 Stewart Hysteresis Parameters for Steel Frame / Wood Panel Shear Walls

Group	Wood Panel	Size	Srew Pattern	K_0 (kN/mm)	r	Fy (kN)	Fy (kN)	Fu/Fy	Fu (kN)	Fi (kN)	P_{Tri}	Fi/Fy	P_{UNL}	β	α
16	CSP	2' x 8'	6" x 12"	0.33	0.26	3.70	-3.70	1.81	6.70	0.65	0	0.18	2.00	1.10	0.41
18	CSP	2' x 8'	4" x 12"	0.40	0.25	5.50	-5.50	1.79	9.86	1.00	0	0.18	2.40	1.10	0.35
8	CSP	4' x 8'	6" x 12"	1.15	0.20	9.20	-9.20	1.50	13.83	1.50	0	0.16	1.65	1.10	0.41
4	CSP	4' x 8'	4" x 12"	1.05	0.25	12.45	-12.45	1.50	18.70	1.75	0	0.14	2.20	1.10	0.35
10	CSP	4' x 8'	3" x 12"	1.50	0.23	20.45	-20.45	1.50	30.70	2.25	0	0.11	1.65	1.09	0.23
30	CSP	8' x 8'	6" x 12"	2.20	0.18	21.50	-21.50	1.46	31.30	2.70	0	0.13	2.25	1.10	0.41
32	CSP	8' x 8'	4" x 12"	2.40	0.30	28.50	-28.50	1.63	46.40	3.90	0	0.14	2.10	1.09	0.25
34	CSP	8' x 8'	3" x 12"	3.20	0.30	37.00	-37.00	1.71	63.30	4.45	0	0.12	1.70	1.07	0.27
12	DFP	4' x 8'	6" x 12"	1.25	0.16	11.00	-11.00	1.55	17.10	1.00	0	0.09	2.20	1.10	0.41
6	DFP	4' x 8'	4" x 12"	1.55	0.20	15.50	-15.50	1.65	25.50	2.50	0	0.16	1.55	1.10	0.35
14	DFP	4' x 8'	3" x 12"	1.75	0.26	22.00	-22.00	1.65	36.20	3.00	0	0.14	1.55	1.09	0.23
20	OSB	2' x 8'	6" x 12"	0.40	0.28	3.50	-3.50	1.86	6.50	0.65	0	0.19	2.40	1.10	0.41
28	OSB	2' x 8'	4" x 12"	0.57	0.22	6.40	-6.40	1.58	10.12	1.00	0	0.16	1.80	1.10	0.45
22	OSB	4' x 8'	6" x 12"	1.60	0.20	8.40	-8.40	1.61	13.50	1.00	0	0.12	1.75	1.10	0.45
24	OSB	4' x 8'	4" x 12"	2.10	0.23	13.40	-13.40	1.49	20.00	1.40	0	0.10	1.75	1.10	0.45
26	OSB	4' x 8'	3" x 12"	3.00	0.22	17.00	-17.00	1.68	28.50	2.50	0	0.15	1.25	1.10	0.45

For each wall configuration the HYSTERES program was initially tested using the load – displacement results of a representative monotonic test. Two graphs were used to validate the model. First of all, the experimental and the modeled load-displacement curves were superimposed (Figure 5-16). A visual evaluation of the matching of the loading and unloading slopes was then attempted. Since the Stewart model is made from a set of straight-lines, it is very difficult to have a perfect match, especially at the beginning of the loading where the shear wall behaviour is non-linear.

The second graph used in the validation of the parameters for the Stewart model is shown in Figure 5-17. It illustrates the energy dissipated by the experimental monotonic test and by the Stewart model with respect to time. This information is very useful for the confirmation of the selected parameters such that the model mimics the real behaviour of the wall. In seismic design it is important for the analytical model to be accurate with respect to the amount of energy that is dissipated in the structural system. Therefore, the author considered the dissipated energy as a major validation characteristic in the calibration of the models.

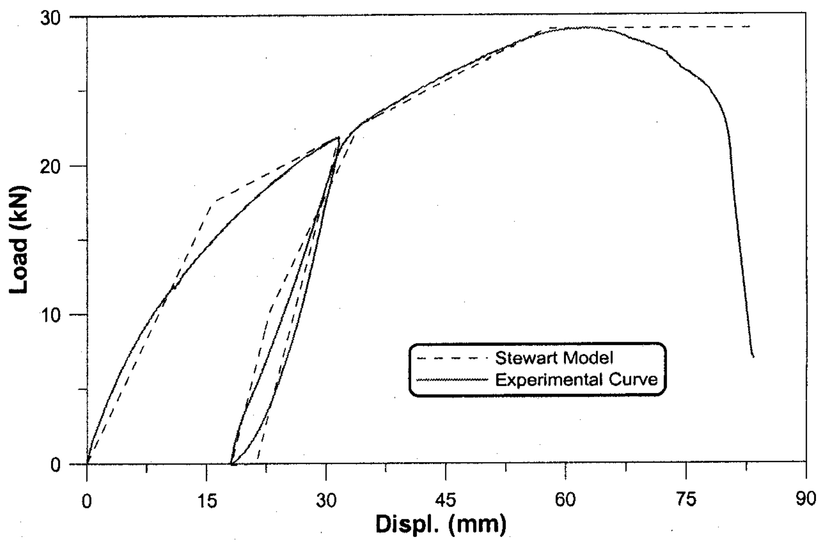

Figure 5-16 Superposition of Stewart Model and Experimental Monotonic Curves (Group 5)

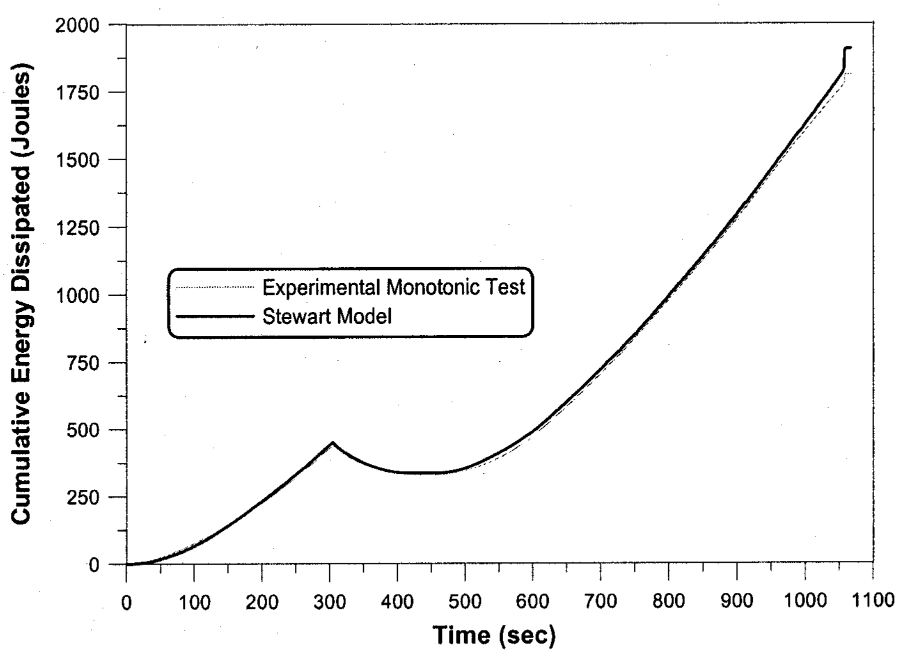

Figure 5-17 Cumulative Energy Dissipated by the Model and Experimental Test (Group 5)

Cyclic test results for each of the 16 different shear wall groups were also used in the calibration of the Stewart Model using HYSTERES. Figures 5-18 and 5-19 illustrate a typical example of the superimposed experimental and modeled load-displacement hysteresis curves and the cumulative energy dissipated for a cyclic test. All cyclic graphs for the 16 groups can be found in Appendix C.

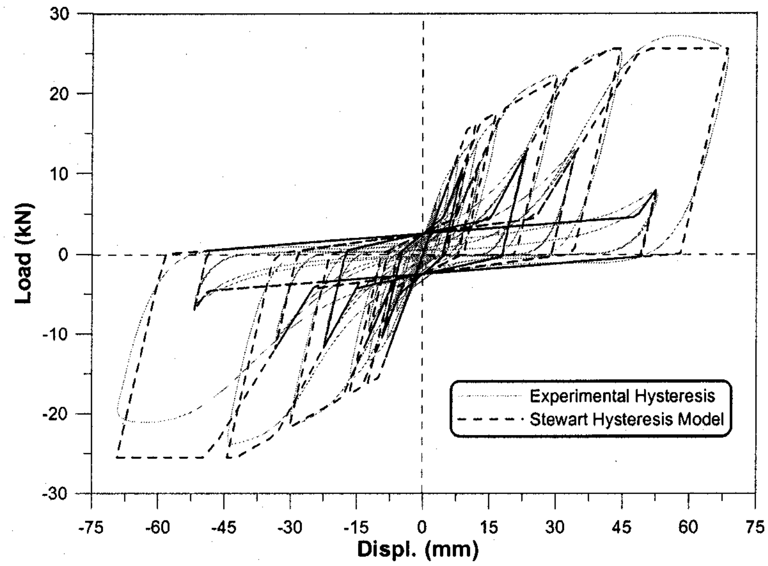

Figure 5-18 Superimposed Experimental and Modeled Hystereses (Group 6)

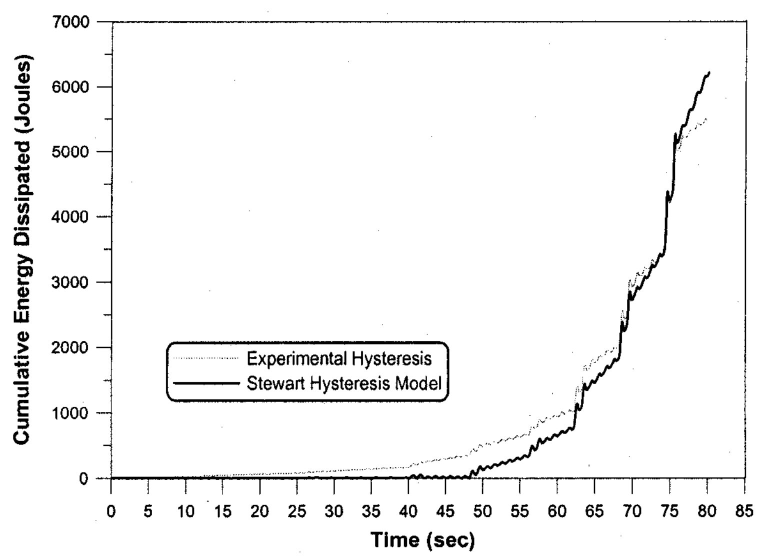

Figure 5-19 Cumulative Energy Dissipated from Experimental Test and Stewart Model Hystereses (Group 6)

The visual validation of the model in Figure 5-18 is achieved by looking at the slopes of the loading and unloading portions of the hysteresis and appreciating their match. The pinched loops are also of major concern since the adjustment of certain factors, especially α and β, modify the amplitude and the slopes of the pinched part of the hysteresis. Certain shear wall groups, especially the larger 2440 x 2440 mm (8'x8') specimens, were more difficult to accurately model due to their asymmetric responses due to the failure of the wall in either a positive or a negative excursion. In that case, an excursion at the same displacement level but in an opposite direction would lead to different resistances and no model can predict such a situation.

5.6.2 MODEL LIMITATIONS

Although the graphs presented above and in Appendix B show good conformity of the Stewart Model with steel frame / wood panel shear walls hystereses, a few limitations have to be considered in the use of this model in a time-history analysis.

First of all, the experimental hysteresis was modeled up to the last stable (intact) loop. The model is not able to represent the failure of the wall and the capacity degradation following that failure. Therefore, following a non-linear time-history analysis, the user would have to manually examine the most solicited walls of the analysed building and verify that the maximum displacement reached when subjected to an earthquake event is less than the wall near-collapse criterion. This criterion was formulated in Chapter 3 as the displacement that corresponds to 80% of the ultimate force on the descending portion of the backbone curve. These values can be found for each test in the test data table in Branston *et al.* (2004) as $\Delta_{net,0.8u}$. In the case where the near-collapse displacement occurs past the 2.5% drift limit, this latter displacement value is used.

Another constraining feature of the Stewart Hysteretic Model is the fact that it has to be calibrated to each wall configuration with the help of full-scale testing. Every slight change in the fasteners spacing or wood panel type causes relatively major impact on the response, and thus the model parameters have to be adjusted accordingly.

Also, the Stewart Model was developed based on a loading protocol different than the one in use within this research project. The several calibration parameters make the adjustment possible such that the CUREE tested walls can be modeled, although it can be a time-consuming task.

5.7 PARTIAL CONCLUSIONS

The hysteretic modeling of a structural element of a system is essential to be able to assess the structural response of the entire structure to seismic excitation in a non-linear time-history analysis program. Different types of hysteretic rules exist for the modelling of wood structures. As seen in this chapter, each has advantages and disadvantages. In general, three types of model exist: the finite element model, the single-degree-of-freedom model and the cyclic analysis model. Although more complete and able to account for minute connection details, a FE model, like the one developed by Dolan, predicts similar results to simpler models. The SDOF models, of which the Stewart Model belongs to, generally have limited applications because they must be calibrated to full-scale experimental data. As mentioned previously, it was not a problem in this research because of the availability of empirical data.

The Stewart Degrading Stiffness Model was chosen to be the best hysteretic rule to apply to steel frame / wood panel shear wall hystereses because of its versatility and ability to be precisely calibrated with the help of its 11 parameters. The pinching and degrading stiffness characteristics are well modeled by this hysteretic rule and the dissipated energy difference between the experimental tests and the models is usually low (±10%). Moreover, the non-linear time-history analysis of a building having shear walls as the SFRS is facilitated by the fact that the Stewart Model is included in the RUAUMOKO software.

CHAPTER 6

CONCLUSIONS AND RECOMMENDATIONS

6.1 SUMMARY

The research presented in this thesis had various objectives. Firstly, a reversed cyclic loading protocol was selected by the author for use in an extensive shear wall test program at McGill University. In order to choose the most appropriate loading regime, nominally identical steel frame / wood panel shear walls were loaded with two pre-selected reversed cyclic protocols and the results were then compared and analysed.

The author was then responsible for the testing and analysis of 20 of the 109 shear walls making up the research program that was undertaken. The Equivalent Energy Elastic-Plastic (EEEP) method was chosen by Branston (2004) and applied by the author to analyse the shear wall design characteristics. Key design parameters such as elastic stiffness, yield resistance and system ductility were extracted from the analysis for each shear wall configuration. In particular, the system ductility was useful in determining the ductility-related seismic force modification factor (R_d) for use with the 2005 NBCC (NRCC, 2004). An overstrength-related force modification factor (R_o) was also determined. Material properties of the wood sheathing and the steel framing were measured by testing.

The final objective of this research was to identify the most appropriate hysteretic model for use with steel frame / wood panel shear walls in the eventuality of performing non-linear time history dynamic analyses.

6.2 *Conclusions*

From the research conducted by the author and from what is presented in this thesis, the following conclusions can be drawn:

1. The CUREE Ordinary Ground Motions reversed cyclic loading protocol (Krawinkler *et al.*, 2000) is well adapted for the testing of steel frame / wood panel shear walls. The obtained test responses and observed failure modes when a specimen is loaded with this regime correspond to what is expected for a shear wall building component loaded during a real design level seismic event. In addition, the CUREE protocol was developed with the notion that multiple earthquakes may occur in the lifetime of the structure.

2. When the Equivalent Energy Elastic-Plastic (EEEP) analysis method is applied to the test response, the system ductility translates into a minimum ductility-related seismic force modification factor (R_d) value of 2.5 provided that a maximum aspect ratio (height : length) of 2:1 for shear walls is respected. An overstrength-related force modification factor (R_o) of 1.8 was also estimated based on the known overstrength information. These R-factors are recommended for use with the 2005 National Building Code of Canada.

3. The Stewart Degrading Hysteresis element (Stewart, 1987) was found to best match the behaviour of a steel frame / wood panel shear wall subject to a reversed cyclic loading protocol. The pinching and degrading stiffness characteristics are well modeled by this hysteretic rule and the difference in dissipated energy between the experimental tests and the models was found to be low (±10%). The element can therefore be included in a more general building model in which steel frame / wood panel shear walls would act as the seismic force resisting system (SFRS). This building model would then be used for non-linear time history dynamic analyses with the Ruaumoko software (Carr, 2000), for example.

4. As part of the ancillary testing program, material properties such as the shear strength, the shear modulus and the rigidity for the wood sheathing were determined using the ASTM D 1037 (1999) standard test method. Although the method gave good results in terms of shear strength, it is recommended that the ASTM D 2719 (1994) test method be used for the determination of the shear modulus and rigidity because the larger specimens are less prone to the boundary effects present in the smaller sections used in the edgewise shear test of ASTM D 1037.

6.3 RECOMMENDATIONS

Even though the research program was quite extensive, i.e. 16 wall configurations with 109 individual walls, the conclusions and trends documented in this thesis are to be appreciated within testing limitations. Additional testing and analysis of diverse shear wall configurations would be interesting, especially those that include a gravity load to simulate the structural weight of floors above. The effect of gravity loads on the lateral resistance of steel frame / wood panel shear walls is an item of ongoing and future research.

For uniformity in research and analysis of shear walls, standardization of a loading protocol is greatly needed. The fact that individual researchers have the freedom to select and apply a chosen protocol, especially with regards to cyclic loading, makes it difficult to compare and incorporate the results of various research programs. An internationally recognized cyclic loading regime would allow for extensive and constructive comparisons of various component details and would help to build a more extensive database of test results and analyses. From the limited research contained herein, the CUREE Ordinary Ground Motion Protocol (Krawinkler *et al.*, 2000) would best be suited for selection as an internationally recognized loading protocol. The CUREE Ordinary Ground Motion Protocol was, however, developed for a design earthquake from California (US) having a 10% in 50 year probability of exceedance. Recent design codes, on the other hand, such as the 2005 version of the National Building Code of Canada, require a 2% in 50 year probability of exceedance. Adjustments are therefore needed.

It is recommended that for verification purposes of the recommended seismic force modification factors R_d and R_o, non-linear time history dynamic analyses of buildings, in which steel frame / wood panel shear walls are incorporated, should be carried out. In addition, shake table testing of multi-storey shear walls should be completed to validate the preliminary force modification factors that have been presented.

References

American Iron and Steel Institute (AISI) (2001). *North American Specification for the Design of Cold-Formed Steel Structural Members*. Washington DC, USA.

American Plywood Association – the Engineered Wood Association, PRP-108 (2001). *Performance Standards and Qualification Policy for Structural-Use Panels*. Tacoma, WA, USA.

American Society for Testing and Materials (ASTM) A 307 (2000). *Standard Specification for Carbon Steel Bolts and Studs, 60000 psi Tensile Strength*. West Conshohocken, PA, USA.

American Society for Testing and Materials (ASTM) A 325 (2002). *Standard Specification for High-Strength Bolts for Structural Steel Joints*. West Conshohocken, PA, USA.

American Society for Testing and Materials (ASTM) A 370 (2002). *Standard Test Methods and Definitions for Mechanical Testing of Steel Products*. West Conshohocken, PA, USA.

American Society for Testing and Materials (ASTM) A 653 (2002). *Standard Specification for Steel Sheet, Zinc-Coated (Galvanized) or Zinc-Iron Alloy-Coated (Galvannealed) by the Hot-Dip Process*. West Conshohocken, PA, USA.

American Society for Testing and Materials (ASTM) D 1037 (1999). *Standard Test Method for Evaluating Properties of Wood-Base Fiber and Particle Panel Materials*. West Conshohocken, PA, USA.

American Society for Testing and Materials (ASTM) D 2719 (1994). *Standard Test Methods for Structural Panels in Shear Through-the-Thickness*. West Conshohocken, PA, USA.

American Society for Testing and Materials (ASTM) E 564 (1995). *Standard practice for static load test for load test for shear resistance of framed walls for buildings*. West Conshohocken, Pennsylvania, USA.

American Society for Testing and Materials (ASTM) E 2126 (2005). *Standard Test Methods for Cyclic (Reversed) Load Test for Shear Resistance of Framed Walls for Buildings*. West Conshohocken, PA, USA.

Applied Technology Council (ATC) (1992). *ATC-24: Guidelines for Cyclic Seismic Testing of Components of Steel Structures*. Redwood City, CA, USA.

Baber, T. and Noori, M.N. (1986). Modeling general hysteresis behavior and random vibration application. *J. Vibration, Acoustics, Stress and Reliability in Des.*, Vol. 108, 411-420

Biblis, E. J. (2001). Edgewise Flexural Properties and Modulus of Rigidity of Different Sizes of Southern Pine LVL and Plywood. *Forest Products Journal*, 51, 81-84

Bouc, R. (1967). Modèle mathématique d'hystérésis. *Acustica*, 24, 16-25.

Branston, A.E., Boudreault, F.A., Rogers, C.A. (2003). *Testing of Steel Frame / Wood Panel Shear Walls – Match Tests of Existing Shear Wall Experiments*. Internal Report, Dept. of Civil Engineering and Applied Mechanics, McGill University, Montreal, Canada.

Branston, A.E. (2004). *Development of a Design Methodology for Steel Frame / Wood Panel Shear Walls*. Master's Thesis, Dept. of Civil Engineering and Applied Mechanics, McGill University, Montreal, Canada.

Branston, A.E., Boudreault, F.A., Chen, C.Y., Rogers, C.A. (2004). *Light Gauge Steel Frame / Wood Panel Shear Wall Test Data: Summer 2003*. Department of Civil Engineering and Applied Mechanics, McGill University, Montreal, QC, Canada.

Canadian Standards Association O86-01 (CSA 086-01) (2001). *Engineering Design in Wood*. Mississauga, Ontario, Canada.

Canadian Standards Association 0121 (CSA 0121) (1978). *Douglas Fir Plywood*. Mississauga, Ontario, Canada.

Canadian Standards Association 0151 (CSA 0151) (1978). *Canadian Softwood Plywood*. Mississauga , Ontario, Canada.

Canadian Standards Association O325 (1992). Construction Sheathing, Mississauga, ON, Canada.

Carr, A.J. (2000). *RUAUMOKO – Inelastic Dynamic Analysis, Version March 15th 2000*. Dept. of Civil Eng., University of Canterbury, Christchurch, New Zealand"

Ceccotti, A. (1995). Design of timber structures in seismic regions. *Timber Engineering STEP 3*. Informationsdienst Holz, Duesseldorf, 16.1 – 16.19 pp.

Ceccotti, A. and Vignoli, A. (1989). A hysteretic behavioural model for semi-rigid joints. *Europe Earthquake Engineering Journal*, V3, 3-9.

Ceccotti, A. and Karacabeyli, E. (2000). Dynamic Analysis of Nailed Wood-Frame Shear Walls. *12th World Conference on Earthquake Engineering (12WCEE 2000)*. Auckland, New Zealand, paper 0720, 1-8.

Ceccotti, A. and Karacabeyli, E. (2002). Validation of Seismic Design Parameters for Wood-Frame Shearwall System. *Can. J. Civ. Eng.*, (29), 484-498.

Ceccotti, A., Follesa, M., Karacabeyli, E. (2000). 3D seismic analysis of multi-storey wood frame construction. *World Conference on Timber Engineering*, Whistler, Canada, paper 1-2-3.

Ceccotti, A., Vignoli, A., Giordano, S. (1994). Testing seismic behaviour of timber structures with semi-rigid joints. *In Proceedings of the 2nd COST C1 Meeting, October 1994*. Czech Technical University, Prague, 447-458.

Chen, C.Y. (2004). *Testing and Performance of Steel Frame / Wood Panel Shear Walls*. Master's Thesis, Dept. of Civil Engineering and Applied Mechanics, McGill University, Montreal, Canada.

COLA-UCI (2001). *Report of a Testing Program of Light-Framed Walls with Wood-Sheathed Shear Panels*. Final Report to the City of Los Angeles Department of Buildings and Safety. University of California, Irvine, Department of Civil and Environmental Engineering, CA, USA.

CUREE – Caltech Woodframe Project (2002). *Recommendations for Earthquake Resistance in the Design and Construction of Woodframe Buildings*. CUREE Publications, Final Review Draft, CA, USA.

Daudeville, L., Davenne, L., Richard, N., Kawai, N. (1998). Étude du comportement parasismique de structures à ossature en bois. *Revue Française de Génie Civil*, 2(6), 651-665.

Della Corte, G., Landolfo, R., Fiorino, L. (2005). Seismic behavior of sheathed cold-formed structures: Numerical tests. *Journal of Structural Engineering, ASCE*. (Accepted).

Dinehart, D. and Shenton III, W. (1998). Comparison of Static and Dynamic Response of Timber Shear Walls. *Journal of Structural Engineering*, June 1998, 686-695.

Dolan, J.D. (1989). *The dynamic Response of Timber Shear Walls*. PhD Thesis, University of British Columbia, Vancouver, B.C., Canada.

Dolan, J.D. (1993). Proposed test method for dynamic properties of connections assembled with mechanical fasteners. *Meeting Twenty-six of the International Council for Building Research Studies and Documentation, Working Commission W18 – Timber Structures*, Athens, GA.

Dowrick, D.J. (1986). Hysteresis loops for timber structures. *Bulletin of the New Zealand National Society of Earthquake Engineering*, Vol 19(20), 143-152.

Filiatrault, A. (1990). Static and Dynamic Analysis of Timber Shear Walls. *Canadian Journal of Civil Engineering*, 17(4), 643-651.

Filiatrault, A., Uang, C-M, Seible, F (2000). Ongoing Seismic Testing and Analysis Program of the CUREE-Caltech Woodframe Project. *Conference Proceeding to the Structures Congress 2000 - Advanced Technology in Structural Engineering*, Philadelphia, PA, USA.

Filiatrault, A. (2002). *Elements of Earthquake Engineering and Structural Dynamics* (second edition). Montreal : École Polytechnique de Montréal.

Findings and recommendations of the City of Los Angeles / SEAOSC Task Force on the Northridge earthquake. (1994). Structural Engineers Association of Southern California, Whittier, CA.

Fischer, D., Filiatrault, A., Folz, B., Uang, C.-M., Seible, F. (2001). *Two-Story Single Family House Shake Table Test Data*. CUREE-Caltech Woodframe Project Report No. W-05, CUREE, Richmond, CA

Foliente, G.C. (1994). Analysis, design, and testing of timber structures under seismic loads. *Proceedings Research Needs Workshop*. University of California-Berkeley, Forest Products Laboratory, Richmond, CA.

Foliente, G.C. (1995). Hysteresis Modeling of Wood Joints and Structural Systems. *Journal of Structural Engineering*, Vol 121 (6), June 1995, 1013-1022.

Foliente, G.C. and Zacher, E.G. (1994). Performance tests of timber structural systems under seismic loads. *Proceedings Research Needs Workshop*. University of California-Berkeley, Forest Products Laboratory, Richmond, CA.

Folz, B. and Filiatrault, A. (2001a). *CASHEW Version 1.1 – A Computer Program for Cyclic Analysis of Wood Shear Walls*. CUREE-Caltech Woodframe Project Report No. W-08, CUREE, Richmond, CA.

Folz, B. and Filiatrault, A. (2001a). Cyclic Analysis of Wood Shear Walls. *Journal of Structural Engineering*, April 2001, 433-441.

Folz, B. and Filiatrault, A. (2002). *SAWS Version 1.1 – A Computer Program for Seismic Analysis of Woodframe Structures*. CUREE-Caltech Woodframe Project Report No. W-21, CUREE, Richmond, CA.

Forest Products Laboratory (1999). *Wood handbook.- wood as an engineering material, Transport and Relaxation Phenomena in Porous Media*. Gen. Tech. Rep. FPL-GTR-113. Madison, WI: U.S. Department of Agriculture, Forest Service, Forest Products Laboratory.

Forintek Wood Products Research Institute. *Technical Expertise*, (On Line). http://www.forintek.ca/public/Eng/E4-Services/1.0need_tech_expertize.html (visited 06/2004).

Foschi, R.O. (1977). Analysis of Wood Diaphragms and Trusses, Part 1: Diaphragms. *Can. J. Civ. Engrg.*, Ottawa, 4(3), 345-362.

Fülöp, L. and Dubina, D. (2002). *Performance of Shear Wall Systems in Seismic Resistant Steel Buildings: Part 1-Experimental Results for Wall Panels.* Politehcnica University of Timisoara, Romania.

Fülöp, L.A.and Dubina, D. (2004a). Performance of wall-stud cold-formed shear panels under monotonic and cyclic loading. Part I: Experimental research. *Thin-Walled Structures*, (42), 321-338.

Fülöp, L.A.and Dubina, D. (2004b). Performance of wall-stud cold-formed shear panels under monotonic and cyclic loading. Part II: Numerical modelling and performance analysis. *Thin-Walled Structures*, (42), 339-349.

Gad, E.F., Duffield, C.F. (1997). Interaction Between Brick Veneer Walls and Domestic Framed Structures when Subjected to Earthquakes. *Proceedings of the 15th Australian Conference on the Mechanics of Structures and Materials*, Melbourne Victoria, Australia, 323-329.

Gad, E.F., Duffield, C.F., Chandler, A.M., Stark, G. (1998). Testing of Cold-formed Steel Framed Domestic Structures. *Proceedings of the 11th European Conference on Earthquake Engineering*, Paris, France.

Gad, E.F., Chandler, A.M., Duffield, C.F., Hutchinson, G.L. (1999a). Earthquake ductility and over-strength in residential structures. *Structural Engineering and Mechanics*, Vol. 8, No. 4, 361-382.

Gad, E.F., Duffield, C.F., Hutchinson, G.L, Mansell, D.S., Stark, G. (1999b). Lateral Performance of Cold-formed Steel-framed Domestic Structures. *Engineering Structures*, Elsevier Science Ltd., Vol. 21, 83-95.

Gad, E.F., Chandler, A.M., Duffield, C.F., Stark, G. (1999c). Lateral Behaviour of Plasterboard-clad Residential Steel Frames. *Journal of Structural Engineering*, ASCE, Vol. 125, No. 1, 32-39.

Gad, E.F. and Duffield, C.F. (2000). Lateral Behaviour of Light Framed Walls in Residential Structures. *Proceedings of the 12th World Conference on Earthquake Engineering*, Auckland, New Zealand, Paper 1663.

Gatto, K. and Uang, C.M. (2002). *Cyclic Response of Woodframe Shearwalls: Loading Protocol and Rate of Loading Effects*. CUREE-Caltech Woodframe Project Report No. W-13, CUREE, Richmond, CA.

He, M., Lam, F. and Prion, G.L. (1998). Influence of Cyclic test Protocols on Performance of Wood-Based Shear Walls. *Can. J. Civ. Eng.*, (25), 539-550.

Heidebrecht, A. (2003). Overview of Seismic Provisions of the Proposed 2005 Edition of the National Building Code of Canada. *Can. J. Civ. Eng.*, (30), 241-254.

Heine, C.P. (2001). *Simulated response of degrading hysteretic joints with slack behavior.* PhD Thesis, Virginia Polytechnic Institute and State University, VA, USA.

Humar, J. and Mahgoub, A. (2003). Determination of Seismic Design Forces by Equivalent Static Load Method. *Can. J. Civ. Eng.*, (30), 287-307.

International Code Council (ICC) (2003). *International Building Code (IBC) 2003.* Falls Church, VA, USA.

International Code Council (ICC-ES) (2003). *Acceptance criteria for shear wall assemblies consisting of wood structural panel sheathing attached to cold-formed steel framing with pneumatic- or gas-power-driven pin fasteners.* ICC Evaluation Service Inc. AC 230, California, USA.

International Code Council (ICC-ES) (2004). *Acceptance criteria for prefabricated wood shear panels.* ICC Evaluation Service Inc. AC 130, California, USA.

International Conference of Building Officials (1994). *Uniform Building Code - ICBO.* Whittier, CA.

International Conference of Building Officials (1997). *Uniform Building Code - ICBO.* Whittier, CA.

International Organization for Standardization (ISO) (2002). *Timber Structures – Joints made with Mechanical Fasteners – Quasi-Static Reversed-Cyclic Test Method.* ISO 16670.3:2002, TC 165 WG7.

Isoda, H., Folz, B., Filiatrault, A. (2002). *Seismic Modeling of Index Woodframe Buildings.* CUREE-Caltech Woodframe Project Report No. W-12, CUREE, Richmond, CA.

Jamison, J.B. (1997). *Monotonic and cyclic performance of structurally insulated panel shear walls.* Masters Thesis, Virginia Polytechnic Institute and State University, VA, USA.

Kannan, A.E. and Powell, G.H. (1973). *DRAIN-2D: a general purpose computer program for dynamic analysis of inelastic plane structures.* University of California, Report EERC 73-6, Berkeley, CA,USA.

Karacabeyli, E. and Ceccotti, A. (1998). Nailed wood-frame shear walls for seismic loads: Test results and design considerations. *Structural Engineering World Wide*, Paper T207-6, San Francisco, CA, USA.

Karacabeyli, E., Dolan, J.D., Ceccotti, A. (1999). Discussion on the paper: Comparison of Static and Dynamic Response of Timber Shear Walls. *Journal of Structural Engineering*, July 1999, 796-797.

Krawinkler, H. (1996). Cyclic loading histories for seismic experimentation on structural components. *Earthquake Spectra, 12 (1)*, 1-12.

Krawinkler, H., Parisi, F., Ibarra, L., Ayoub, A., Medina, R. (2000). *Development of a Testing Protocol for Woodframe Structures*. CUREE-Caltech Woodframe Project Report No. W-02, CUREE, Richmond, CA.

Landolfo, R., Della Corte, G., Fiorino, L. (2004). Testing of sheathed cold-formed steel stud shear walls for seismic performance evaluation. *13th World Conference on Earthquake Engineering*, paper 2697, August 2004, Vancouver, Canada.

Martin, É. (2002). *Inelastic Response of Steel Roof Deck Diaphragms under Simulated Dynamically Applied Seismic Loading*. Master's Thesis, Département des génies civil, géologique et des mines, École Polytechnique de Montréal, QC, Canada.

Medearis, K. and Young, D.H. (1964). "Energy absorption of structures under cyclic loading." *Journal of the Structural Division ASCE 90 (STI)*: 61-91.

Miranda, E. and Bertero, V.V. (1994). Evaluation of Strength Reduction Factors for Earthquake-Resistant Design. *Earthquake Spectra*, Vol. 10 (2).

Mitchell, D., Tremblay, R., Karacabeyli, E., Paultre, P., Saatcioglu, M., Anderson, D.L. (2003). Seismic Force Modification Factors for the Proposed 2005 Edition of the National Building Code of Canada. *Can. J. Civ. Eng.*, (30), 308-327.

National Research Council of Canada (NRCC) (1990). *National Building Code of Canada 1990 (NBCC), 10th Edition*. Canadian Commission on Building and Fire Codes, Ottawa, Ontario, Canada.

National Research Council of Canada (NRCC) (1995). *National Building Code of Canada 1995 (NBCC), 11th Edition*. Institute for Research in Construction, Ottawa, Ontario, Canada.

National Research Council of Canada (NRCC) (2004). *National Building Code of Canada 2005 (NBCC), 12th Edition Draft*. Institute for Research in Construction, Ottawa, Ontario, Canada.

Nassar, A. and Krawinkler, H. (1991). *Seismic demands for SDOF and MDOF systems, John Blume Earthquake Engineering Research Center Report No. 95*, Department of Civil Engineering, Stanford University, Stanford, CA.

Newark, N.M. and Hall, W.J. (1982). *Earthquake Spectra and Design*. Engineering Monograph, Earthquake Engineering Research Institute, Berkeley, CA, USA.

Parasin, A.V. and Stieda, C.K.A. (1985). *Recommendations for Allowable Stresses for Canadian Softwood Plywood.* Council of Forest Industries of British Columbia, Report 131. Vancouver, B.C.

Park, R. (1989). Evaluation of Ductility of Structures and Structural Assemblages from Laboratory Testing. *Bulletin of the New Zealand National Society for Earthquake Engineering*, Vol. 22, No. 3, 155-166.

Paulay, T. and Priestley, M.J.N. (1992). *Seismic Design of Reinforced Concrete and Masonry Buildings*. J. Wiley, New York, USA.

Porter, M.L. (1987). Sequential Phased Displacement (SPD) Procedure for TCCMAR Testing. *Proceedings of the Third Meeting of the Joint Technical Coordinating Committee on Masonry Research, U.S. - Japan Coordinated Earthquake Research Program*, Tomamu, Japan.

Powell,G.H. (1993). *DRAIN-2DX User's guide.* Department of Civil Engineering, University of California, Berkeley, CA, USA.

Prakash, V. and Powell, G.H. (1993). *DRAIN-2DX, DRAIN-3DX and DRAIN-BUILDING: Base Program and Design Documentation.* Department of Civil Engineering, University of California, Berkeley, CA, USA.

Richard, N., Davenne, L., Daudeville, L., Prion, H., Lam, F. (2001). Influence des connexions sur la résistance au contreventement de murs à ossature en bois. *Annales Génie Civil Bois*, (5), 35-44.

Rogers, C.A., Branston, A.E., Boudreault, F.A., Chen, C.Y. (2004). Steel Frame / Wood Panel Shear Walls: Preliminary Design Information for use with the 2005 NBCC. *13th World Conference on Earthquake Engineering*, Vancouver, B.C., Canada.

Rose, J.D. (1998). *Preliminary testing of wood structural panel shear walls under cyclic (reversed) loading. Report No. 158*. APA The Engineered Wood Association, Tacoma, WA.

SAC/BD (1997). *Protocol for fabrication, inspection, testing and documentation of beam-column connection tests and other experimental specimens*. SAC Steel Project Background Document, Report No. SAC/BD-97/02, SAC Joint Venture, Sacramento, CA.

Salenikovich, A.J. and Dolan, J.D. (2003). The Racking Performance of Shear Walls with various aspect ratios. Part 2. Cyclic tests of fully anchored walls. *Forest Products Journal*, Nov/Dec 2003, Vol. 53 (11/12), 37-45.

Salenikovich, A.J., Dolan, J.D., Easterling, W.S. (2000). Racking Performance of Long Steel-Frame Shear Walls. *Fifteenth International Specialty Conference on Cold-Formed Steel Structures*, St-Louis, MO, USA.

Serrette, R., Nguyen, H., Hall, G. (1996). *Shear Wall Values for Light Weight Steel Framing*. Report No. LGSRG-3-96, Santa Clara University, Department of Civil Engineering, Santa Clara, CA, USA.

Serrette, R., Encalada, J., Hall, G., Matchen, B., Nguyen, H., Williams, A. (1997). *Additional Shear Wall Values for Light Weight Steel Framing*. Report No. LGSRG-1-97, Santa Clara University, Department of Civil Engineering, Santa Clara, CA, USA.

Serrette, R., Morgan, K.A., Sorhouet, M.A. (2002). *Performance of Cold-Formed Steel-Framed Shear Walls: Alternative Configurations*. Report No. LGSRG-06-02, Santa Clara University, Department of Civil Engineering, Santa Clara, CA, USA.

Simpson Strong-Tie Co. Inc. (2001). *Light Gauge Steel Construction Connectors*. Dublin, USA.

Smith, G.R. (1974). *The Derivation of Allowable Unit Stresses for Unsanded Grades of Douglas Fir Plywood.* Council of Forest of British Columbia, Report 105. Vancouver, B.C.

Soltis, L.A., Gromala, D.S., Tuomi, R.L. (1981). "Seismic performance of low-rise wood buildings." Pages 78-91 in Gupta, A.K., ed. *Seismic performance of low rise buildings – State of the art and research needs.* American Society of Civil Engineers, New-York, NY.

Stewart, W.G. (1987). *The Seismic Design of Plywood Sheathed Shear Walls.* PhD Thesis, University of Canterbury, New-Zealand.

Structural Engineers Association of Southern California (SEOSC), (1997). *Standard Method of Cyclic (Reversed) Load Test for Shear Resistance of Framed Walls for Buildings.* SEAOSC, Whitten, CA.

Sugiyama, H. (1984). Japanese experience and research on timber buildings in earthquakes. *Proc. Pacific Timber Engineering Conference*, Auckland, New Zealand (2), pp. 431-438.

Suzuki, S., Nawa, D., Miyamoto, K., Shibusawa, T. (2000). Shear Through-Thickness Properties of Wood-Based Panels Determined by the Two-Rail Shear and the Edgewise Shear Methods (in Japanese). *J. Soc. Mat. Sci. Japan* (49), 395-400.

Suzuki, S. and Miyagawa, H. (2003). Effect of Element Type on the Internal Bond Quality of Wood-Based Panels Determined by Three Methods. *Journal of Wood Science*, (49), 513-518.

van de Lindt, J.W. and Walz, M. (2003). Development and Application of Wood Shear Wall Reliability Model. *Journal of Structural Engineering*, March 2003, 405-413.

van de Lindt, J.W. (2004). Evolution of Wood Shear Wall Testing, Modelling, and Reliability Analysis: Bibliography. *Journal of Structural Engineering*, February 2004, 44-53.

Yang, W. (2003). *Inelastic Seismic Response of Steel Roof Deck Diaphragms Including Effects of Non-Structural Components and End Laps*. Master's Thesis, Département des génies civil, géologique et des mines, École Polytechnique de Montréal, QC, Canada.

Zhao, Y. (2002). *Cyclic Performance of Cold-Formed Steel Stud Shear Walls*. Masters Thesis, Dept. of Civil Engineering and Applied Mechanics, McGill University, Montreal, Canada.

APPENDIX A

REVERSED CYCLIC TEST PROTOCOLS

Table A-1 : Serrette-SPD cyclic protocol for test 3-A

FME =	20.0mm	Screw Pattern:	102 / 305 mm
		Sheathing:	CSP

Displ. (% FME)	Target (corr.) mm	Actuator Input mm	No. Of cycles
25%	5.00	7.035	3
50%	10.00	13.380	3
75%	15.00	19.265	3
100%	20.00	25.155	3
125%	25.00	31.175	3
150%	30.00	36.955	3
175%	35.00	42.620	3
200%	40.00	48.330	3
225%	45.00	54.065	3
250%	50.00	60.080	3
275%	55.00	65.815	3
300%	60.00	71.430	3
325%	65.00	76.920	3
350%	70.00	82.350	3
375%	75.00	87.755	3
400%	80.00	93.075	3
425%	85.00	99.025	3
450%	90.00	104.400	3

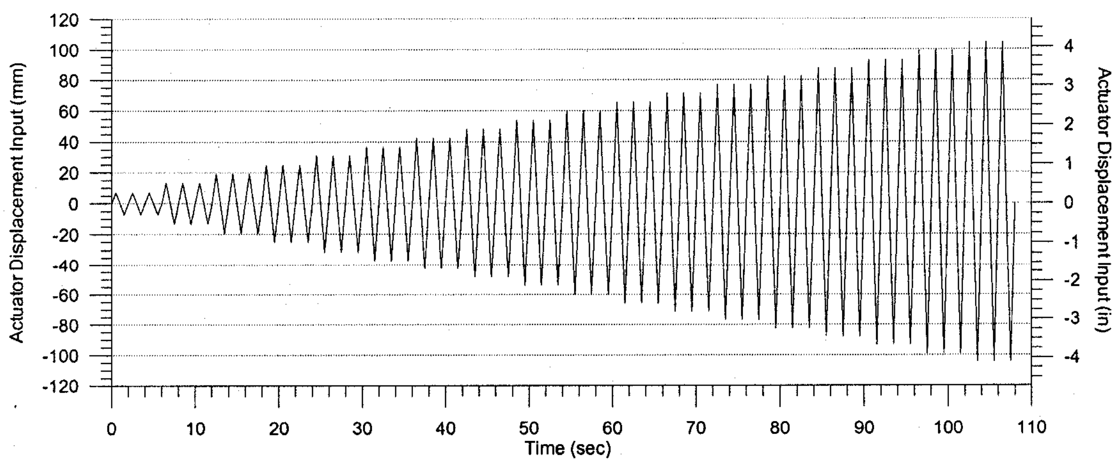

Figure A-1 : Serrette-SPD cyclic protocol for test 3-A

Table A-2 : Serrette-SPD cyclic protocol for tests 3-B,C

FME =	20.0mm	Screw Pattern:	102 / 305 mm
		Sheathing:	CSP

	Target (corr.)	Actuator Input	
Displ. (% FME)	mm	mm	No. Of cycles
25%	5.00	7.035	3
50%	10.00	13.380	3
75%	15.00	19.265	3
100%	20.00	25.155	3
125%	25.00	31.175	3
150%	30.00	36.955	3
175%	35.00	42.620	3
200%	40.00	48.330	3
225%	45.00	54.065	3
250%	50.00	60.080	3
275%	55.00	65.815	3
300%	60.00	71.430	3
325%	65.00	76.920	3
350%	70.00	82.350	3
375%	75.00	87.755	3
400%	80.00	93.075	3
425%	85.00	99.025	3
450%	90.00	104.400	3

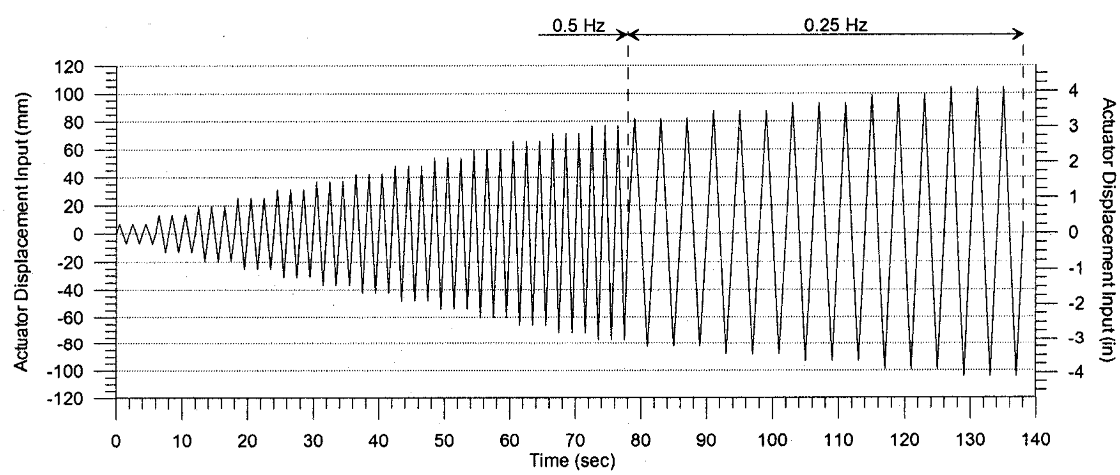

Figure 2 : Serrette-SPD cyclic protocol for tests 3-B,C

Table A-3 : CUREE cyclic protocol for tests 4-A,B,C

Δ=0.6*Δ_m =	46.78mm	Screw Pattern:	102 / 305 mm
		Sheathing:	CSP

Displ.	Target (corr.) mm	Actuator Input mm	No. Of cycles
0.050 Δ	2.339	3.824	6
0.075 Δ	3.509	5.590	1
0.056 Δ	2.632	4.270	6
0.100 Δ	4.678	7.278	1
0.075 Δ	3.509	5.590	6
0.200 Δ	9.357	13.241	1
0.150 Δ	7.018	10.418	3
0.300 Δ	14.035	18.835	1
0.225 Δ	10.526	14.658	3
0.400 Δ	18.713	24.405	1
0.300 Δ	14.035	18.835	2
0.700 Δ	32.748	40.980	1
0.525 Δ	24.561	31.587	2
1.000 Δ	46.783	57.318	1
0.750 Δ	35.088	43.668	2
1.500 Δ	70.175	84.002	1
1.125 Δ	52.631	64.251	2

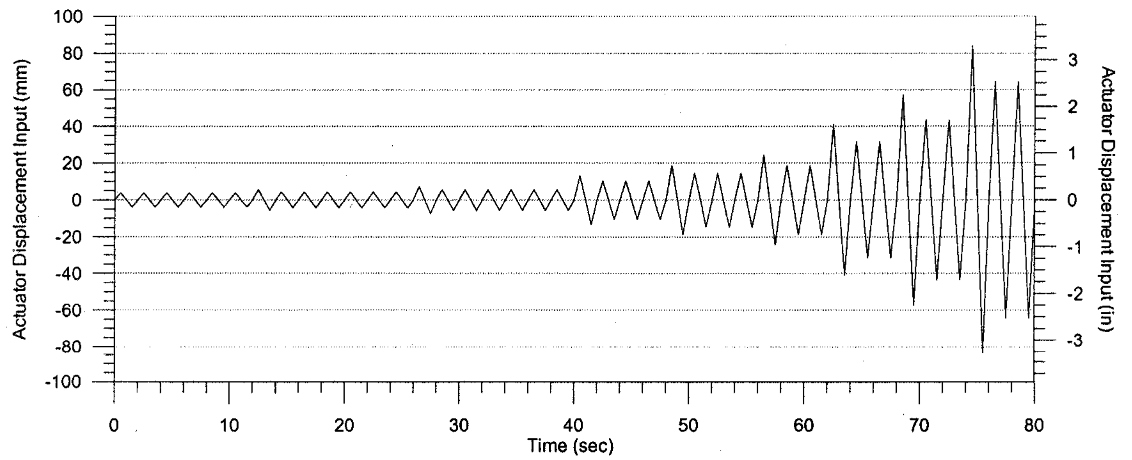

Figure A-3: CUREE cyclic protocol for tests 4-A,B,C

Table A-4 : CUREE cyclic protocol for tests 6-A,B,C

$\Delta = 0.6 * \Delta_m$	45.50mm	Screw Pattern:	102 / 305 mm
		Sheathing:	DFP

	Target (corr.)	Actuator Input	
Displ.	mm	mm	No. Of cycles
0.050 Δ	2.275	2.747	6
0.075 Δ	3.413	4.120	1
0.056 Δ	2.559	3.090	6
0.100 Δ	4.550	5.493	1
0.075 Δ	3.413	4.120	6
0.200 Δ	9.100	10.987	1
0.150 Δ	6.825	8.240	3
0.300 Δ	13.651	16.480	1
0.225 Δ	10.238	12.360	3
0.400 Δ	18.201	21.973	1
0.300 Δ	13.651	16.480	2
0.700 Δ	31.851	38.453	1
0.525 Δ	23.889	28.840	2
1.000 Δ	45.502	54.933	1
0.750 Δ	34.127	41.200	2
1.500 Δ	68.253	82.400	1
1.125 Δ	51.190	61.800	2
2.000 Δ	91.004	109.866	1
1.500 Δ	68.253	82.400	2

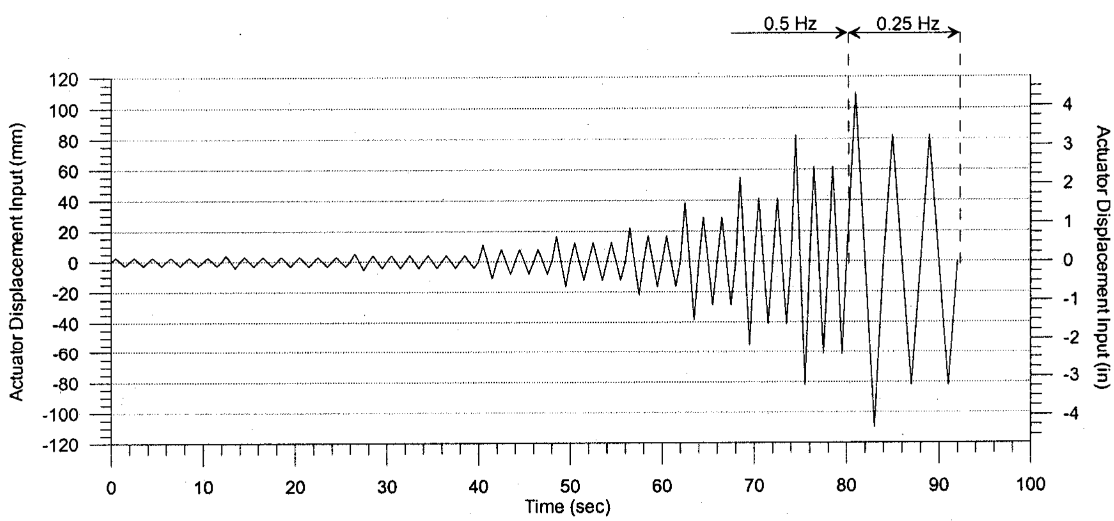

Figure A-4 : CUREE cyclic protocol for tests 6-A,B,C

APPENDIX B

DESIGN VALUES CALCULATIONS WITH AN EXCEL SPREADSHEET

B.1 BACKGROUND INFORMATION

An Excel™ spreadsheet was created using Visual Basic™ Macros to ease the design values and R-Factors computation following the series of tests completed during the summer 2003 at McGill University.

The testing protocol used for all the cyclic tests was the "*CUREE-Caltech Testing Protocol for Deformation Controlled Quasi-Static Cyclic Testing for Ordinary Ground Motions*" (Krawinkler *et al.* 2002).

Five different versions of the CUREE Protocol have been used during the summer 2003 test series depending on the length and frequency selected. They are:

1. Max. amplitude at 1.5Δ without freq. change (all at 0.5 Hz) – 80 sec.
2. Max. amplitude at 2.0Δ without freq. change (all at 0.5 Hz) – 86 sec.
3. Max. amplitude at 1.5Δ with freq. change (0.5 Hz until 1.0Δ and 0.25 Hz after) – 92 sec.
4. Max. amplitude at 2.0Δ with freq. change (0.5 Hz until 2.0Δ and 0.25 Hz after) – 92 sec.
5. Max. amplitude at 2.0Δ with freq. change (0.5 Hz until 1.5Δ and 0.25 Hz after) – 98 sec.

B.2 GENERAL INPUT PROCEDURES

The test files usually contain unwanted rows of acquired data due to the fact that the recording usually started before the actual testing. All unnecessary rows have to be deleted; which means a certain number of rows at the beginning of the test (before the actuator started to move) have to be deleted as well as all the rows that came after the last trailing cycle.

Make sure **the order of the acquisition channels are in the same column order shown in Figure B-1** (unnecessary columns are hidden but have not been deleted).

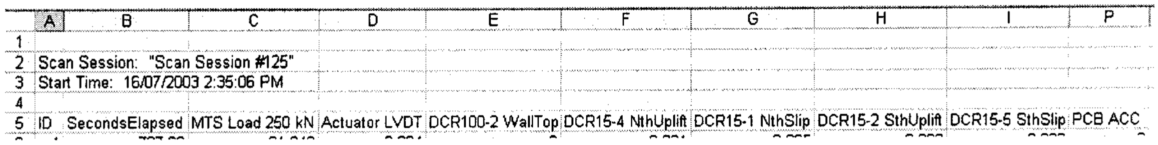

	A	B	C	D	E	F	G	H	I	P
1										
2	Scan Session: "Scan Session #125"									
3	Start Time: 16/07/2003 2:35:06 PM									
4										
5	ID	SecondsElapsed	MTS Load 250 kN	Actuator LVDT	DCR100-2 WallTop	DCR15-4 NthUplift	DCR15-1 NthSlip	DCR15-2 SthUplift	DCR15-5 SthSlip	PCB ACC

Figure B-1 : Columns order in the spreadsheet to be imported in "EEEP_curee.xls"

B.2.1 IMPORTING DATA TO THE "EEEP_CUREE.XLS" WORKBOOK

When opening the "EEEP_curee.xls" workbook, you see three spreadsheets: "Data", "Energy" and "EEEP". Copy the data from the original file to the "EEEP_curee.xls" - "Data" spreadsheet. The range of selection will depend on the protocol used but will range from A6:T"last row". Paste it at the same location in the EEEP_curee spreadsheet (cell A6).

You then see the total time of the protocol in the cell "M4" and you have to select the type of CUREE protocol with which the wall was tested from the drop down list in "J4". You need to know if the max displacement was 1.5Δ or 2.0Δ.

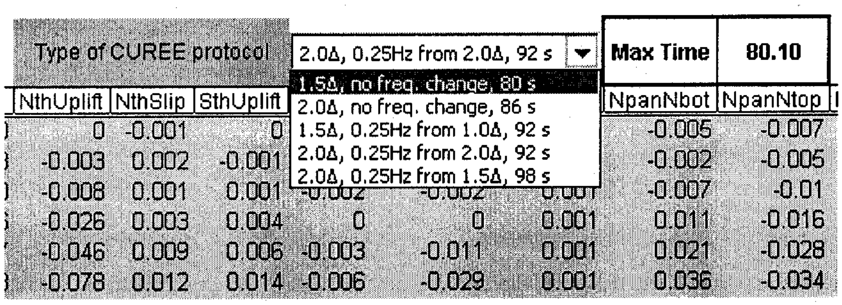

Figure B-2 : Type of Curee Protocol selection

Once you have selected the protocol, follow these steps:

1. Click the "Hide Columns" Hide Columns button;

2. Enter the wall length in cell "Z1";

3. Click the "Plot Backbone" Plot Backbone button;

B.2.2 CREATING THE BACKBONE CURVE

A new chart sheet is created when the "Plot backbone" button is pressed. A few modifications have to be done to the curves before continuing with the computation. Figure B-3 shows what the graph should look like:

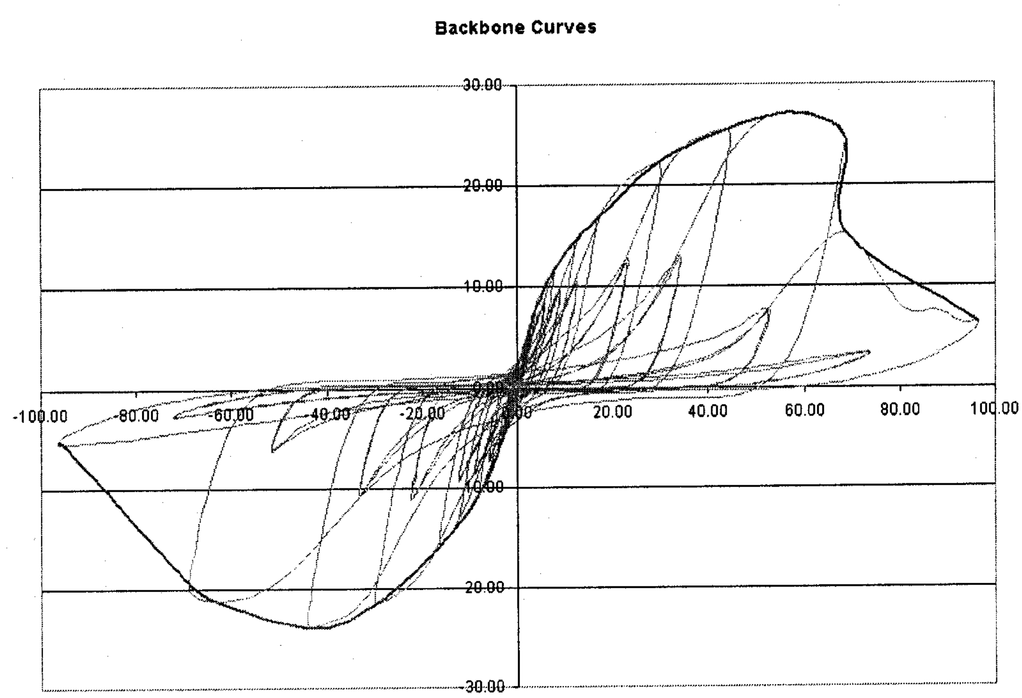

Figure B-3 : Backbone curves as they appear when plotted automatically

On the positive backbone curve, the maximum displacement did not occur at the same location as the maximum force. The user may have to modify the source data of the backbone curves to get a smoothed curve. The data is located on the "Data" spreadsheet and is in the grey shaded range "AC31:AD57". In the example shown above, the coordinate (69.00,15.04) should be deleted to obtain a smoother curve. When deleting the coordinate, the user has to drag up the other data to obtain one uniform range of data.

Backbone Curve	
Displ. (mm)	Load (kN)
-96.50	-5.25
-95.41	-5.43
-69.12	-19.36
-63.26	-21.11
-43.21	-23.88
-29.38	-21.46
-16.15	-15.63
-11.98	-13.33
-7.92	-10.50
-4.20	-6.41
-3.20	-5.13
0.00	0.00
0.00	0.00
2.94	6.34
3.78	7.56
7.71	11.51
11.93	14.32
16.40	16.51
29.60	22.17
43.77	25.45
57.97	27.14
68.77	24.59
69.00	15.04
96.45	6.25

Backbone Curve	
Displ. (mm)	Load (kN)
-96.50	-5.25
-95.41	-5.43
-69.12	-19.36
-63.26	-21.11
-43.21	-23.88
-29.38	-21.46
-16.15	-15.63
-11.98	-13.33
-7.92	-10.50
-4.20	-6.41
-3.20	-5.13
0.00	0.00
0.00	0.00
2.94	6.34
3.78	7.56
7.71	11.51
11.93	14.32
16.40	16.51
29.60	22.17
43.77	25.45
57.97	27.14
68.77	24.59
96.45	6.25

Backbone Curve	
Displ. (mm)	Load (kN)
-96.50	-5.25
-95.41	-5.43
-69.12	-19.36
-63.26	-21.11
-43.21	-23.88
-29.38	-21.46
-16.15	-15.63
-11.98	-13.33
-7.92	-10.50
-4.20	-6.41
-3.20	-5.13
0.00	0.00
0.00	0.00
2.94	6.34
3.78	7.56
7.71	11.51
11.93	14.32
16.40	16.51
29.60	22.17
43.77	25.45
57.97	27.14
68.77	24.59
96.45	6.25

Figure B-4 : Modifications to the backbone curve data range

When the modifications are done (could be one or two points to delete for the positive and negative curves), the user has to find the trendline that fits the best the backbone curve (both positive and negative). The procedure is to right-click on one of the backbone curve, select "Add trendline", select a polynomial type to the order "6" and check the "Set intercept=0" and "Display equation on chart" options under the "Options" tab. The objective here is to get trendlines that match as good as possible the real backbone curves so it is possible that the user would have to change the order of the polynomial trendlines a few times. To do so, right-click again on the trendline and select a different order. The user should keep in mind that the trendline should match as best as possible the backbone curve **from the origin to ±0.8*v_{peak}.** The display of the equations just helps remember the order of the polynomial equations which will have to be typed on the "EEEP" spreadsheet. Once you found the two best match for both the positive and the negative backbone curves, you should have something like Figure B-5 (the trendlines are in dotted lines).

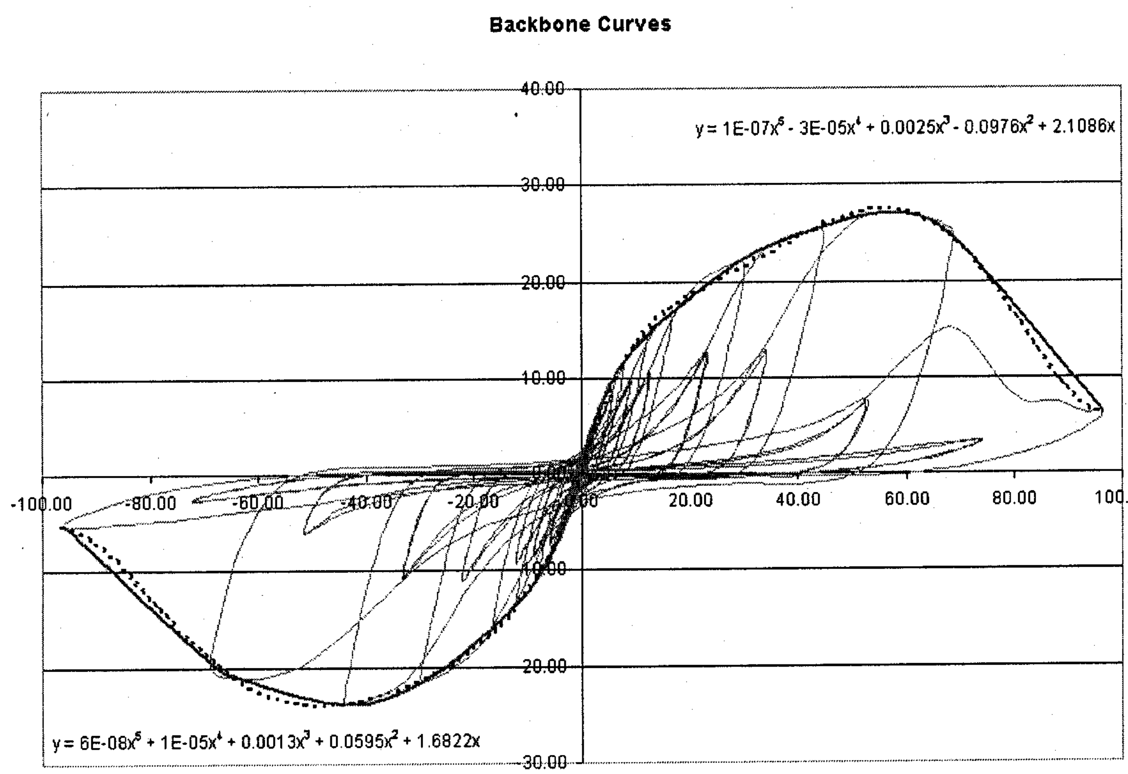

Figure B-5 : Backbone curves and fitted trendlines

As previously mentioned, the workbook also compute the total dissipated energy (not normalized) on the "Energy" spreadsheet. Charts like the ones shown in Figure B-6 will be computed for each test.

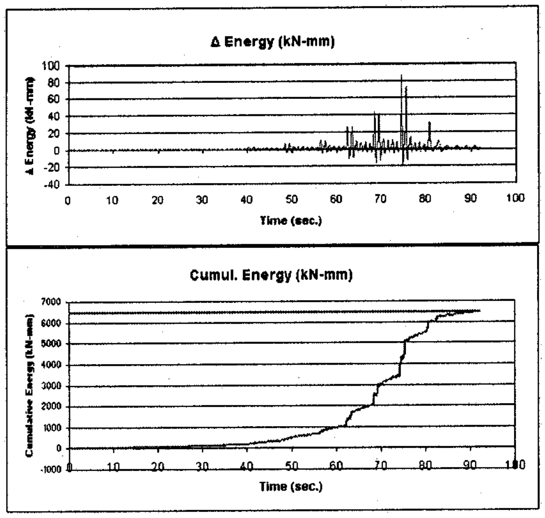

Figure B-6 : Dissipated Energy Charts

B.2.3 EQUIVALENT ENERGY ELASTIC-PLASTIC CURVES (EEEP CURVES)

On the spreadsheet "EEEP", the user only has to enter the order of the positive and negative polynomial equations of the trendlines in cells "G2" and "G3" respectively. The spreadsheet then gives out the $\mathbf{R_d}$ **factor** and the average v_{yield} in kN/m (see Figure B-7). Click on the "Plot EEEP" button to plot the Equivalent Energy Elastic-Plastic curves and the backbone curves. Figure B-8 shows the chart sheet the user should obtain.

Order of positive trendline equation	5
Order of negative trendline equation	4

	Negative	Positive	Units
F_{peak}	-23.88	27.14	kN
$F_{failure}$	-19.11	21.71	kN
$0.4{*}F_{peak}$	-9.55	10.86	kN
F_{yield}	-21.38	23.31	kN
K_e	1.26	1.60	kN/mm
Ductility (μ)	4.16	5.45	-
Δ_{yield}	-17.01	14.60	mm
Δ_{peak}	-43.21	57.97	mm
$\Delta_{failure}$	-70.70	79.60	mm
$\Delta_{0.4Fpeak}$	-7.60	6.80	mm
$Area_{Backbone}$	1329.85	1685.58	kN-mm
$Area_{EEEP}$	1329.85	1685.58	kN-mm
Check	OK	OK	

Plot EEEP

Save your file before clicking on "Reset"

Reset

R_d=	2.93	
V_{yield}=	18.33	kN/m

Figure B-7 : EEEP Parameters

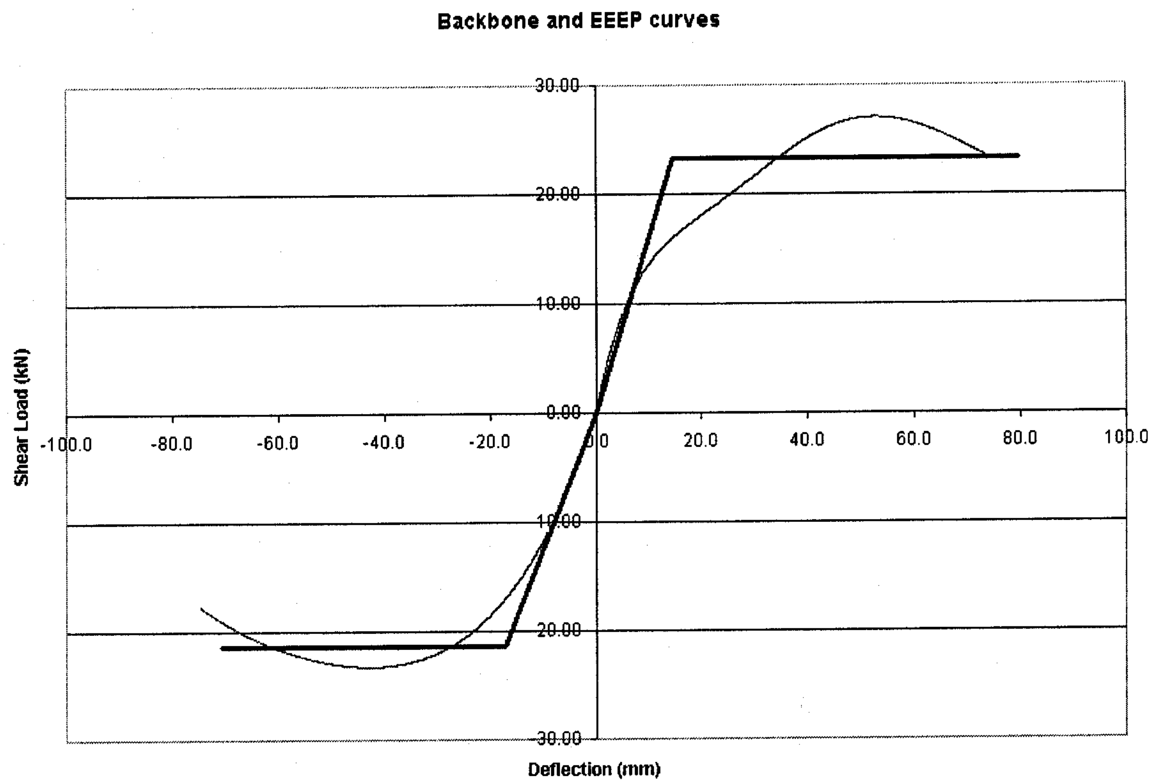

Figure B-8 : EEEP and Backbone curves

APPENDIX C

EXPERIMENTAL HYSTERESES
VS
STEWART MODEL HYSTERESES

Group	Wood Panel	Size	Srew Pattern	K_0 (kN/mm)	r	Fy (kN)	Fy (kN)	Fu/Fy	Fu (kN)	Fi (kN)	P_{Tri}	Fi/Fy	P_{UNL}	β	α
4	CSP	4' x 8'	4" x 12"	1.05	0.25	12.45	-12.45	1.50	18.70	1.75	0	0.14	2.20	1.10	0.35

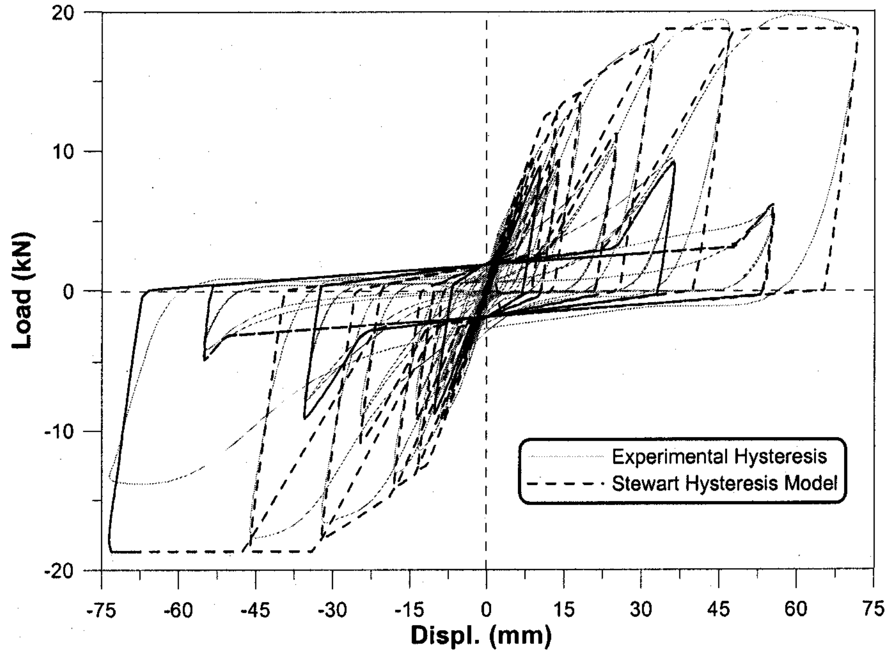

Figure C-1 : Superimposed Experimental and Modeled Hystereses (Group 4)

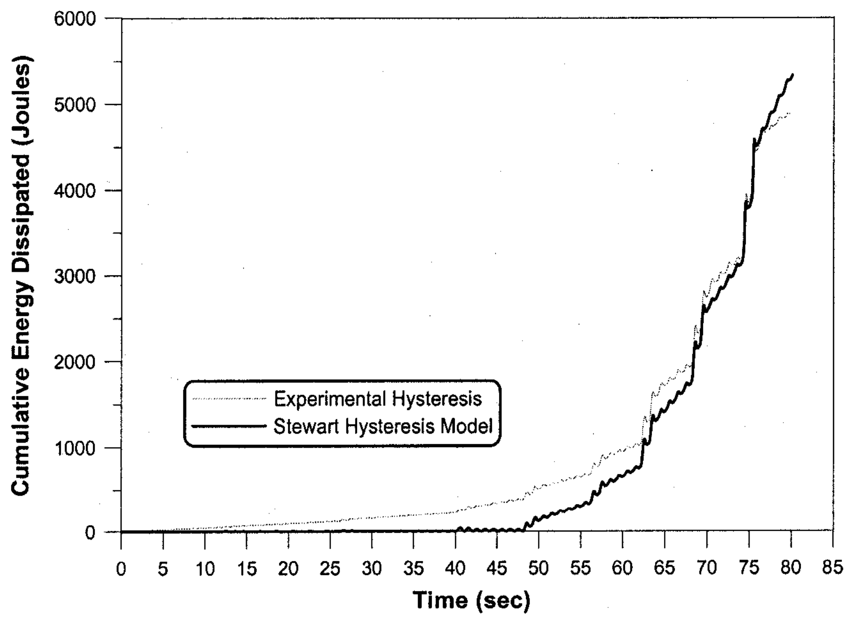

Figure C-2 : Cumulative Energy Dissipated from Experimental Test and Stewart Model Hystereses (Group 4)

Group	Wood Panel	Size	Srew Pattern	K_0 (kN/mm)	r	Fy (kN)	Fy (kN)	Fu/Fy	Fu (kN)	Fi (kN)	P_{Tri}	Fi/Fy	P_{UNL}	β	α
6	DFP	4' x 8'	4" x 12"	1.55	0.20	15.50	-15.50	1.65	25.50	2.50	0	0.16	1.55	1.10	0.35

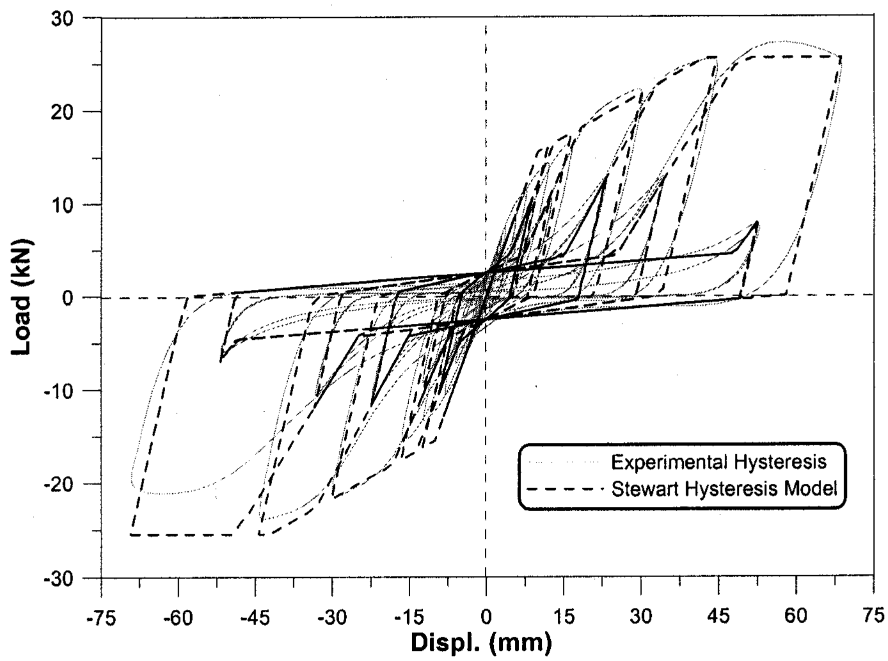

Figure C-3 : Superimposed Experimental and Modeled Hystereses (Group 6)

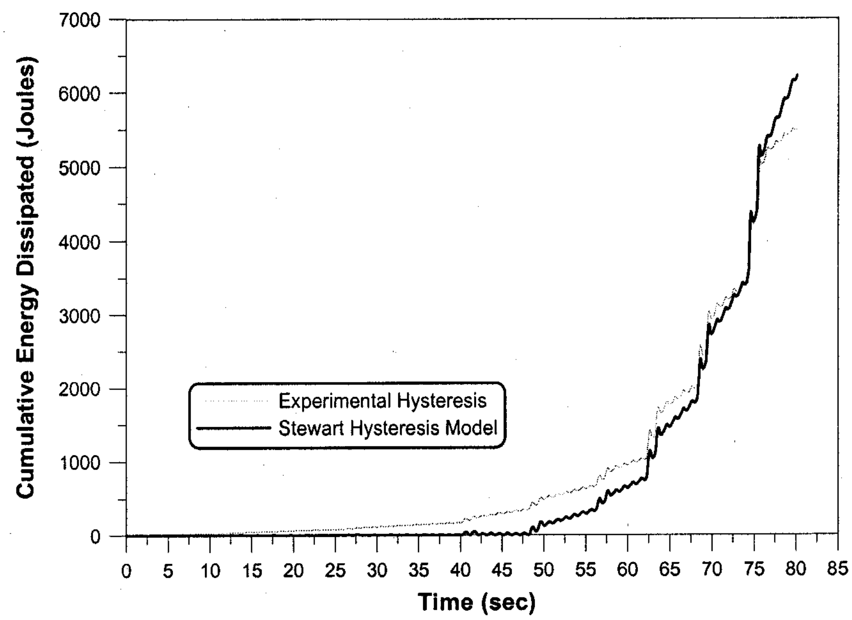

Figure C-4 : Cumulative Energy Dissipated from Experimental Test and Stewart Model Hystereses (Group 6)

Group	Wood Panel	Size	Srew Pattern	K_0 (kN/mm)	r	Fy (kN)	Fy (kN)	Fu/Fy	Fu (kN)	Fi (kN)	P_{Tri}	Fi/Fy	P_{UNL}	β	α
8	CSP	4' x 8'	6" x 12"	1.15	0.20	9.20	-9.20	1.50	13.83	1.50	0	0.16	1.65	1.10	0.41

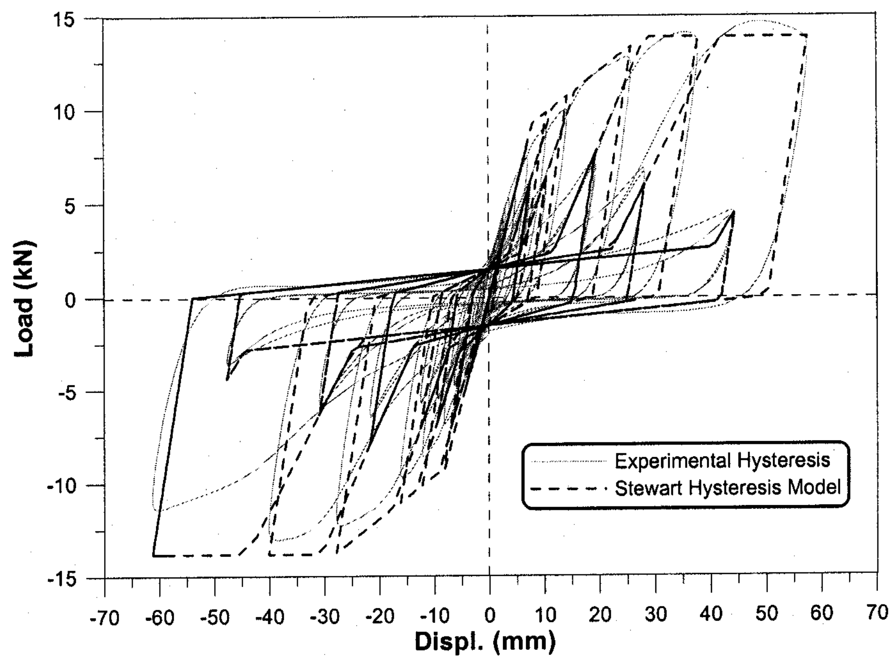

Figure C-5 : Superimposed Experimental and Modeled Hystereses (Group 8)

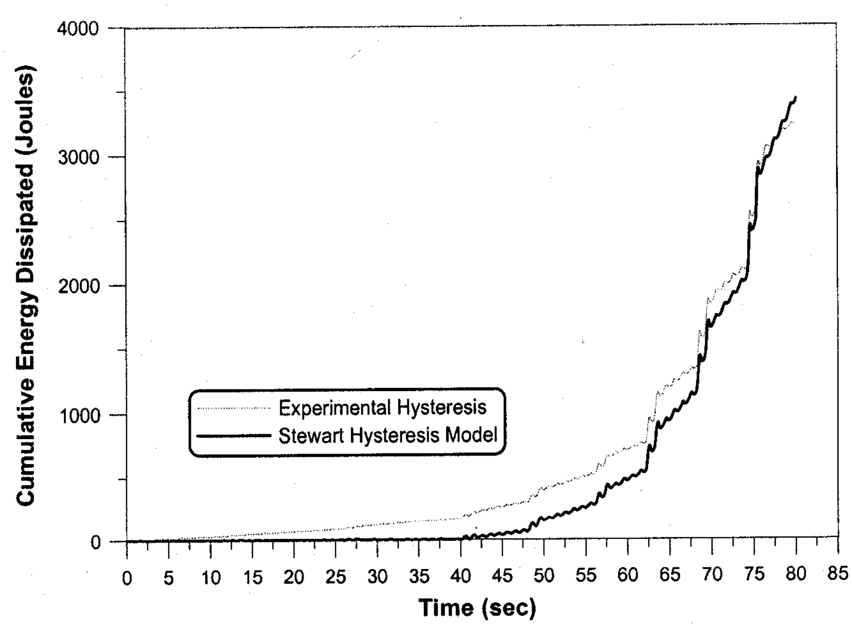

Figure C-6 : Cumulative Energy Dissipated from Experimental Test and Stewart Model Hystereses (Group 8)

Group	Wood Panel	Size	Srew Pattern	K_0 (kN/mm)	r	Fy (kN)	Fy (kN)	Fu/Fy	Fu (kN)	Fi (kN)	P_{Tri}	Fi/Fy	P_{UNL}	β	α
10	CSP	4' x 8'	3" x 12"	1.50	0.23	20.45	-20.45	1.50	30.70	2.25	0	0.11	1.65	1.09	0.23

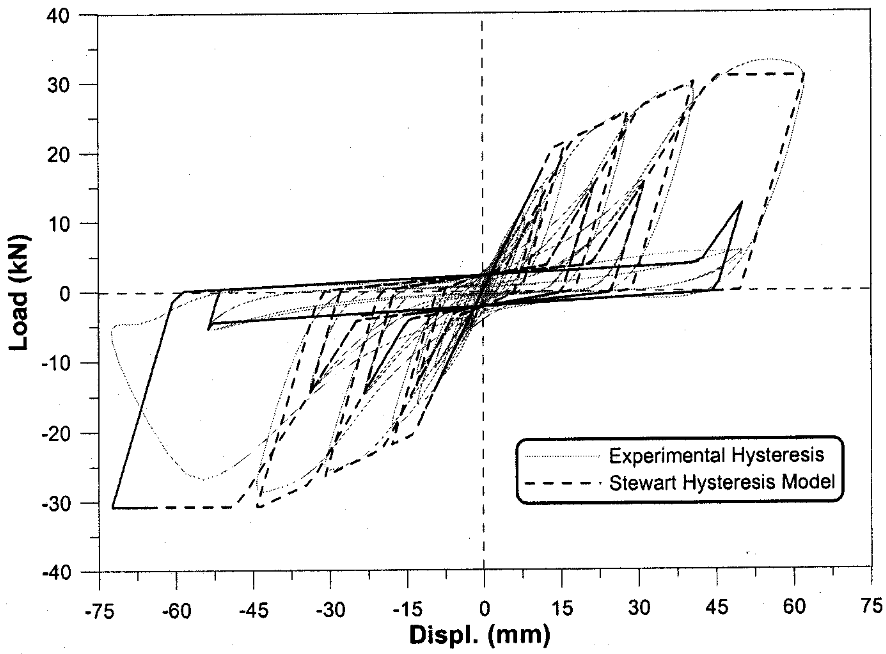

Figure C-7 : Superimposed Experimental and Modeled Hystereses (Group 10)

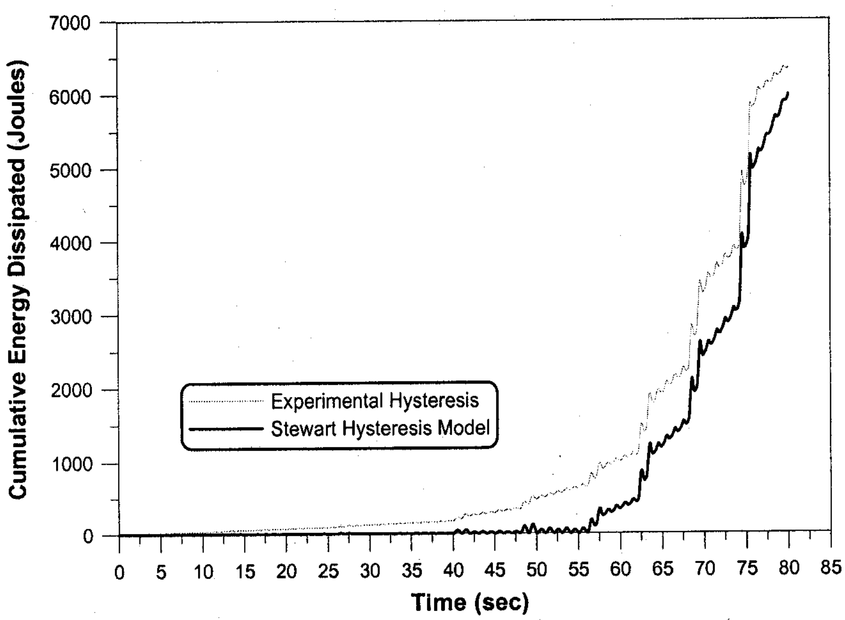

Figure C-8 : Cumulative Energy Dissipated from Experimental Test and Stewart Model Hystereses (Group 10)

Group	Wood Panel	Size	Srew Pattern	K_0 (kN/mm)	r	Fy (kN)	Fy (kN)	Fu/Fy	Fu (kN)	Fi (kN)	P_{Tri}	Fi/Fy	P_{UNL}	β	α
12	DFP	4' x 8'	6" x 12"	1.25	0.16	11.00	-11.00	1.55	17.10	1.00	0	0.09	2.20	1.10	0.41

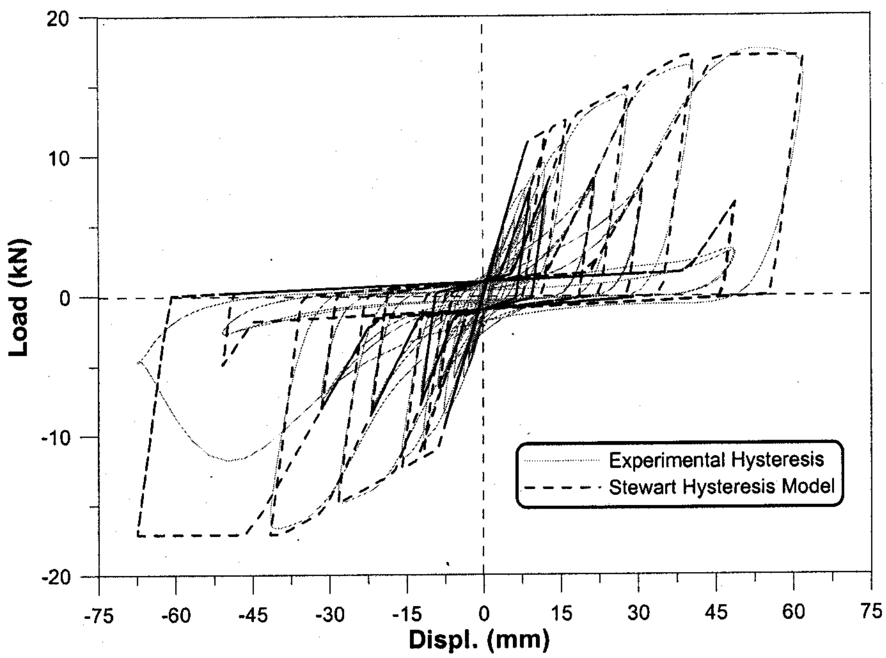

Figure C-9 : Superimposed Experimental and Modeled Hystereses (Group 12)

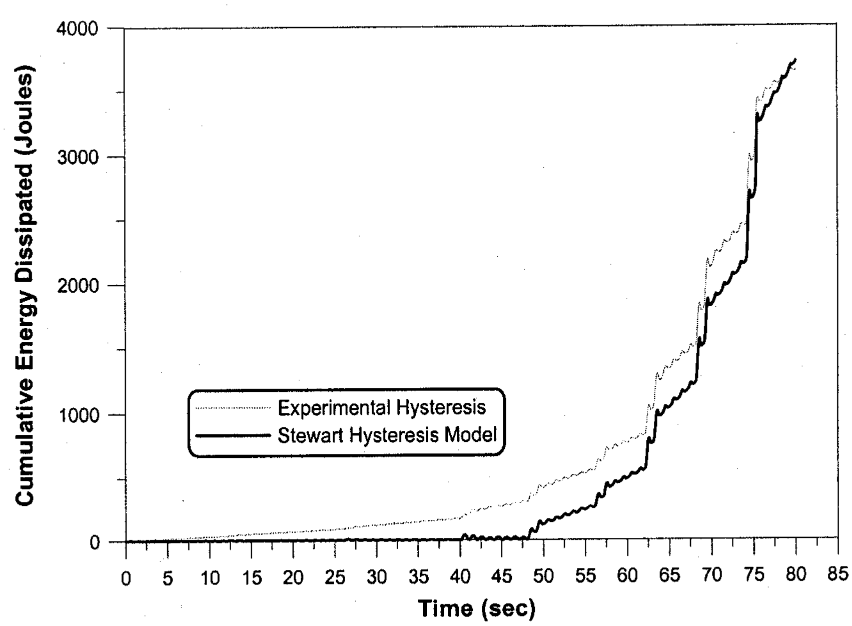

Figure C-10 : Cumulative Energy Dissipated from Experimental Test and Stewart Model Hystereses (Group 12)

Group	Wood Panel	Size	Srew Pattern	K_0 (kN/mm)	r	Fy (kN)	Fy (kN)	Fu/Fy	Fu (kN)	Fi (kN)	P_{Tri}	Fi/Fy	P_{UNL}	β	α
14	DFP	4' x 8'	3" x 12"	1.75	0.26	22.00	-22.00	1.65	36.20	3.00	0	0.14	1.55	1.09	0.23

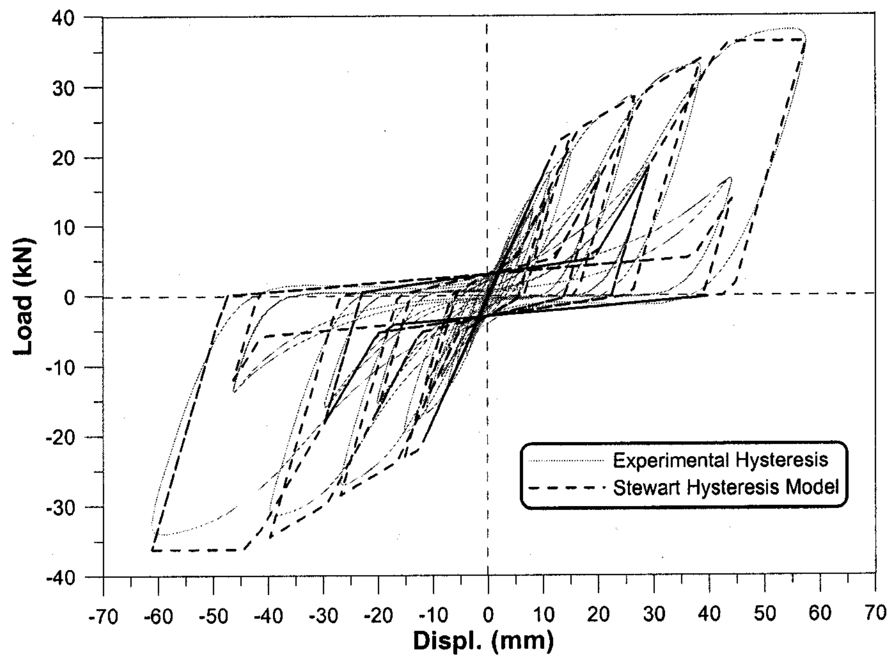

Figure C-11 : Superimposed Experimental and Modeled Hystereses (Group 14)

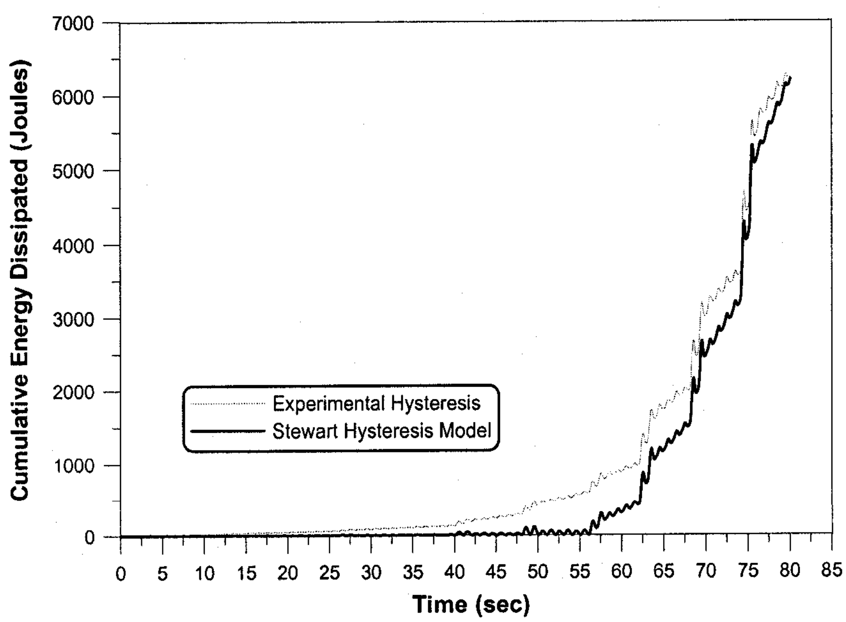

Figure C-12 : Cumulative Energy Dissipated from Experimental Test and Stewart Model Hystereses (Group 14)

Group	Wood Panel	Size	Srew Pattern	K_0 (kN/mm)	r	Fy (kN)	Fy (kN)	Fu/Fy	Fu (kN)	Fi (kN)	P_{Tri}	Fi/Fy	P_{UNL}	β	α
16	CSP	2' x 8'	6" x 12"	0.33	0.26	3.70	-3.70	1.81	6.70	0.65	0	0.18	2.00	1.10	0.41

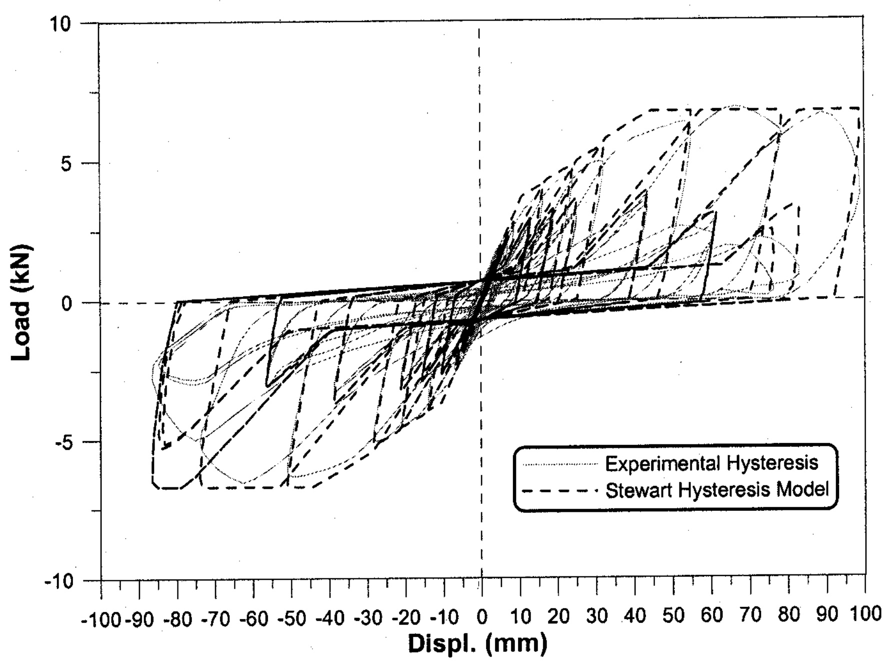

Figure C-13 : Superimposed Experimental and Modeled Hystereses (Group 16)

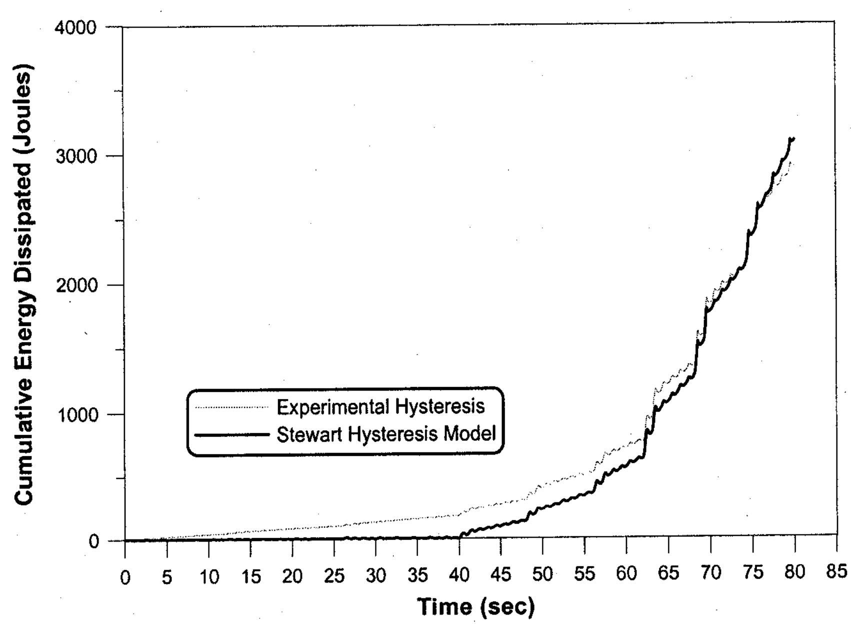

Figure C-14 : Cumulative Energy Dissipated from Experimental Test and Stewart Model Hystereses (Group 16)

Group	Wood Panel	Size	Srew Pattern	K_0 (kN/mm)	r	Fy (kN)	Fy (kN)	Fu/Fy	Fu (kN)	Fi (kN)	P_{Tri}	Fi/Fy	P_{UNL}	β	α
18	CSP	2' x 8'	4" x 12"	0.40	0.25	5.50	-5.50	1.79	9.86	1.00	0	0.18	2.40	1.10	0.35

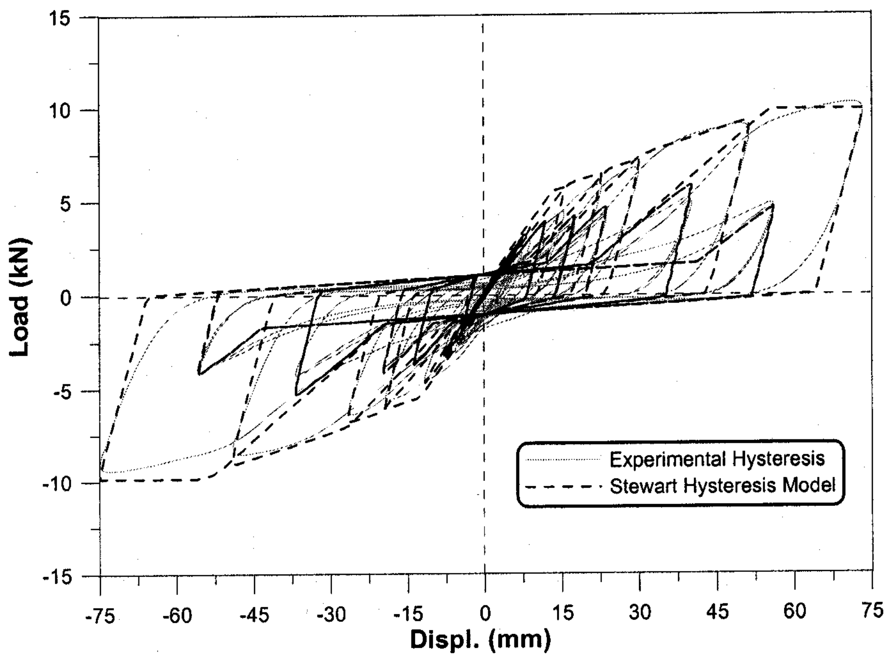

Figure C-15 : Superimposed Experimental and Modeled Hystereses (Group 18)

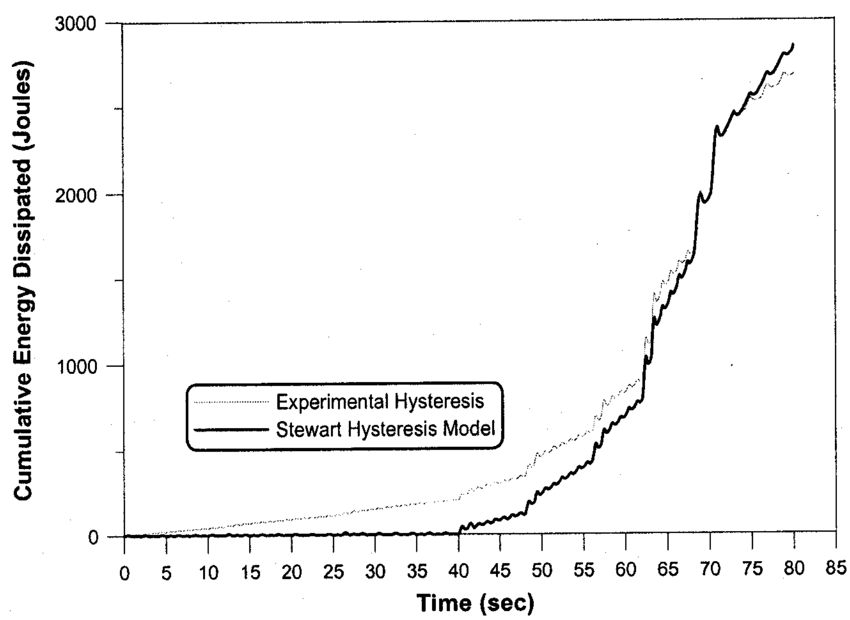

Figure C-16 : Cumulative Energy Dissipated from Experimental Test and Stewart Model Hystereses (Group 18)

Group	Wood Panel	Size	Srew Pattern	K_0 (kN/mm)	r	Fy (kN)	Fy (kN)	Fu/Fy	Fu (kN)	Fi (kN)	P_{Tri}	Fi/Fy	P_{UNL}	β	α
20	OSB	2' x 8'	6" x 12"	0.40	0.28	3.50	-3.50	1.86	6.50	0.65	0	0.19	2.40	1.10	0.41

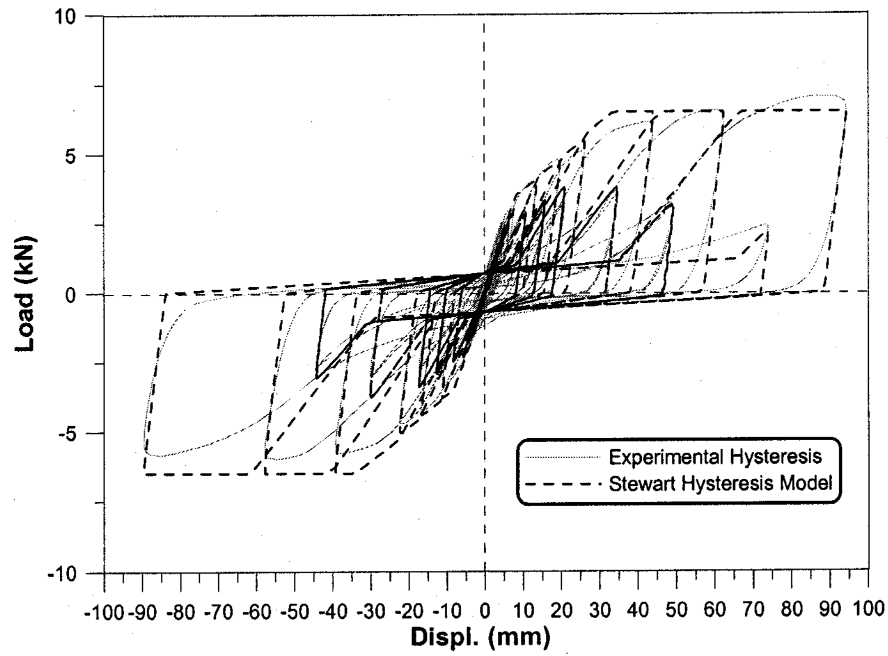

Figure C-17 : Superimposed Experimental and Modeled Hystereses (Group 20)

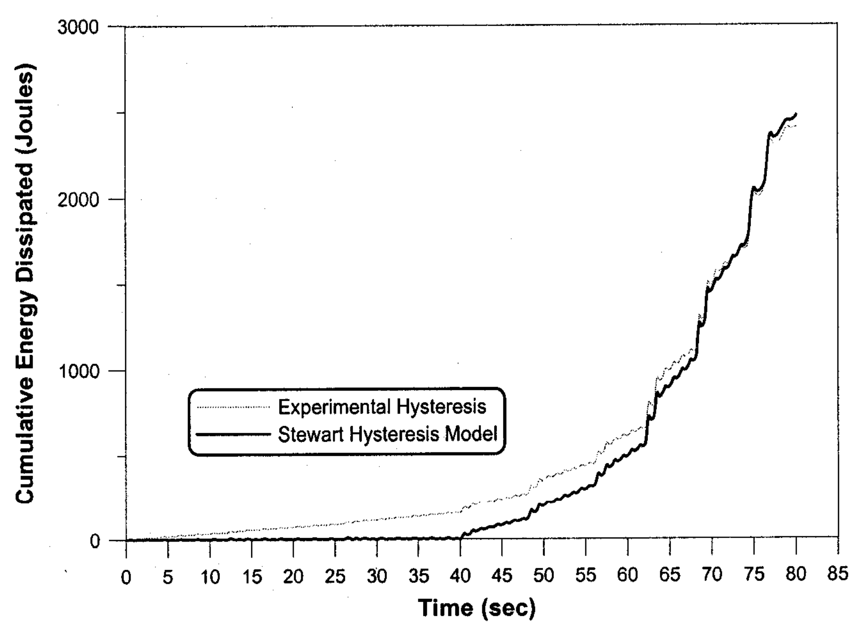

Figure C-18 : Cumulative Energy Dissipated from Experimental Test and Stewart Model Hystereses (Group 20)

Group	Wood Panel	Size	Srew Pattern	K_0 (kN/mm)	r	Fy (kN)	Fy (kN)	Fu/Fy	Fu (kN)	Fi (kN)	P_{Tri}	Fi/Fy	P_{UNL}	β	α
22	OSB	4' x 8'	6" x 12"	1.60	0.20	8.40	-8.40	1.61	13.50	1.00	0	0.12	1.75	1.10	0.45

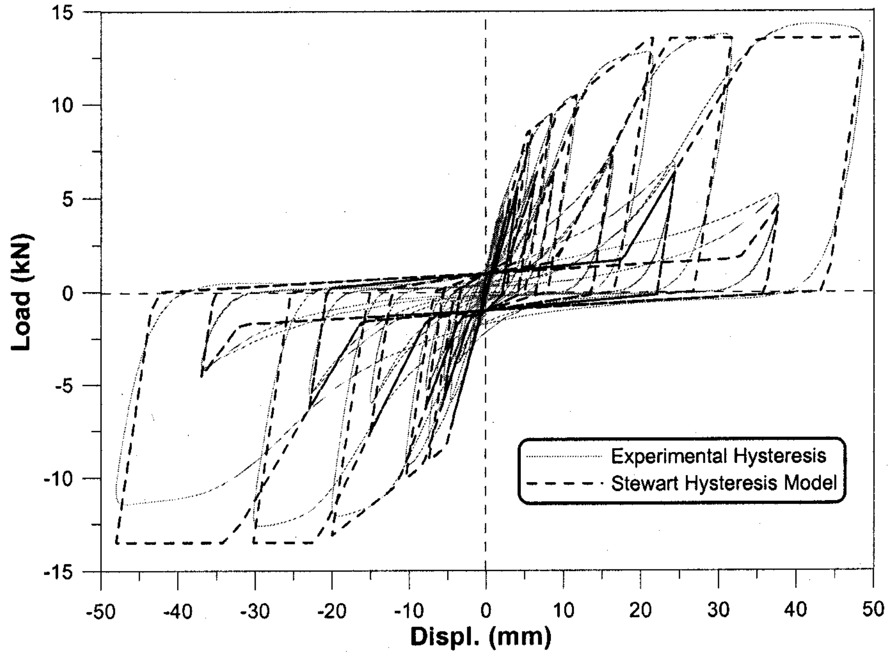

Figure C-19 : Superimposed Experimental and Modeled Hystereses (Group 22)

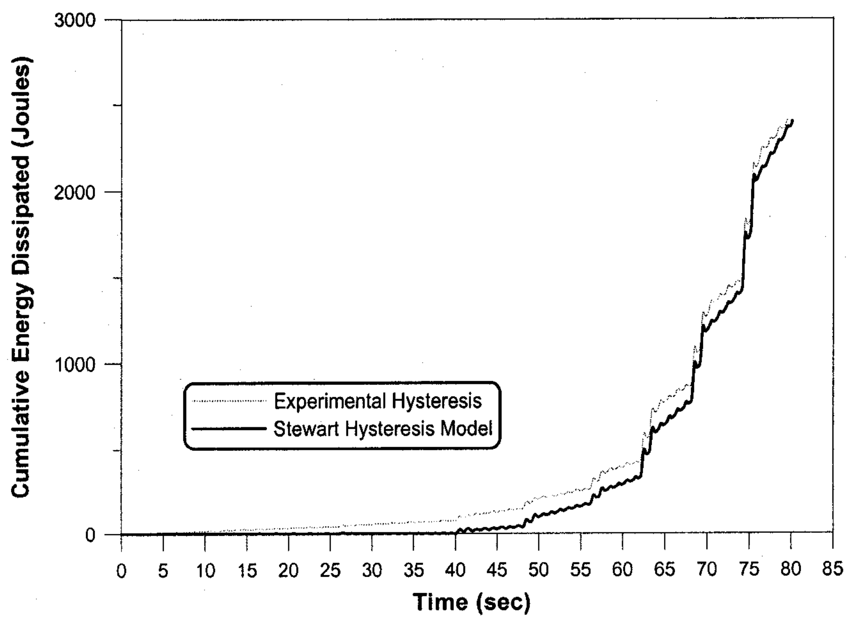

Figure C-20 : Cumulative Energy Dissipated from Experimental Test and Stewart Model Hystereses (Group 22)

Group	Wood Panel	Size	Srew Pattern	K_0 (kN/mm)	r	Fy (kN)	Fy (kN)	Fu/Fy	Fu (kN)	Fi (kN)	P_{Tri}	Fi/Fy	P_{UNL}	β	α
24	OSB	4' x 8'	4" x 12"	2.10	0.23	13.40	-13.40	1.49	20.00	1.40	0	0.10	1.75	1.10	0.45

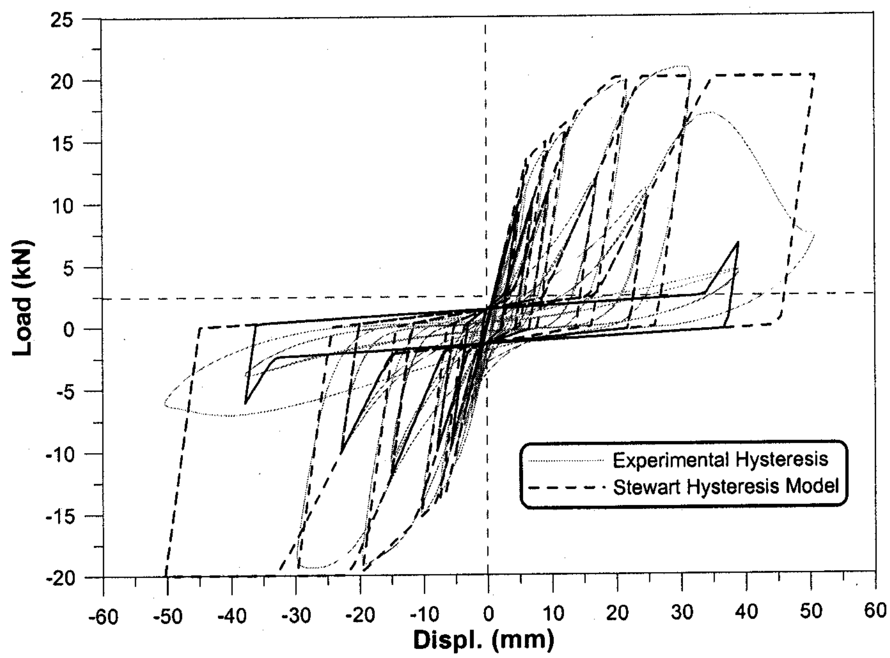

Figure C-21 : Superimposed Experimental and Modeled Hystereses (Group 24)

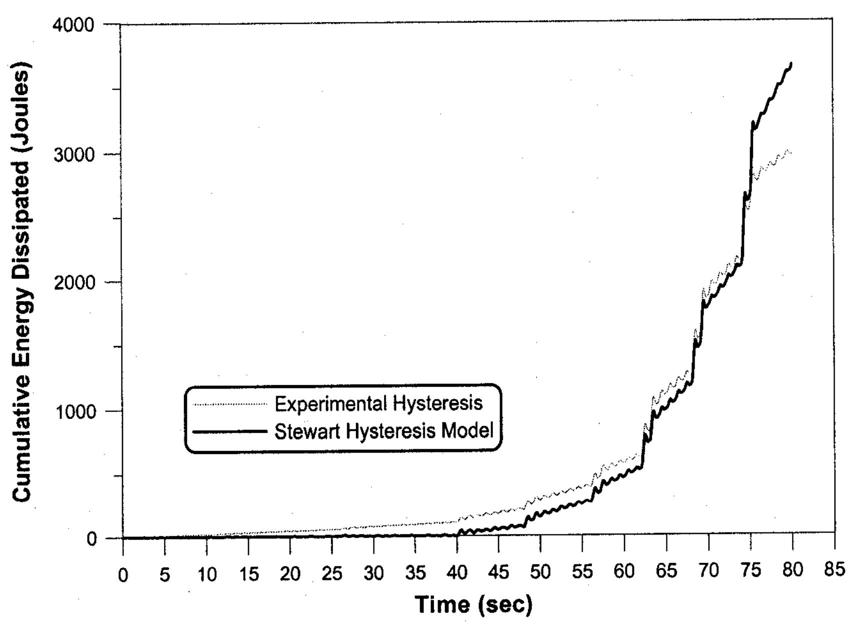

Figure C-22 : Cumulative Energy Dissipated from Experimental Test and Stewart Model Hystereses (Group 24)

Group	Wood Panel	Size	Srew Pattern	K_0 (kN/mm)	r	Fy (kN)	Fy (kN)	Fu/Fy	Fu (kN)	Fi (kN)	P_{Tri}	Fi/Fy	P_{UNL}	β	α
26	OSB	4' x 8'	3" x 12"	3.00	0.22	17.00	-17.00	1.68	28.50	2.50	0	0.15	1.25	1.10	0.45

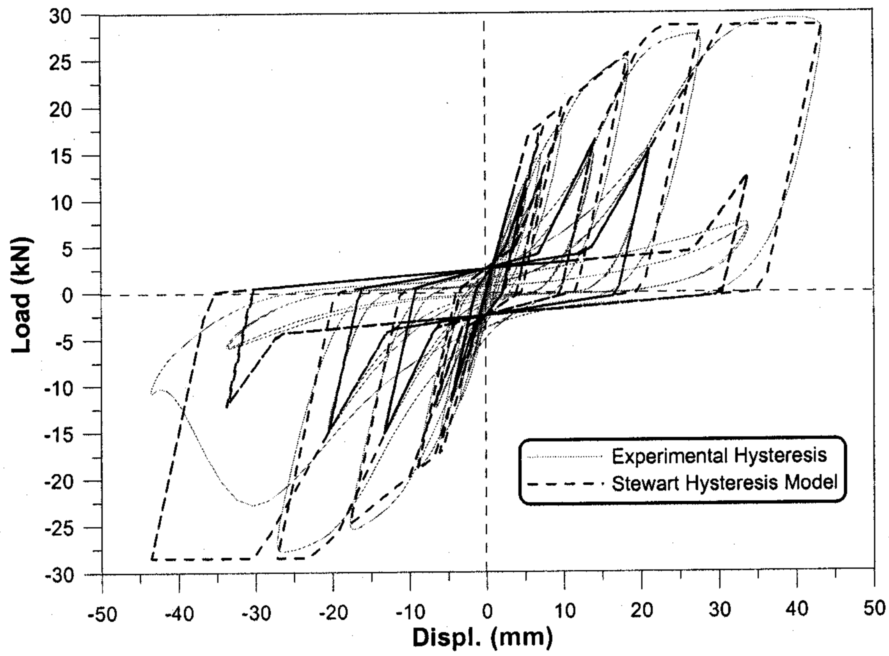

Figure C-23 : Superimposed Experimental and Modeled Hystereses (Group 26)

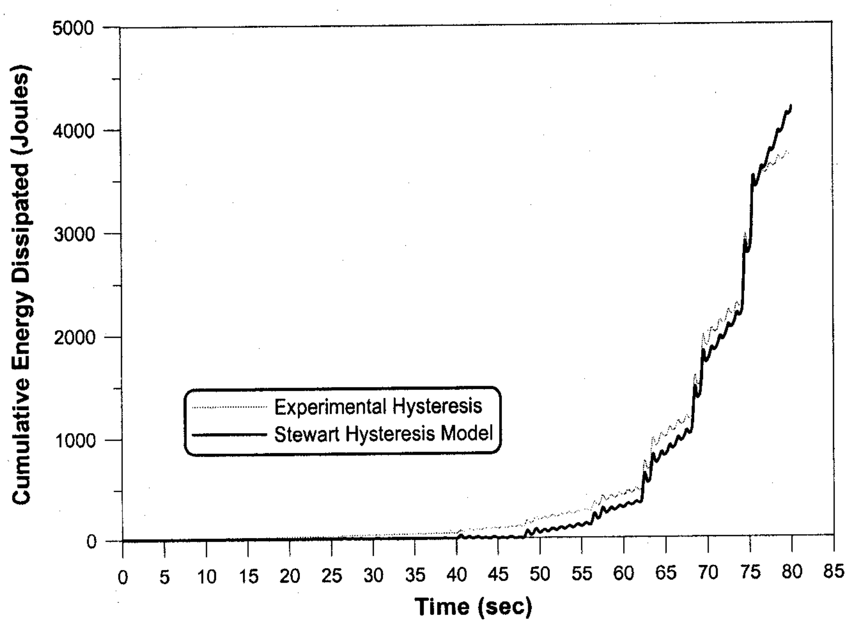

Figure C-24 : Cumulative Energy Dissipated from Experimental Test and Stewart Model Hystereses (Group 26)

Group	Wood Panel	Size	Srew Pattern	K_0 (kN/mm)	r	Fy (kN)	Fy (kN)	Fu/Fy	Fu (kN)	Fi (kN)	P_{Tri}	Fi/Fy	P_{UNL}	β	α
28	OSB	2' x 8'	4" x 12"	0.57	0.22	6.40	-6.40	1.58	10.12	1.00	0	0.16	1.80	1.10	0.45

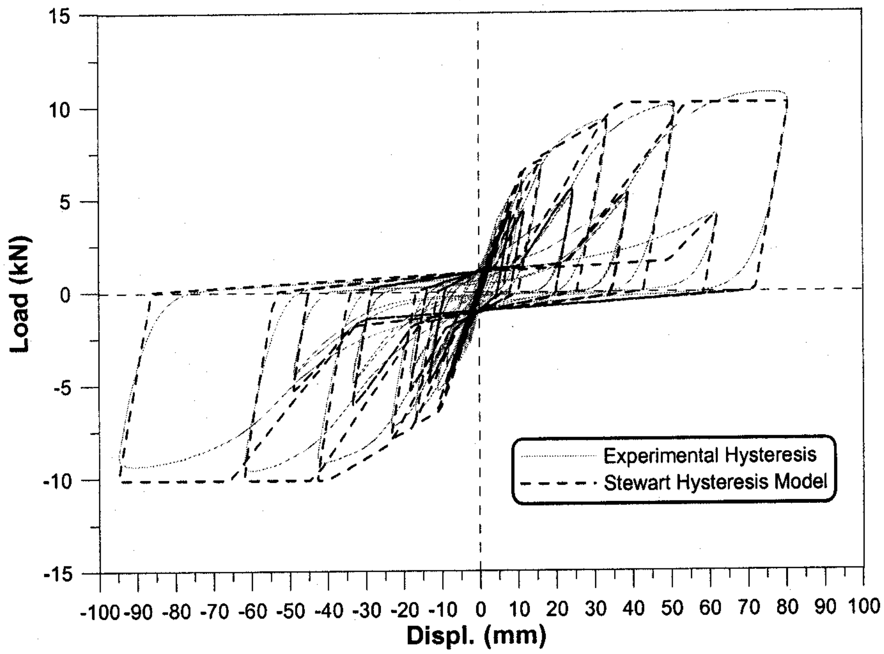

Figure C-25 : Superimposed Experimental and Modeled Hystereses (Group 28)

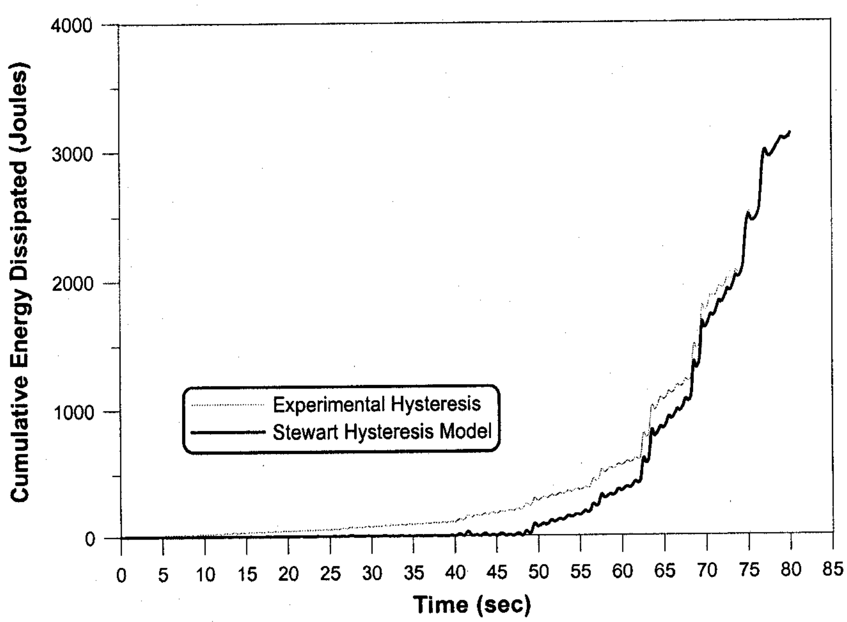

Figure C-26 : Cumulative Energy Dissipated from Experimental Test and Stewart Model Hystereses (Group 28)

Group	Wood Panel	Size	Srew Pattern	K_0 (kN/mm)	r	Fy (kN)	Fy (kN)	Fu/Fy	Fu (kN)	Fi (kN)	P_{Tri}	Fi/Fy	P_{UNL}	β	α
30	CSP	8' x 8'	6" x 12"	2.20	0.18	21.50	-21.50	1.46	31.30	2.70	0	0.13	2.25	1.10	0.41

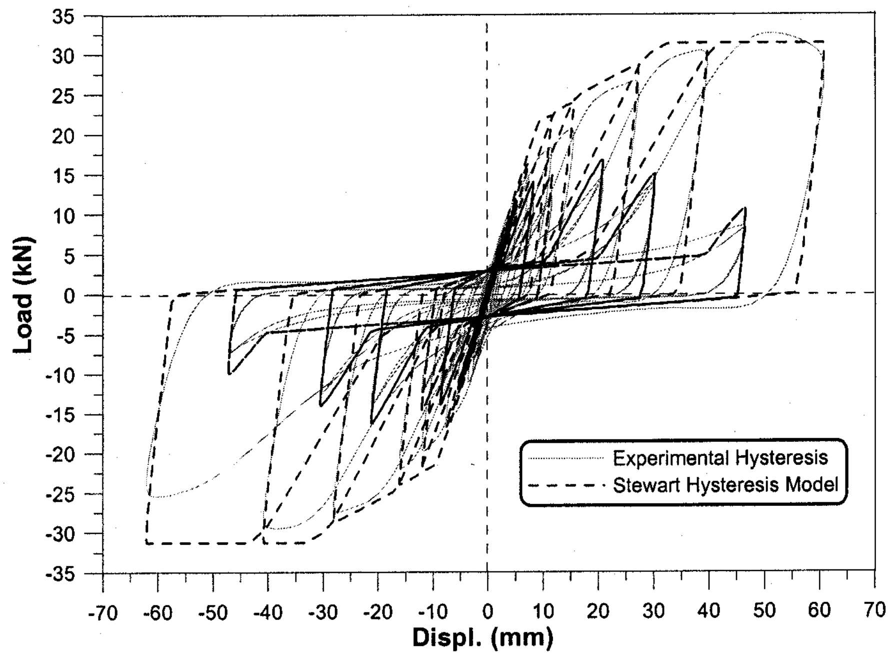

Figure C-27 : Superimposed Experimental and Modeled Hystereses (Group 30)

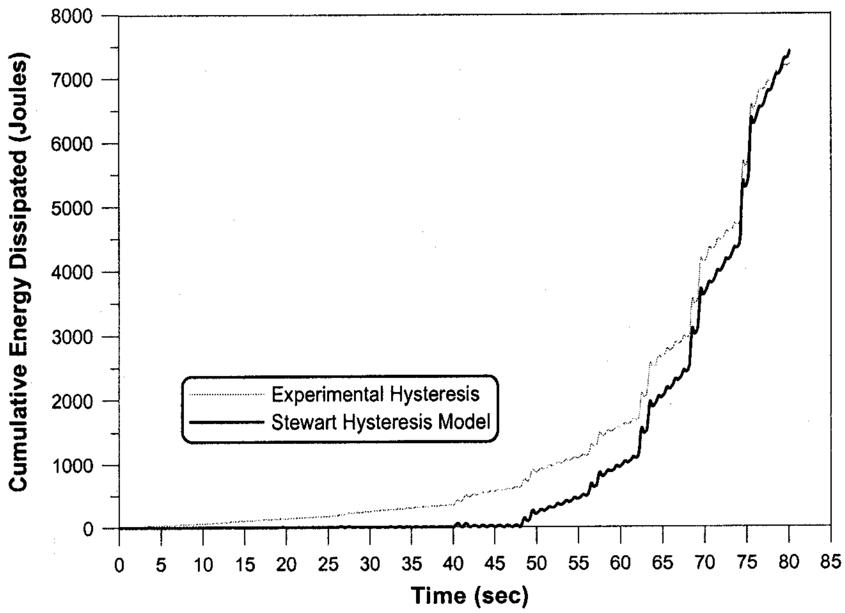

Figure C-28 : Cumulative Energy Dissipated from Experimental Test and Stewart Model Hystereses (Group 30)

Group	Wood Panel	Size	Srew Pattern	K_0 (kN/mm)	r	Fy (kN)	Fy (kN)	Fu/Fy	Fu (kN)	Fi (kN)	P_{Tri}	Fi/Fy	P_{UNL}	β	α
32	CSP	8' x 8'	4" x 12"	2.40	0.30	28.50	-28.50	1.63	46.40	3.90	0	0.14	2.10	1.09	0.25

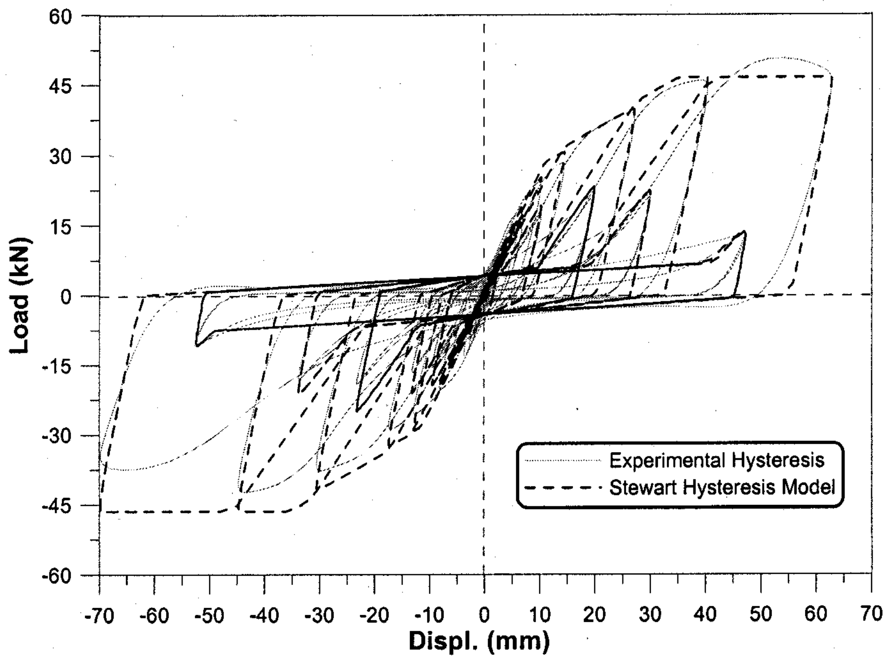

Figure C-29 : Superimposed Experimental and Modeled Hystereses (Group 32)

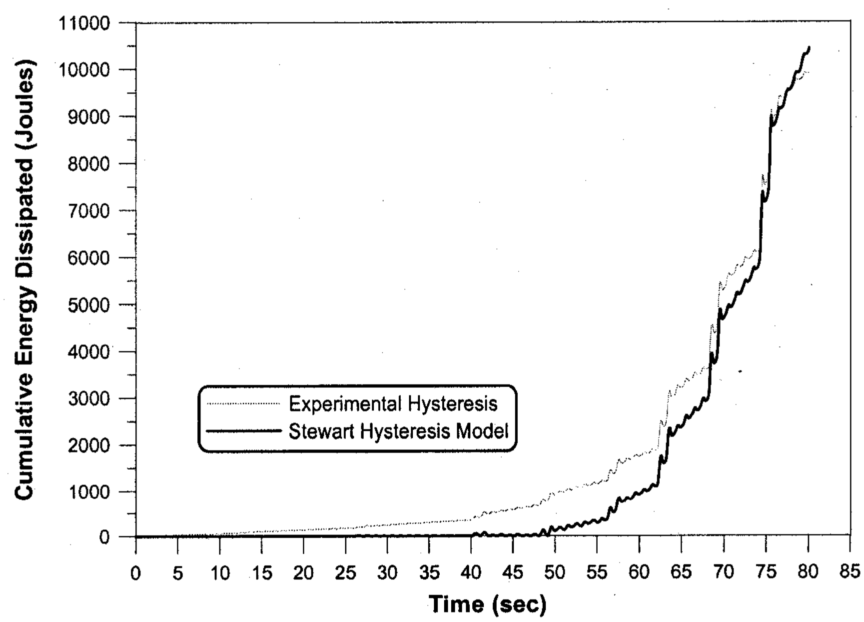

Figure C-30 : Cumulative Energy Dissipated from Experimental Test and Stewart Model Hystereses (Group 32)

Group	Wood Panel	Size	Srew Pattern	K_0 (kN/mm)	r	Fy (kN)	Fy (kN)	Fu/Fy	Fu (kN)	Fi (kN)	P_{Tri}	Fi/Fy	P_{UNL}	β	α
34	CSP	8' x 8'	3" x 12"	3.20	0.30	37.00	-37.00	1.71	63.30	4.45	0	0.12	1.70	1.07	0.27

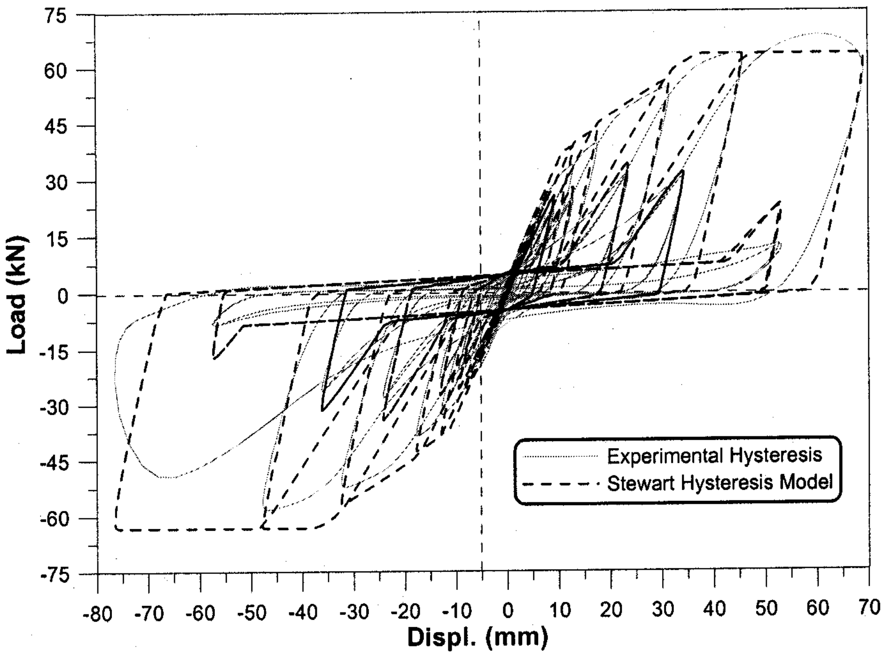

Figure C-31 : Superimposed Experimental and Modeled Hystereses (Group 34)

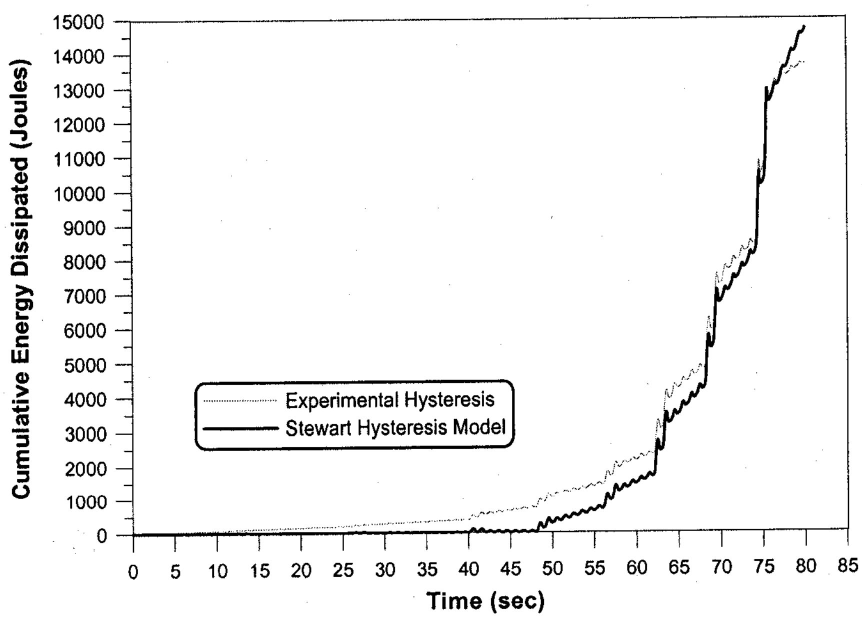

Figure C-32 : Cumulative Energy Dissipated from Experimental Test and Stewart Model Hystereses (Group 34)